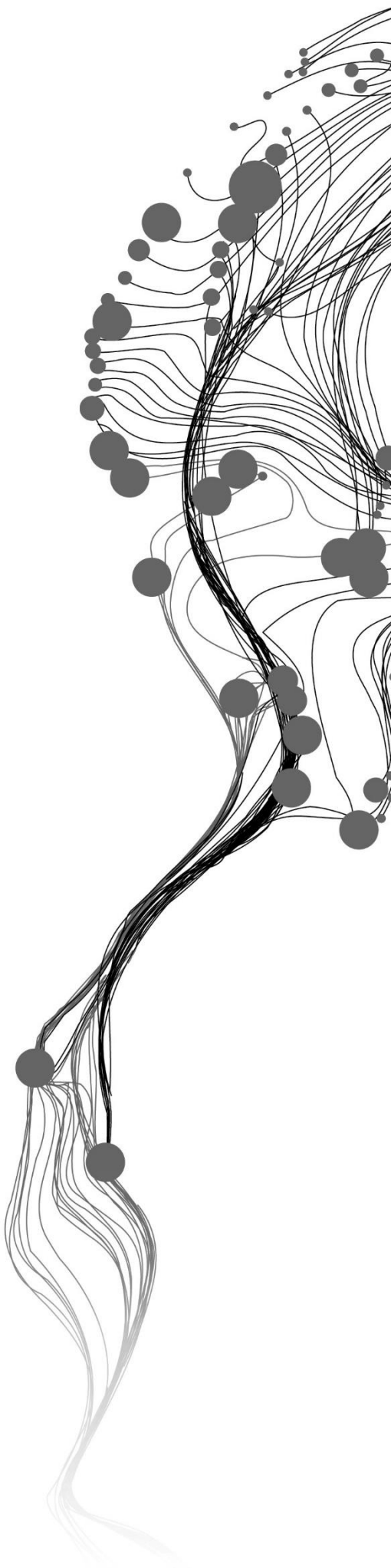


# **LAKE TANA WATER BALANCE ASSESSMENT BY THE EFFECT OF CLIMATE CHANGE AND LAND USE INTERVENTIONS**

BETELHEM WOLDERUFAEL GEBRETSADIK  
September, 2021

SUPERVISORS:  
Dr. Ing. T.H.M, Rientjes  
Dr. ir.M.J. Booij





# **LAKE TANA WATER BALANCE ASSESSMENT BY THE EFFECT OF CLIMATE CHANGE AND LAND USE INTERVENTIONS**

BETELHEM WOLDERUFAEL GEBRETSADIK  
Enschede, The Netherlands, September 2021

Thesis submitted to the Faculty of Geo-Information Science and Earth  
Observation of the University of Twente in partial fulfilment of the  
requirements for the degree of Master of Science in Geo-information Science  
and Earth Observation.

Specialization: Water Resources and Environmental Management

**SUPERVISORS:**

Dr. Ing. T.H.M, Rientjes

Dr. ir.M.J. Booij

**THESIS ASSESSMENT BOARD:**

Prof. Dr. Z.Su (Chair)

Dr. Alemseged Haile (External Examiner, Arba Minch University, Ethiopia)

#### DISCLAIMER

This document describes work undertaken as part of a programme of study at the Faculty of Geo-Information Science and Earth Observation of the University of Twente. All views and opinions expressed therein remain the sole responsibility of the author, and do not necessarily represent those of the Faculty.



## ABSTRACT

Lake Tana is the largest lake in Ethiopia, which is located in the upper Blue Nile Basin. The lake has a significant impact on society regarding income generation and food security since the community's livelihood around the lake depends on agriculture, fisheries, livestock production, and water transportation. In line with this, there are a number of water resource developments in the Lake Tana sub-basin, such as hydropower, large-scale irrigation, and water supply projects. Accordingly, the lake's sustainability is expected to be affected as a result of climate change and land use interventions. This study assesses the impact of climate change and land use interventions on the water balance of Lake Tana by using the water evaluation and planning (WEAP) model. The land use interventions this study focused on were the large-scale irrigation projects and dam constructions in the Lake Tana sub-basin. To assess the change in the lake's water balance, two time horizons were selected: baseline period (1991-2005) and future period (2041-2070). The water balance simulation of the WEAP was performed under four scenarios: baseline period (scenario 1), baseline period with land use interventions (scenario 2), future period (scenario 3), future period with land use interventions (scenario 4). Bias corrected ensemble mean of three dynamically downscaled RCM models under RCP4.5 and RCP8.5 emission scenarios were used for this study. The HBV rainfall-runoff model simulated streamflow from 19 catchments (gauged and ungauged). To estimate the irrigation demand of the 11 planned irrigation schemes, the AquaCrop model was used. The WEAP simulation result shows that the mean annual lake level of the baseline scenario is 1786.45 m.a.s.l. According to the WEAP simulation result, the mean annual lake water level of the baseline period under planned irrigation schemes and dam construction could decline by about 1.2 m when compared to scenario 1. The future period (scenario 3) revealed a mean annual lake water level decline of 0.51 m and 1.74 m for RC4.5 and RCP8.5 emission scenarios, respectively. The drop in water level under the RCP8.5 emission scenario is more significant than the RCP4.5 due to lower lake precipitation and higher open water evaporation because of increasing temperature for the RCP8.5 emission scenario compared to the RCP4.5 scenario. The mean annual water level under the combined effect of climate change and land use intervention will likely result in a decline of 2.78 m and 5.16 m water levels under RCP4.5 and RCP8.5 emission scenarios, respectively. According to the result, the combined impact of future development and climate change is more significant than the climate change impact.

Evaluation of the sustainable water supply to the planned irrigation schemes was performed under the full implementation of the water resource developments. Findings indicate that for scenario 2, the irrigation schemes' unmet water demand is 19.4% of total water demand. WEAP results indicate that the unmet demand under scenario 4 is 11.4% and 20.5 % under the RCP4.5 and RCP8.5 scenarios, respectively. The unmet demand of the environmental flow requirement showed that the unmet demand is less than 1% for scenario 2 and RCP4.5 under scenario 4. While the unmet demand for the environmental flow requirement of scenario 4 of the RCP8.5 is around 4%.

## ACKNOWLEDGEMENTS

First and foremost, I thank the Almighty GOD for His mercy and blessing upon me during my journey in ITC and all my life.

I would like to express my sincere gratitude to the Netherlands Government through the Orange Knowledge Programme (OKP) for granting me this opportunity and supporting me financially.

Very special thanks to my supervisors, Dr.Ing. Tom Rientjes and Dr.ir.M.J.Booij for their guidance, encouragement, and constructive comments throughout the thesis work. The weekly discussions and your valuable support and guidance helped me to gain a lot of knowledge. Without you, this work would not have been realized.

I would also like to express my appreciation to all Water Resources and Environmental Management department staff at the ITC community who helped me during this thesis work. Special acknowledgment goes to Ir. Arno Van Lieshout. Mr. Bas Retsios and Kingsley, I am so grateful for your technical support.

I would like to thank also Ethiopian Ministry of Water Resources and the National Meteorological Agency for providing hydrological and meteorological data.

Last but not least, I would like to thank my wonderful family for their unlimited support throughout my life. I will always do my best to make you proud.

Betelhem Wolderufael Gebretsadik

[Betelhemwy1@gmail.com](mailto:Betelhemwy1@gmail.com)

# TABLE OF CONTENTS

---

1.	INTRODUCTION.....	1
1.1.	General.....	1
1.2.	Problem Statement.....	2
1.3.	Main Objective.....	3
1.4.	Specific Objectives.....	3
1.5.	Research Questions.....	3
1.6.	Research Hypotheses.....	3
2.	LITERATURE REVIEW.....	4
2.1.	Climate Models.....	4
2.2.	Downscaling Technique.....	4
2.3.	Emission Scenarios.....	4
2.4.	Hydrological Models.....	5
2.5.	Water Evaluation and Planning Model (WEAP).....	5
2.6.	Related Studies.....	6
3.	STUDY AREA AND DATA PREPARATION.....	9
3.1.	Study Area.....	9
3.2.	Data Processing for Baseline Period and Future Climate Change Projections.....	13
4.	METHODOLOGY.....	27
4.1.	WEAP Modelling.....	28
4.2.	Water Balance Components of Lake Tana.....	36
4.3.	HBV Modelling.....	38
4.4.	AquaCrop Modelling.....	44
5.	RESULTS.....	49
5.1.	Climate Projections.....	49
5.2.	Lake Water Balance Components.....	54
5.3.	Irrigation Requirement.....	64
5.4.	Water Balance.....	67
6.	DISCUSSION.....	75
6.1.	Projected Change in Climate Variables.....	75
6.2.	Rainfall-Runoff Modelling.....	75
6.3.	Irrigation Requirement.....	76
6.4.	Water Balance of Lake Tana under Baseline Period.....	76
7.	CONCLUSION AND RECOMMENDATION.....	78
7.1.	Conclusion.....	78
7.2.	Limitations and Assumptions.....	79
7.3.	Recommendations.....	79

## LIST OF FIGURES

---

Figure 3-1: Location of the study area .....	9
Figure 3-2: Planned and completed irrigation schemes in Lake Tana sub-basin after (Halcrow, 2010) .....	12
Figure 3-3: Spatial distribution of meteorological stations and hydrological stations and basins .....	13
Figure 3-4: Double mass curve analysis for Delgi, Dangila, Deke Istifanos and Gondar stations .....	15
Figure 3-5: Long-term annual average precipitation in each meteorological station with its elevation.....	16
Figure 3-6: Precipitation-elevation relation in Lake Tana sub-basin.....	16
Figure 3-7: Distribution of mean monthly precipitation for respective stations (1991-2005). .....	17
Figure 3-8: Relation between station temperature and average temperature.....	17
Figure 3-9: Mean monthly temperature with elevation .....	18
Figure 3-10: Mean monthly temperature of 6 meteorological stations over the period 1991-2005.....	18
Figure 3-11: Mean annual temperature-elevation relation in Lake Tana sub-basin.....	19
Figure 3-12: Lake Tans basin area overlain by a 44 × 44 km grid showing RCA4 RCM maximum temperature on January 1 <sup>st</sup> , 2041. Locations of the meteorological stations are also indicated. ....	21
Figure 3-13: Long term monthly mean precipitation comparison of observed and RCM data in Megech, Ribb catchment.....	22
Figure 3-14: Long term monthly mean temperature comparison of observed and RCM data in Megech, Ribb catchment.....	23
Figure 3-15: Bias corrected precipitation data of ensemble RCMs .....	25
Figure 3-16: Bias corrected mean temperature data of ensemble RCMs .....	26
Figure 3-17: Bias corrected wind speed data of ensemble RCMs.....	26
Figure 4-1: Flowchart of the research .....	27
Figure 4-2: WEAP schematization for baseline and future period scenario (scenario 1&3).....	29
Figure 4-3: WEAP schematization for baseline and future period with land use interventions scenario (scenario 1&3).....	30
Figure 4-4: Reservoir storage zones (Source: Sieber (2005)) .....	34
Figure 4-5: Schematic representation of HBV model (IHMS, 2006), modified by (Perera, 2009) .....	38
Figure 4-6: Flowchart on AquaCrop modelling.....	44
Figure 5-1: Annual temperature of Lake Tana for baseline and future period under RCP4.5 and RCP8.5 emission scenario .....	49
Figure 5-2: Projected monthly changes of Lake Tana mean temperature for the future period under RCP4.5 and RCP8.5 emission scenarios .....	50
Figure 5-3: Annual mean temperature of catchments for baseline and future period under RCP4.5 and RCP8.5 emission scenario .....	50
Figure 5-4: Projected monthly changes catchment mean temperature for the future period under RCP4.5 and RCP8.5 emission scenarios.....	51
Figure 5-5: Annual catchment precipitation for baseline and future period under RCP4.5 and RCP8.5 emission scenario .....	51
Figure 5-6: Projected changes in monthly mean precipitation of catchments for the future period under RCP4.5 and RCP8.5 emission scenarios .....	52
Figure 5-7: Annual catchment PET for baseline and future period under RCP4.5 and RCP8.5 emission scenario.....	53
Figure 5-8: Projected changes in monthly catchment PET for the future period under RCP4.5 and RCP8.5 emission scenario .....	53
Figure 5-9 Model calibration results of Gilgel Abay and Gumara catchment.....	55

Figure 5-10: Model validation result of Gilgel Abay and Gumara catchment from 2004-2005.....	56
Figure 5-11: Lake Tana's annual precipitation for baseline and future period under RCP4.5 and RCP8.5 emission scenario.....	58
Figure 5-12: Projected changes in monthly Lake precipitation for the future period under RCP4.5 and RCP8.5 emission scenario.....	58
Figure 5-13: Lake Tana's annual evaporation for baseline and future period under RCP4.5 and RCP8.5 emission scenario.....	59
Figure 5-14: Projected change in monthly lake evaporation for the future period under RCP4.5 and RCP8.5 emission scenario.....	59
Figure 5-15: Projected five-year average lake evaporation and precipitation for RCP4.5 and RCP8.5 scenarios.....	60
Figure 5-16: Lake Tana's annual inflow for baseline and future period under RCP4.5 and RCP8.5 emission scenario.....	61
Figure 5-17: Projected change in monthly inflow for the future period under RCP4.5 and RCP8.5 emission scenario.....	61
Figure 5-18: Evaluation of <i>Beta</i> coefficient for Lake Tana outflow computation (1991-2005).....	62
Figure 5-19: Observed and simulated lake level (1991-2005) as a result of outflow computation.....	62
Figure 5-20: Flow upstream of the six irrigation dams.....	63
Figure 5-21: Mean monthly evaporation and precipitation for Ribb and Gilgel Abay Dams.....	63
Figure 5-22: Monthly gross irrigation requirement.....	64
Figure 5-23: Gross irrigation requirement of the baseline period.....	65
Figure 5-24: Observed and simulated lake levels for the period 1991-2005.....	67
Figure 5-25: Annual Lake level for baseline under land use interventions scenario.....	68
Figure 5-26: Annual Lake level for baseline and future scenario.....	68
Figure 5-27: Annual Lake level under scenario 1 ,2 ,3 & 4.....	69
Figure 5-28: Monthly Lake level under scenario 1, 2, 3 & 4.....	70
Figure 5-29: Cumulative value of water balance components for baseline and future period (RCP4.5 and RCP8.5).....	73

## LIST OF TABLES

---

Table 3-1: Major gauged and ungauged catchment in the Lake Tana sub-basin (Perera, 2009).....	11
Table 3-2: Planned irrigation schemes in Lake Tana sub-basin .....	12
Table 3-3: Summary of and missing precipitation data (1991-2005).....	14
Table 3-4: Selected RCMs and driving GCMs for this study .....	20
Table 3-5: RMSE, MAE, R <sup>2</sup> between observed and RCMs monthly precipitation in Megech and Ribb catchments over 1991-2005 .....	24
Table 4-1: Environmental flow requirement(m <sup>3</sup> /s) downstream the planned irrigation dams(Halcrow, 2011) .....	32
Table 4-2: Demand prioritization .....	32
Table 4-3: Reservoir operation data for the planned dams.....	35
Table 4-4: Calibrated model parameters for gauged catchment 1991-2000 (Perera, 2009).....	41
Table 4-5: Physical catchment characteristics for regionalization method (Perera, 2009).....	42
Table 4-6: Catchment area upstream proposed irrigation dams .....	43
Table 4-7: Default soil parameters of AquaCrop model.....	46
Table 5-1: Evaluation of Previously calibrated parameters.....	54
Table 5-2: Calibrated model parameters for Gilgel Abay and Gumara catchment.....	54
Table 5-3: HBV model parameters for gauged catchments.....	55
Table 5-4: HBV model validation result for Gilgel Abay and Gumara catchments from 2004-2005 .....	56
Table 5-5: Developed Regional model equation .....	57
Table 5-6: Validation of a regional model of the gauged catchment from 2003-2005.....	57
Table 5-7: Mean annual evaporation and precipitation of irrigation dams .....	63
Table 5-8: Annual gross irrigation requirement for baseline and future period under land use intervention scenario.....	65
Table 5-9: Annual water use rate of each irrigation scheme (Mm <sup>3</sup> /ha).....	66
Table 5-10: Results of mean annual water level simulation for each scenario.....	70
Table 5-11: Monthly minimum and maximum lake level for each scenario .....	71
Table 5-12: Lake Tana water balance components (Mm <sup>3</sup> /year) .....	71
Table 5-13: Number of months under the minimum recommended lake level by EEPCO .....	73
Table 5-14: Unmet demand of irrigation schemes (Mm <sup>3</sup> /year).....	74
Table 5-15: Unmet demand of environmental flow requirement (Mm <sup>3</sup> /year).....	74

# 1. INTRODUCTION

## 1.1. General

The sustainability of water resources and the local ecosystems can significantly be affected by climate and land use change (Zhang, Nan, Xu, & Li, 2016). According to Loucks (2000), sustainability of water resources is the consistent water supply for current and future demands, regardless of climate change, land use change, and other human and natural activities. Climate change is defined as a long-term weather pattern change (e.g., precipitation and temperature) due to increased greenhouse concentration in the atmosphere (Rahman, 2013). IPCC (2021) indicated that by CO<sub>2</sub> emissions, a possible increase of 1.5°C in the global temperature would occur within the next two decades compared to the historical period 1850 - 1900. Under high emission scenarios, the increase in surface temperature may reach 3.3°C to 5.7°C by 2100. African countries are among the most exposed areas to climate change and variability (IPCC, 2001). IPCC (2014) showed that the average precipitation would possibly decrease in mid-latitude and subtropical dry regions, while it will possibly increase in wet areas. The report further explained that although precipitation patterns are not well understood in Eastern Africa, the change in patterns for the past thirty to forty years was the leading cause of recurrent droughts and heavy rainfall. Water planners and managers do not usually account for variations in climate trends when building water supply systems such as dams (Mukheibir, 2007). However, climate change is becoming a significant threat to water resource management by affecting precipitation trends worldwide (Mukheibir, 2007). Even though it has not been adequately addressed, the impact of climate change can result in lower lake water levels and river base flow. Besides, it can negatively affect irrigation and groundwater supply to the community (Lambin, 1997).

Land use land cover change (LULC) can be caused by human activities such as urbanization, deforestation, and agriculture expansion. Changes can be diffused in time or abrupt by interventions such as dam construction and large-scale irrigation planning. These changes due to land use interventions can affect water flow and the water balance (Rawat & Kumar, 2015). Changes in LULC also affect the water availability of an area (Sajikumar & Remya, 2015). The change in LULC is high in Africa's tropical mountain area because of the rise in population and increased human pressure for a living (Lambin, 1997). Also, LULC might negatively affect the economy of low-income and developing countries like Ethiopia that largely depends on agriculture (Welde & Gebremariam, 2017). Though the effect of changes in LULC may be very high, the fundamental mechanisms causing the hydrological impact of land-use change on streamflow are less understood yet (Wang et al., 2018).

The integrated effect of climate change and land use intervention might negatively affect water resource availability and sustainability. Therefore, understanding the impact of climate change and LULC on water resources is very important for sustainable water resource planning and management. Also, it provides support for decision-makers for national water resource planning and allocation.

## 1.2. Problem Statement

As the primary source of the Blue Nile River and the largest lake in Ethiopia, the water assessment of lake Tana basin by climate change, land use interventions, and their impact on the lake's water balance have high relevance for the society on the lakeshore. Kim & Kaluarachchi (2009) reported that the Blue Nile River basin at large is greatly affected by climate and water resource variability, wetter, and warmer climate in the period 2040-2069. Setegn (2011) indicated that the Lake Tana basin would be negatively affected due to climate change and water resource abstractions.

Lake Tana has a significant impact on society regarding income generation, and food security since the livelihood of the community around the lake depends on agriculture, fisheries, and livestock production. Those sectors are sensitive to climate and land use changes and interventions. The lake also has a significant economic impact on the country through hydropower generation, tourism, and food production. Therefore, fully understanding the lake's water dynamics is crucial that profoundly supports the government and decision-makers on water resource planning and management of the sub-basin.

Ethiopia's Federal Democratic Republic Government identified the lake Tana basin as one of the most important regions for various socio-economic developments. Some 15 dams and river diversion structures are planned or already built along the tributary rivers that flow to Lake Tana to store the runoff water. Water reservoirs by dam constructions in the basin should serve agricultural production and hydropower generation to accommodate the population growth and food production (Shewit et al., 2017). Based on a recent study by Dessie et al. (2017), different irrigation schemes are planned to irrigate more than 115,000 ha of land in the Tana sub-basin.

Consequently, the expansion of the agricultural land and building dams around the basin affects the lake's natural inflow, influencing the lake's water balance. A preliminary study by (McCartney et al., 2010) indicated that as a result of dam construction and planned irrigation schemes, lowering of Lake Tana Lake levels by 44 cm is projected, and the average surface area will decrease by 30 km<sup>2</sup>, which is 1% of the total lake area and up to 80 km<sup>2</sup> (2.6% of the lake area) through some dry seasons. Tadesse (2008) indicated that the lake's water resources development would drop the lake's average water level by 33 cm and reduce the lake's average surface area by 23 km<sup>2</sup>, as a consequence of dam construction and planned irrigation schemes. Reported findings are not based on a holistic approach and consider outdated emission scenarios. Also, the effects of land intervention schemes by dam-reservoir construction are not well assessed. From a scientific point of view, there is an urgent need to assess Lake Tana's sustainability that considers the most recent emission scenarios and land intervention schemes and modelling tools to estimate Lake inflows and water use by planned irrigation schemes.

### **1.3. Main Objective**

The main objective of this research is to assess the impact of climate change and land use interventions on the water balance of Lake Tana.

### **1.4. Specific Objectives**

The specific objectives are:

1. To evaluate future projections of precipitation and temperature change.
2. To model at monthly and annual time step in and outflows to Lake Tana under the effect of climate change.
3. To quantify the baseline and future water demand of planned large-scale irrigation developments in the sub-basin at a monthly and annual time step and the effects on the lake water balance.
4. To evaluate the sustainability of lake Tana under the combined effect of climate change and planned land use interventions.

### **1.5. Research Questions**

The following research questions are developed to achieve these research objectives.

- To what extent will the precipitation and temperature of the Lake Tana sub-basin change for the future period?
- How much will Lake Tana's in and out flow change due to the effects of climate change?
- What will be the annual and monthly variation of the lake's water balance components under the effect of climate change?
- Will Lake Tana be sustainable by the integrated effect of climate change and planned dam constructions for large-scale irrigation developments?

### **1.6. Research Hypotheses**

- The increase in potential evaporation due to the rise in annual temperature by climate change will affect available water resources in the Lake Tana sub-basin area and negatively affect the water storage of Lake Tana.
- Since the lake inflow reduces due to planned irrigations, dam, and reservoir construction, the lake will not be sustainable.
- The effect of land use interventions has more pronounced effects on lake sustainability than the effect of climate change.

## 2. LITERATURE REVIEW

### 2.1. Climate Models

Understanding past, current, and future climate patterns give insight into how to mitigate climate change impacts. The study of those patterns over long periods requires sophisticated climate models. Climate models help to understand the effects of anthropogenic emissions and climate change on the earth system. The models use mathematical methods to simulate the processes and interactions that affect the earth's climate. These models predict how climate conditions change in an area over future periods(decades) due to natural and human activities. Global circulation models (GCMs) are a type of climate model that provides quantitative estimates of future climate change continental and global and scale and over long periods. In order to use the information of the GCMs on a local and regional scale, downscaling methods are applied.

### 2.2. Downscaling Technique

GCMs have a coarse resolution of 100 to 200 km grid size and obstruct impacts assessments at a regional and local scale. Thus, a downscaling approach should be applied to assess impacts on hydrological processes on a regional and local scale. Two downscaling techniques are distinguished: that are statistical and dynamic/regional downscaling. Statistical downscaling methods use statistical relationships between past global and regional climate patterns to project the future climate. Assuming that the relationships would be the same for the future periods, the method applies this statistical relationship for future projections. This method requires minimum computing time but has the limitation that it assumes that the past relationship between global and regional climate patterns would carry for the future. The other downscaling method that scales global scale GCM model outcomes to regional scale is the dynamic downscaling method. This method is a computationally intensive technique but is quite advantageous in resolving atmospheric processes that occur in a sub GCM grid compared to statistical downscaling. The regional modelling technique uses initial conditions, surface boundary conditions, time-dependent lateral meteorological conditions of the GCMs. In this method, GCM outputs are downscaled to a smaller scale using a higher resolution dynamic model known as the regional climate model (RCM). RCM model domains do not cover the entire globe but apply model domains that cover global sub-regions at a finer spatial grid scale.

### 2.3. Emission Scenarios

The calculations in the climate models are based on greenhouse emission scenarios. The climate models take the information about the probability of human emission of greenhouse gases and how that would affect the future climate. Based on those hypothetical emissions, the climate models calculate the future patterns of different climate variables, such as precipitation and temperature. The emission/ radiation scenarios are based on future green gas emissions. IPCC (2000) published a Special Report on Emissions Scenarios (SRES). The scenarios are based on four narrative storylines labelled A1, A2, B1, and B2. These emission scenarios are based on a possible socio-economic change in the future, how the socio-economic developments drive greenhouse gas emissions, and the levels to which those emissions would rise in the 21st century.

The IPCC (2013) fifth assessment report has agreed on a new set of scenarios, which focuses on the level of greenhouse gas concentration in the atmosphere in 2100. The new scenarios are called Representative Concentration Pathways (RCPs) and consist of a very low forcing level scenario (RCP2.6), medium scenarios (RCP4.5/RCP6) high emission scenarios (RCP8.5). RCP2.6, RCP4.5, RCP6, RCP8.5 associates to radiative forcing is 2100 equal to 2.6 W/m<sup>2</sup>, 4.5 W/m<sup>2</sup>, 6W/m<sup>2</sup>, and 8.5 W/m<sup>2</sup>, respectively. Unlike SRES, RCPs start with radiative, forcing pathways not with detailed socioeconomic narratives or scenarios (van Vuuren et al., 2011). The radiative forcing is determined by changes in greenhouse gas concentration, measured by a change in the amount of solar energy received per second per square meter of land (W/m<sup>2</sup>).

## **2.4. Hydrological Models**

Hydrologic models are simplified conceptual representations of reality. Hydrological models are a valuable tool for water resource planning and management. The application of hydrological models has become essential to study the response of hydrological systems to various natural and anthropogenic activities. Hydrological models have a wide variety of applications in rainfall-runoff estimation and understanding the different water balance processes. Nowadays, hydrological models are considered an important tool to study the potential impact of climate and land use change.

There are different hydrological models, depending on the amount of information/data provided for the modelling, the modelling approach, the model structure, and the mathematical equation used. Hydrological models can be classified as empirical, conceptual, and physical-based models based on the modelling approach. According to Rientjes (2015), the empirical model approach is observational and experiment oriented. This modelling approach takes information only from the existing data. They do not consider the physical features and processes of a hydrological system. At the same time, the physical-based modelling approach involves understanding the principle of physical process and uses the mathematical representation to express real phenomena in a catchment. They use measurable variables (state variables) and use the principle of conservation of mass, momentum, and energy to model the processes of a hydrological system. In the conceptual model approach relatively, simple mathematical relations are applied to simulate the real-world system. Conceptual modelling approach uses semi-empirical equations, and model parameters are evaluated through calibration. Contrary to the physical model approach, the conceptual modelling approach requires a large number of meteorological and hydrological data for calibration. According to Rientjes (2015), the conceptual modelling approach is mostly used in rainfall-runoff and hydraulic modelling.

For this study, the HBV rainfall-runoff model was used to simulate the rainfall-runoff relations in the Tana sub-basin. The selection of the model was based on its proven performance to study the climate change impacts. Krysanova et al. (1999) listed some advantages of using the HBV rainfall-runoff model: 1) It can cover the most significant runoff generating process by robust and simple structure, (2), HBV accounts for different topographic settings by defining elevation zones within the sub-basins or basins, (3) The performance of the model has been tested in different conditions in over 40 countries. HBV has been widely used in climate impact assessment studies in Lake Tana sub-basin. Some of the studies were performed in the sub-basin are (Wale, 2008; Perera, 2009; Nigatu et al., 2016).

## **2.5. Water Evaluation and Planning Model (WEAP)**

Studying the sustainability of lakes and different water resources under climate change and land use interventions requires an integrated water resource tool that can model the complete water system. The Water Evaluation and Planning (WEAP) model is an integrated system that incorporates water demand, hydrology, water quality, water

supply, and groundwater. The model operates on the basic principle of water balance. WEAP allows users to develop water use and allocation scenarios that serve to assess the impact of different developments. The development of scenarios in the WEAP model is based on “what if?” questions. The scenarios can answer a broad range of questions such as, what if future climate patterns change? What if the future population grows? The WEAP scenarios are based on an assumption of how the future water resource will likely be affected due to changes in climate patterns, population growth, and land-use change. Droogers and Aerts (2005) indicated that WEAP scenarios could model aspects that cannot directly be influenced, such as population growth and climate change

The model has been applied in different lakes and basins of the world and showed a good performance in addressing climate change and water demand assessments. Hagan (2007) used the model in Ghana to assess small reservoirs in the upper volta basin. The model has also been used in different basins of Ethiopia. The study by Arsiso et al. (2017) is one of the studies performed in Ethiopia. The study used the WEAP model to evaluate water demand and supply in Addis Ababa, Ethiopia, under the impact of Climate Change and urbanization for 2039. The study used the WEAP model to evaluate the change in the storage volume and water level of Legedadi/Dire and Gefersa reservoirs due to climate change and urbanization. Gedefaw et al. (2019) applied the WEAP model to evaluate the impact of climate change and irrigation expansion on the Awash River Basin's water resource. The study assessed Awash River Basin's water demand, supply, and shortage under three different future period horizons. The model has also been applied in the Upper Blue Nile basin by (McCartney et al., 2010). Those studies only considered the effect of planned water resource development on the basin's hydrology without considering climate change's impact on the basin. Specific to the Tana sub-basin, Alemayehu et al. (2010) used the WEAP model to evaluate the effect of planned irrigation and water supply developments on lake Tana water level. Reported findings of the conducted studies on the UBN basin and Lake Tana sub-basin did not take into account Lake Tana inflow from the ungauged catchments. A study by Zeleke (2015) used the WEAP model to evaluate the variability and change in water resource availability for water resource development projects in the Lake Tana sub-basin. The study used RCA4 RCM data under the RCP4.5 emission scenario and incorporated water abstraction demands of Hydropower, irrigation, and water supply projects. The study has not performed a detailed irrigation demand assessment since water requirements of the irrigation schemes were obtained from feasibility studies. The study computed the water level change of Lake Tana on a monthly basis.

## **2.6. Related Studies**

### **2.6.1. Climate Change in Ethiopia and UBN Basin using RCPs**

Different climate change impact studies have been performed in Ethiopia using the RCP scenarios. A recent study conducted by Bekele et al. (2019) at Keleta watershed in the Awash River basin used statistically downscaled GCM data and RCP 4.5 and RCP 8.5 representative concentration pathways. The study showed that minimum and maximum temperature and average precipitation would increase for the mid and the end of the century for both emission scenarios, subsequently increasing the runoff by 70%. Another study performed by Arsiso et al. (2017) in Addis Ababa, the capital city of Ethiopia, used statistically downscaled climate model data under RCP 4.5 (mid-range) and RCP 8.5 (high) emission scenarios. According to the study, the water level of the city's two main water supply reservoirs, named Legedadi/Dire and Gefersa, will likely reduce for the future projection years between 2023 and 2039.

There are some studies in the UBN basin that used the latest emission scenarios (RCPs). A study in the Gilgal Abay watershed by Ayele et al. (2016) used seven GCMs with high and medium-low Representative Concentration Pathways (RCP 4.5 and RCP 8.5) for 2021-2040 and 2081-2100. Thus, although the magnitude of the change is

different between the models and the emission scenarios, all models predicted an increase and decrease of runoff in the wet and dry seasons, respectively. This is mainly due to the increase in precipitation for the wet season and the reduction in the dry season. It is reported that evapotranspiration will likely decrease in the dry season and increase in the wet season for all models and both RCPs. The decrease of evapotranspiration in the dry season is highly influenced by decreased precipitation rather than temperature, which showed an increasing pattern for both seasons. The study further indicated that the increase in precipitation and runoff would increase the inflow to the lake, and it would also increase the probability of flash floods. Likewise, Woldesenbet et al. (2018) assessed the response of a catchment to climate and land use change in the upper Blue Nile sub-basins, using representative concentration pathways (RCP 6.0) for the period 2016-2030. The study stated that the future climate would be warmer and wetter. It also revealed an increase of future precipitation in the main rainy season and on an annual scale compared to the baseline period. Furthermore, the change in the magnitude of the water balance components (evapotranspiration, surface runoff, and baseflow) is more significant under the combined effect of LULC and climate change. It also indicates that the integrated impact of land use change and climate change is higher on the streamflow response at the outlet of the Tana watershed.

### **2.6.2. Climate Change Studies in UBN Basin using RCMs**

Findings in the Upper Blue Nile region indicated uncertainties of the GCMs in future climate projections. For instance, Taye et al. (2011) found an unclear pattern of future mean volume and high/low flow in the lake catchment under A1B and B1 emission scenarios using the 17 General Circulation Model (GCM). Setegn et al. (2011) also indicated that the GCMs' rainfall projections are not consistent with the temperature projections, which show a uniformly increasing trend. However, only a few studies have been performed using regional circulation climate models (RCMs). An example of a study performed using RCM is the study conducted by (M. P. McCartney & Menker Girma, 2012). The study focuses on the impact of planned water resource development and climate change on the Blue Nile River of the Ethiopian portion, using a regional climate model (COSMO-CLM version 4) and A1B emission scenario. The study indicated that the basin hydrology will be affected by climate change. Besides, it also stated that the annual flow from lake Tana will reduce by approximately 74% without considering the effect of water resource development in the basin. Another example of a study using the regional circulation models is the study performed by Haile et al. (2017) on the upper Blue Nile basin. Six dynamically downscaled global circulation models (GCMs) were used to simulate future climate impact on the basin under the RCP 4.5. Consequently, depending on the season, the annual evapotranspiration will increase, also the annual rainfall will increase by -2.8 to 2.7% for the future period between 2041 to 2070. The study stated that an increase in soil moisture deficit and a stream flow reduction might be expected for future simulated periods.

Although RCMs have a finer resolution and are better than the GCMs with their smaller scale, uncertainties have been noticed in a simulation of future rainfall and temperature projection. Haile & Rientjes (2015) evaluated eight dynamically downscaled regional climate models (RCMs) rainfall simulations in the upper Blue Nile basin. As a result, the models have shown shortcomings in estimating light daily rainfall and heavy daily rainfall amount. Also, almost all eight models underestimate the rainfall in the dry season and the mean annual rainfall. An ensemble mean of multiple regional climate models was recommended as such can capture different aspects of rainfall than the individual models and better monthly rainfall distribution. A similar study was conducted in the Jemma sub-basin of the Upper Blue Nile Basin (Worku et al., 2018). In this study, the performance of ten dynamically downscaled RCMs in modelling rainfall climatology was evaluated. The ensemble means of the ten RCMs simulation performed better in simulating the seasonal rainfall pattern and showed a better correlation with the observed annual and rainy season (June, July, August, September) rainfall than the single RCM models.

### **2.6.3. LULC Change Studies in UBN Basin**

Some studies typically addressed the impact of land use change in the UBN basin. Rientjes et al. (2011) focused on evaluating the change in the landcover of the upper Gilgel Abay & the hydrological effect of the change. According to the study, the land that has been covered by forest has reduced from 50.9% (in 1973) to 16.7% (in 2001). And monthly rainfall shown a decreasing pattern followed by a declined annual flow of the catchment.

There are some studies that targeted the integrated impact of climate change and land use change on the basin's hydrology. Woldesenbet et al. (2018) assessed the integrated effect of climate and land use land cover change in the Upper Blue Nile sub-basins using the soil and water assessment tool (SWAT). The research analysed the streamflow response to future (2016-2030) land use change and climate variation scenarios. Consequently, streamflow at the Tana watershed outlet would be increased under the effect of climate & LULC. However, the LULC scenario performed in the research does not consider the impact of water resource developments in the basin.

### **2.6.4. Summary of Literature on Climate Change**

Based on previous studies, the overall conclusion is that the lake Tana sub-basin will experience a significant climate variation for the mid and late 21st century. These will have a potential impact on the hydrology of the basin and the lake's water balance. The minimum and maximum temperature will be projected to increase for both the wet and dry seasons. In addition, a shift in the rainy season will likely be expected. Also, an intense and long rainy season will be anticipated for the future periods, which could probably extend to November. The dry season will experience much lower precipitation. Though the pattern is inconsistent, annual rainfall will likely increase for the future period. This increase in maximum and minimum temperature will significantly increase the evaporation of the lake. Consequently, affecting the lake's sustainability and the sustainable supply of water to the water resource developments, such as the irrigation schemes in the basin.

Studies on the impact of LULC indicate that change in LULC affects the hydrology of Lake Tana's sub-basin. And, the effect is higher under the combined effect of climate and LULC change. This study focused on assessing the separate and combined effect of climate and land use interventions on the sustainability of Lake Tana. Ensembles mean of multiple RCMs with emission scenarios of RCP4.5 and RCP8.5 was used. A baseline period between 1991- 2005 and a medium-term future projection period between 2041 and 2070 is used for the assessment. WEAP model was used to study the sustainability of Lake Tana under climate change and land use interventions (water resource development interventions) on a monthly and annual basis. The lake water inflow from each catchment was estimated using HBV rainfall-runoff modelling, and the AquaCrop model is used to compute the water demand by the planned irrigation schemes.

### 3. STUDY AREA AND DATA PREPARATION

#### 3.1. Study Area

Lake Tana is located in the Lake Tana sub-basin of the Upper Blue Nile basin. Lake Tana sub-basin is the second-largest sub-basin of the Blue Nile basin, covering 15,000 km<sup>2</sup>. Lake Tana is one of the primary sources of the Blue Nile River and a major freshwater resource provider in Ethiopia (50%) (Stave et al., n.d.). It is the third largest lake in the Upper Blue Nile Basin and the largest lake in Ethiopia, with a surface area of 3060 km<sup>2</sup>. The lake is located in the northwest highlands between 36.89 °E to 38.25 °E longitude and 10.95 °N to 12.78 °N latitude. Tana has an approximate width of 66 km, 64 km length, and maximum and a minimum depth of 7.2 m and 14 m, respectively (Wale, 2008). The average altitude of the Lake is approximately 1786 m.a.s.l. A minimum lake level of 1784.75 m.a.s.l. was set by Ethiopian Electric Power Corporation (EEPCO) to allow for a minimum draught needed for navigation in Lake Tana (SMEC, 2008).

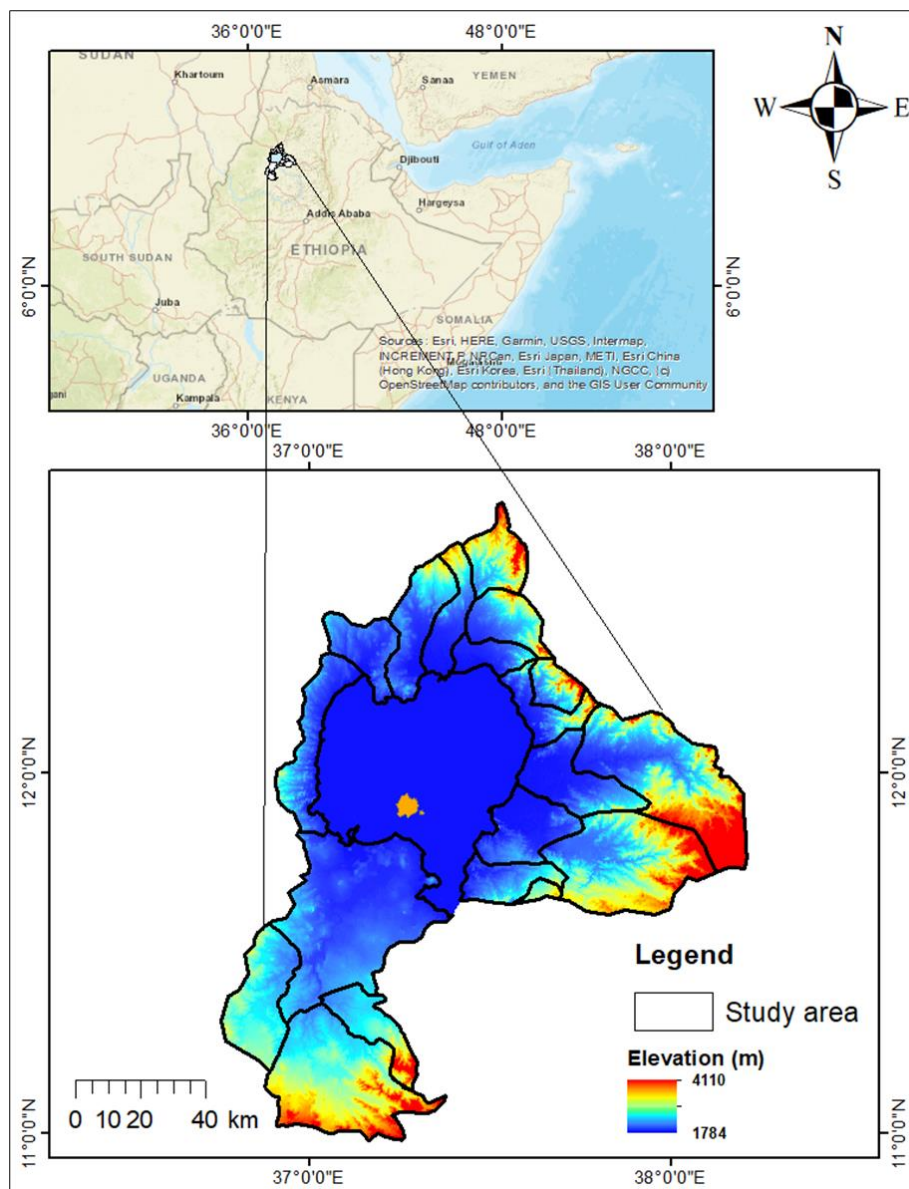


Figure 3-1: Location of the study area

### 3.1.1. Climate

The Lake Tana area is characterized by its mild climate as a result of its elevation (Wale, 2008). The climate of the sub-basin is mainly dominated by tropical monsoon and is mainly divided into two seasons: the dry season (between October and April) and the wet season (between June to September). The water resource of the Lake Tana sub-basin and the whole of the Blue Nile river is mainly influenced by rainfall (Kebede et al. 2006). The rainfall pattern of the area is spatially highly variable; its variability is mainly influenced by the terrain orientation in the area (Gebremichael et al., 2007).

The Lake Tana region has an annual average temperature of 20.2 °C at Bahir Dar station and 20.6 °C (Wale, 2008). The sub basin's temperature drops by 5.8 °C for every 1000m increase of elevation (Conway, 2000). The elevation of the area ranges from 1784 to 4109 m. This variation has a high impact on the climate of the region.

### 3.1.2. Soil and Landcover

Most soils in the Tana sub-basin are derived from weathered basalt. In low-lying areas of the sub-basin, specific to east and north of Lake Tana and the part of Gilgel Abay's soil has developed on alluvial sediments. As per the FAO soil group classification, which was previously collected from the EMWR GIS department and obtained from the ITC archive for the purpose of this study, the dominant soil in the Lake Tana sub-basin is Leptosols, Luvisols, Nitisols, and Vertisols. According to FAO soil groups (WRB, 2007) description, the soil types are explained as follows.

The Leptosols are characterized by their gravelly, stony and shallow nature. Those types of soils are common in mountainous areas. Luvisols are soils with a higher accumulation of clay in the subsoil than the topsoil due to pedogenetic processes. This soil has moderate to high water and nutrient storage capacity. The other dominant soil type in Tana sub-basin is Nitisols. These soils are well-drained, deep, and red tropical soils. It is known for its substantial accumulation of clay. Thirty percent or more of Nitisols is occupied by clay and blocky structure. Because of their deep structure and high nutrient content, Nitisols are the most fertile soil among the tropical soils. Vertisols are the other dominant soil type in the Tana sub-basin. Those soil types are distinguished by their heavy clay content with a high portion of expansive clay minerals. The soils expand and shrink with a variation of moisture content. During the dry period, the soils shrink, and they create deep cracks. While it will expand during the wet season. The percentage of the soil types covering each catchment in the Lake Tana sub-basin, can be found in Appendix B.

Landcover classification previously collected from EMWR and later updated by Landsat ETM+, was obtained from the ITC archive for this study. Thus, as per the classification data, the land cover of the Tana sub-basin is mainly classified as forest, grassland, cropland, bare land, urban and built-up area, woody savannah, and water body.

### 3.1.3. Hydrology of the Study Area

Lake Tana is surrounded by floodplain wetlands in most directions and is fed by 40 rivers. Among the rivers feeding the Lake, four major tributary rivers contribute more than 93% of the inflow to the lake (Setegn, 2010). This river is Gilgel Abay, Ribb, Megech, Gumara. The representative area of the gauged and ungauged catchments is presented in Table 3-1 as delineated by Perera (2009). According to the study, the mean annual inflow to the lake from the gauged and ungauged catchments for the year between 1994-2003 is 1781 mm.

Table 3-1: Major gauged and ungauged catchment in the Lake Tana sub-basin (Perera, 2009)

Gauged catchments	Area(km <sup>2</sup> )	Ungauged catchment	Area(km <sup>2</sup> )
Ribb	1408	Ungauged Ribb	736
Gilgel Abay	1657	Ungauged Gilgel Abay	2072
Gumara	1281	Ungauged Gumara	287
Megech	531	Ungauged Megech	437
Koga	298	Ungauged Gumero	424
Gumero	163	Ungauged Garo	365
Garo	98	Ungauged Gelda	364
Gelda	26	Ungauged Dema	325
Kelti	608	Tana West	546
		Ungauged Gabi Kura	427

The lake has only one outlet, which flows to the Blue Nile River. Until 1996, the flow to the Blue Nile was natural. In 1996, the river's flow started to be regulated by two radial gates, following the construction of Chara Chara Weir to regulate Tiss Abay I hydropower generation. In 2001, the outflow to the Blue Nile River was further regulated by additional five gates to improve the flow to the Tiss Abay II hydropower plant. After the Chara Chara Weir operation, the lake's water level started to drop, reaching a minimum level of 1784.46 m.a.s.l. on the 6th of June 2003.

#### 3.1.4. Irrigation Developments in Tana Sub-basin

The government of Ethiopia identified potential irrigatable areas (842,870 ha) in Upper Blue Nile Basin. For the Tana and Beles sub-basins, a potential irrigatable area of 159,580 ha is identified. Under the Tana growth corridor, there are ongoing and planned water resource projects along the rivers that flow to Lake Tana. The ongoing and planned water resources projects include six dams to provide water to the irrigation schemes. These are: Koga, Jema, Ribb, Gilgel Abay, Gumara and Megech. Koga is a completed project while Rib and Megech dams are under construction, whereas other dams undergo a feasibility study. Besides that, most of the irrigation schemes are supported by the dams; there are also a considerable number of irrigation projects supported by direct pumping from the Lake (Halcrow, 2010). Figure 3-2 shows the location of the planned irrigation schemes and dams in the Lake Tana sub-basin.

Table 3-2: Planned irrigation schemes in Lake Tana sub-basin

Project	Irrigable Area(ha)	Abstraction source	Status
Koga	7000	Koga Dam	Completed
Jema	7559	Jema Dam	Detail feasibility and design document
Gilgel Abay	11250	Gilgel Abay Dam	Detail design document
Rib	14460	Rib Dam	Completed
Gumara	14800	Gumara Dam	Detail design document
Megech	14621	Megech Dam	Under Construction
Northeast Tana	3903	Lake Tana (Pump Irrigation)	Detail feasibility
Northwest Tana	6719	Lake Tana (Pump Irrigation)	Detail feasibility
Southwest Tana	5132	Lake Tana (Pump Irrigation)	Detail feasibility
Megech Robit	6024	Lake Tana (Pump Irrigation)	Detail feasibility and design
Megech Serbera	4040	Lake Tana (Pump Irrigation)	Completed

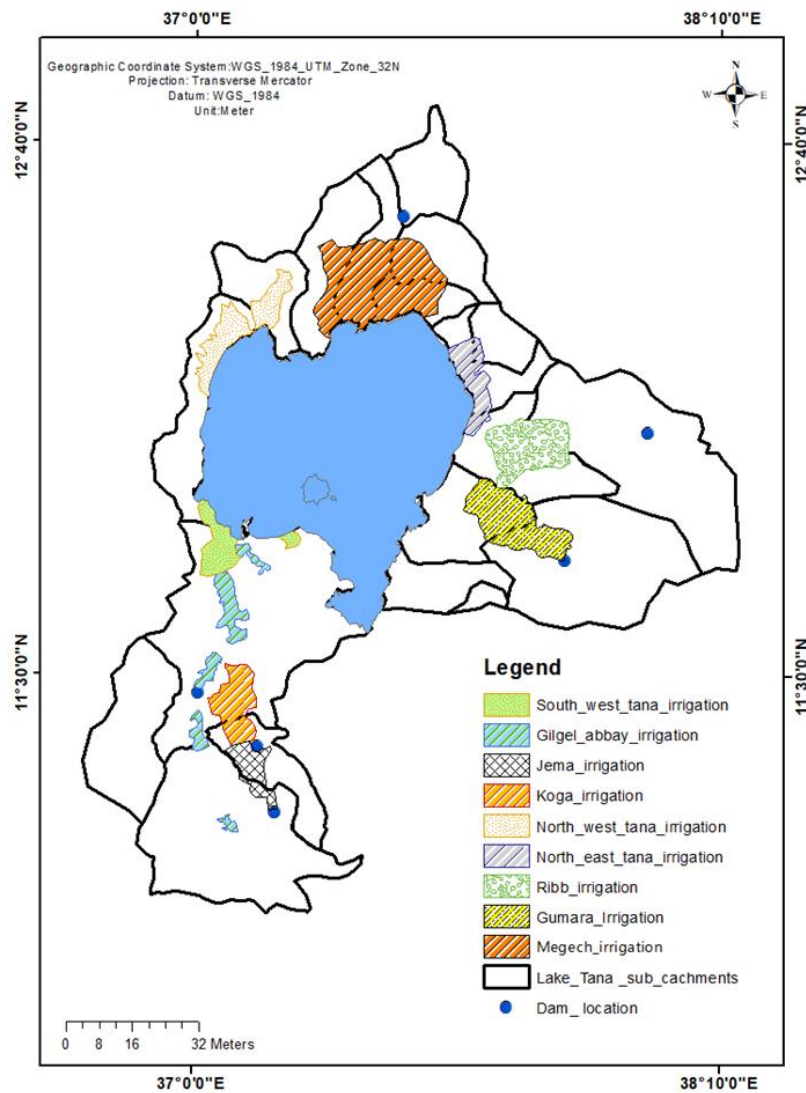


Figure 3-2: Planned and completed irrigation schemes in Lake Tana sub-basin after (Halcrow, 2010)

## 3.2. Data Processing for Baseline Period and Future Climate Change Projections

### 3.2.1. Observed Data

Daily meteorological data of 13 stations inside and close to Lake Tana Sub-basin, covering the period 1991-2005, were collected from the National Meteorological Agency (NMA) of Ethiopia. Precipitation is measured in all thirteen stations. However, other meteorological data of minimum temperature, maximum temperature, relative humidity, wind speed, sunshine hour are measured in few stations. Thus, 13 precipitation stations and 6 evaporation stations were selected based on their spatial distribution in the sub-catchments and data availability. The following figure shows the spatial distribution of the meteorological stations selected for this study.

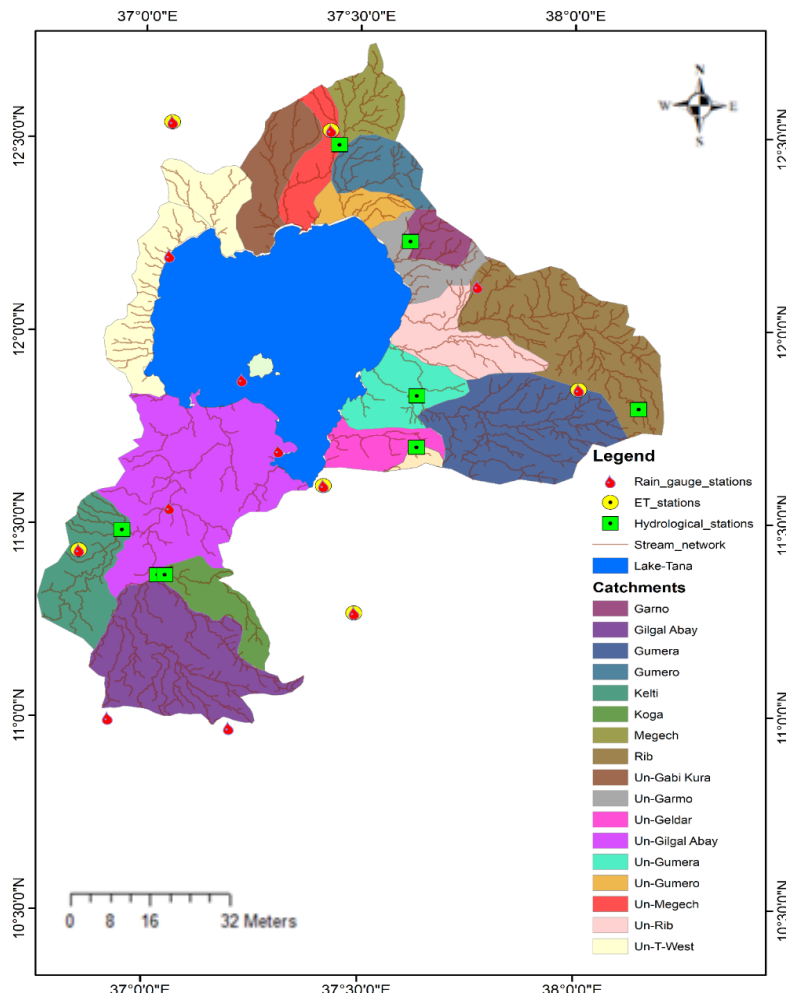


Figure 3-3: Spatial distribution of meteorological stations and hydrological stations and basins

#### 3.2.1.1. Precipitation

The precipitation dataset had many missing records for several stations. Screening of the meteorological data showed that there are a lot of missing data. The percentage of the missing precipitation data for the 13 stations is as shown in Table 3-3. Enfranz, Sekela, and Addis Zemen stations have a higher number of missing precipitation data. Whereas Adet and Zege have a smaller number of missing data.

Table 3-3: Summary of and missing precipitation data (1991-2005)

Station	Longitude	Latitude	Altitude	Period	Missing data (%)
Adet	37.47	11.3	2080	1991-2005	1.72
Addis Zemen	37.87	12.1	2117	1991-2005	18.9
Aykel	37.05	12.5	2160	1991-2005	9.95
Bahir Dar	37.42	11.6	1828	1991-2005	9.02
Dangila	36.85	11.3	2126	1991-2005	8.63
Delgi	37.03	12.2	1865	1991-2005	6.66
Gondar	37.42	12.6	2074	1991-2005	5.03
Deki Istifanos	37.27	11.9	1799	1991-2005	3.89
Debre Tabor	38.01	11.9	2714	1991-2005	6.95
Enfranz	37.68	12.2	1889	1991-2005	20
Enjibara	36.9	11	2760	1991-2005	6.73
Sekela	37.22	11	2584	1991-2005	21.7
Zege	37.32	11.7	1786	1991-2005	1.7

Missing precipitation data gaps were filled using a method of the arithmetic mean. The missing record of the target stations (stations with missing records) is estimated by the arithmetic mean of the nearby stations. Two and three nearby stations are considered for the computation of the missing record of the target station. The method assumes an equal weight of the neighbouring stations to calculate the missing precipitation value. Missing precipitation  $P_x$  is calculated as:

$$P_x = \frac{1}{m} \sum_{i=1}^m P_i \quad [3-1]$$

Where  $P_x$  is the missing gauge precipitation,  $m$  indicates the number of neighbouring stations;  $P_i$  is recorded precipitation at the  $i^{\text{th}}$  station.

The consistency of precipitation data has been evaluated for each station after the gap-filling of the precipitation data was performed. The consistency of the precipitation data was performed using the double mass curve method, which uses a plot of cumulated values of a given station against accumulated values of the average value of five stations over the same period. Inconsistency of precipitation records can be identified if there are gaps and deviations from the straight lines of the plot.

The result of consistency analysis for all stations shows a straight line and regression coefficient ( $R^2 > 0.99$ ), which indicates the consistency of the precipitation data. The following figures show the double mass curve analysis for Delgi, Dangila, Gondar, and Deke-Istifanos stations.

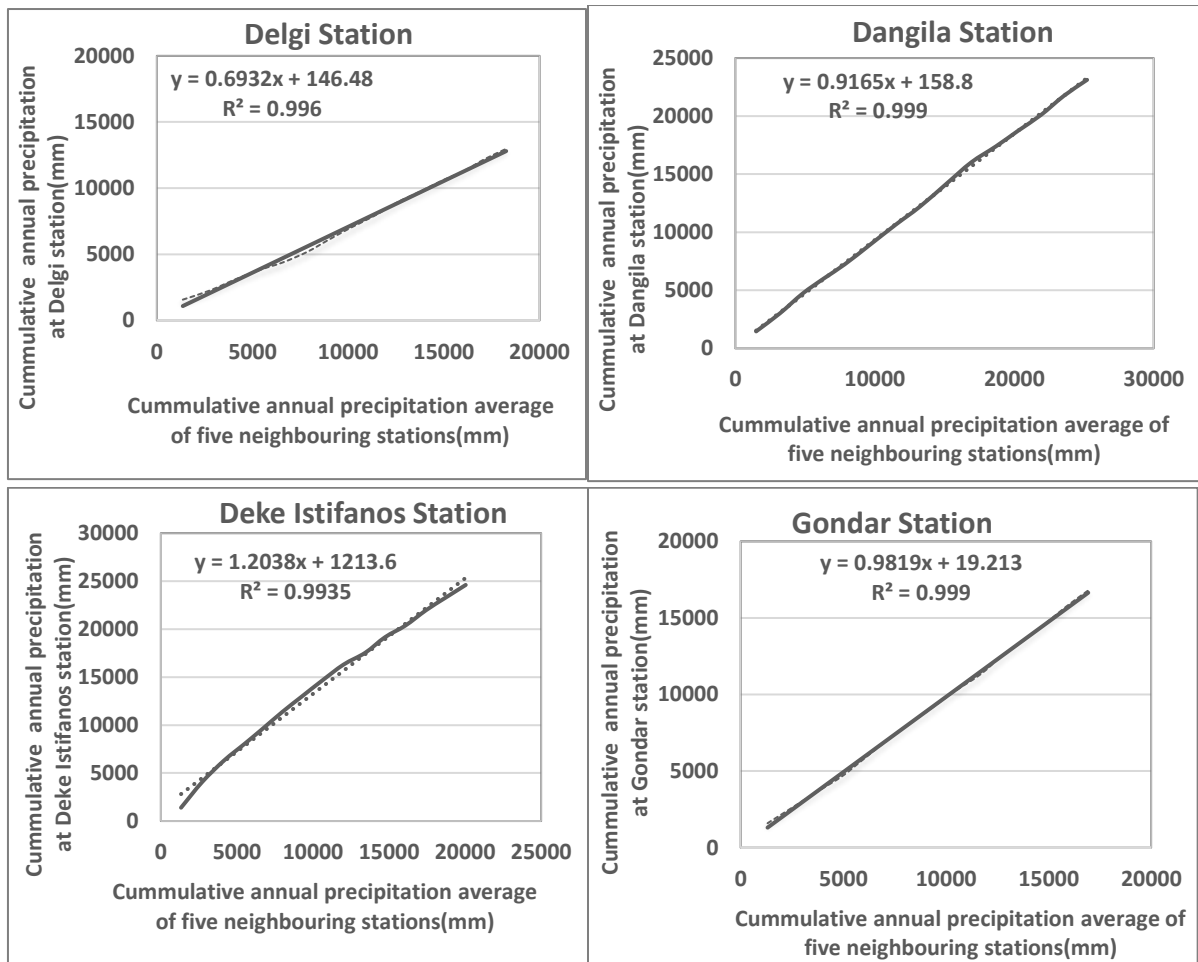


Figure 3-4: Double mass curve analysis for Delgi, Dangila, Deke Istifanos and Gondar stations

To understand the spatial variability of precipitation in the sub-basin, a long-term annual average precipitation (mm/year) was calculated and analysed for all stations from 1991-2005 (see Figure 3-5). According to the analysis, the southern part of the sub-basin receives the highest precipitation of 2278 mm at Enjibara station. And low precipitation amount has been noticed in the northern and some parts of the northwest of the sub-basin. The lowest precipitation amount throughout 1991-2005 is 865mm at Delgi station.

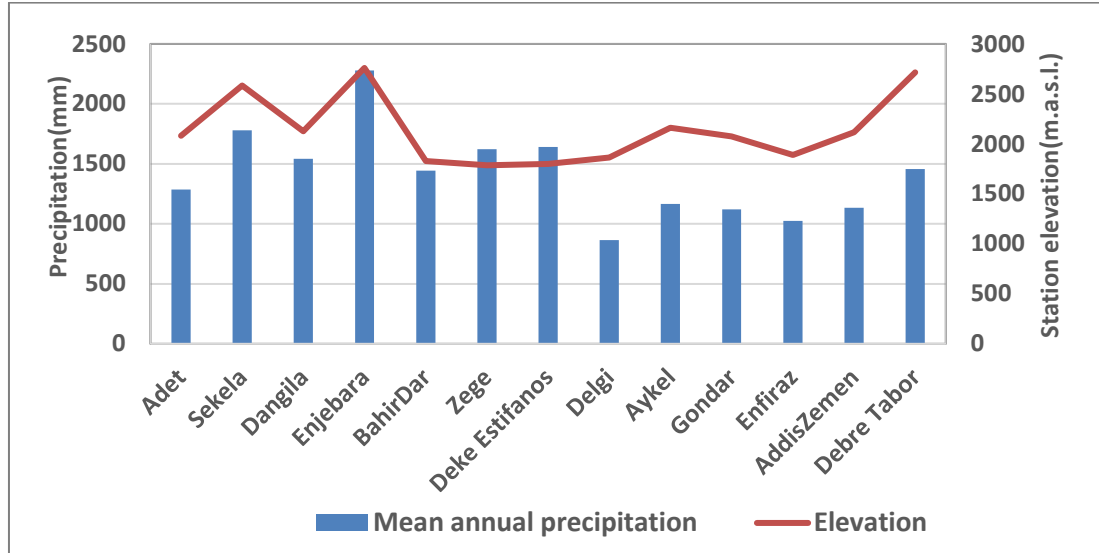


Figure 3-5: Long-term annual average precipitation in each meteorological station with its elevation

The long-term annual mean precipitation and elevation relationship has been analysed by establishing a linear relationship based on the 13 meteorological stations in the sub-basin. As shown in Figure 3-6, only 30% of precipitation variation can be explained by the linear relationship between precipitation and elevation. The 70% of precipitation variation does not show a distinct relationship between elevation and precipitation.

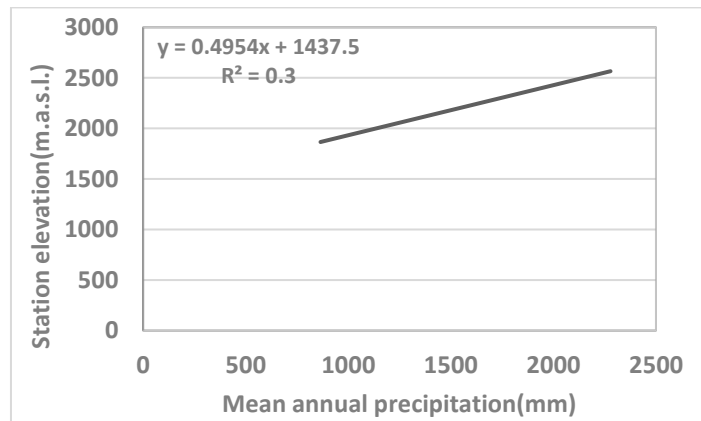


Figure 3-6: Precipitation-elevation relation in Lake Tana sub-basin

Analysis of the long-term monthly mean of the fifteen year precipitation shows that the sub-basin receives a high amount of precipitation in the rainy period (June to August) and low precipitation between October and May (see Figure 3-7).

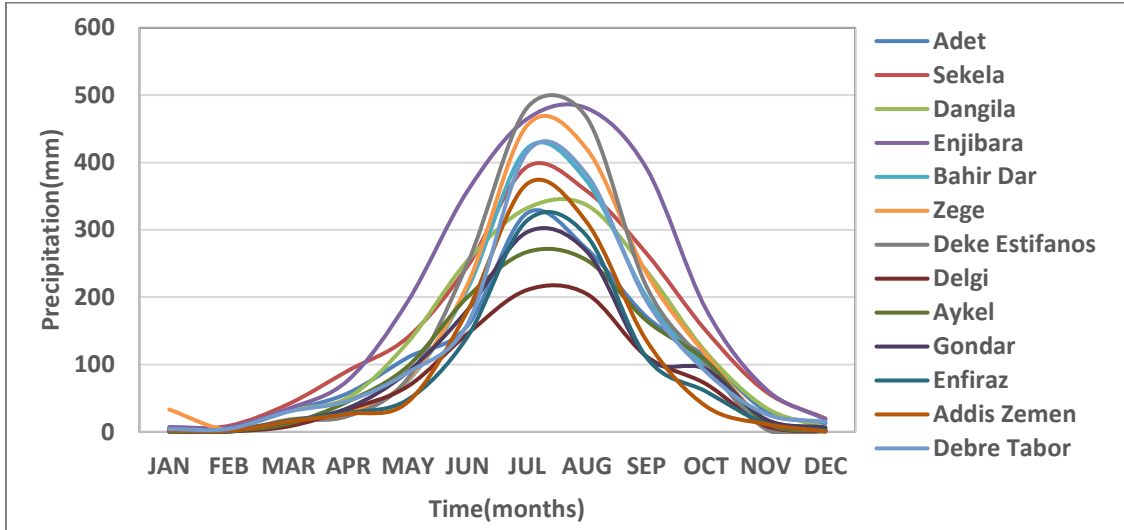


Figure 3-7: Distribution of mean monthly precipitation for respective stations (1991-2005).

**3.2.1.2. Evaporation Data**

Based on data availability of the stations, daily minimum temperature, maximum temperature, relative humidity, and sunshine hour data of 6 meteorological stations of the period from 1991 to 2005 were selected for the computation of the catchment potential evapotranspiration and lake evaporation. The evaporation dataset had many missing records in all selected meteorological stations. Therefore, a linear regression gap-filling technique was used to fill the missing records. Linear regression has been established between the target station (station with missing records) and the average of three nearby stations. Average of a different combination of the closer neighbouring station was used to choose the best correlated neighbouring stations to the target station. The average of a nearby station with a higher  $R^2$  was selected to fill the missing records of the target station. According to the linear regression method, the missing data is given as:

$$Px = m_0 + m_1\bar{p} \tag{3-2}$$

Where  $Px$  is the missing gauge reading,  $m_0$  and  $m_1$  are regression constant and,  $\bar{p}$  is the average gauge reading of neighbouring stations. The following scatter plots show the relation of the maximum temperature of Gondar and Debre Tabor station with the average of the neighbouring stations.

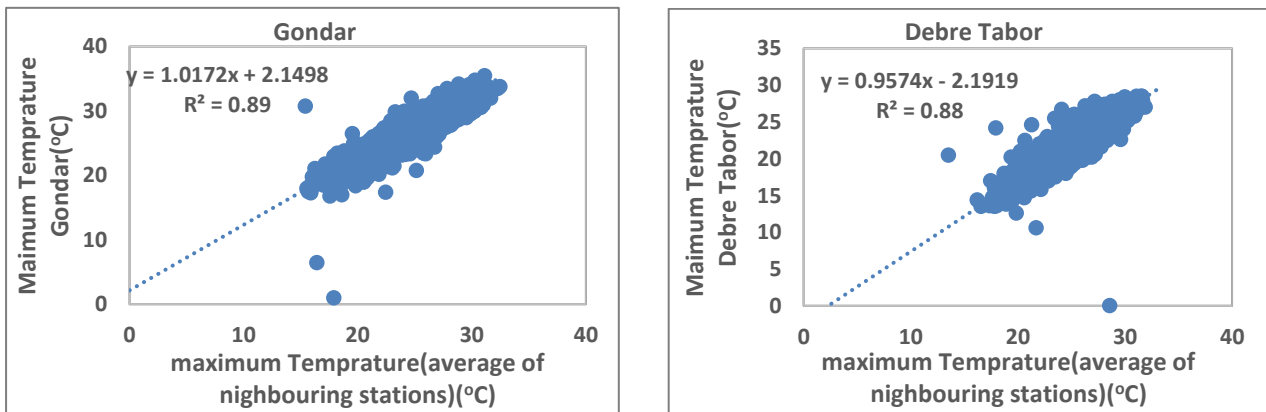


Figure 3-8: Relation between station temperature and average temperature

After the missing temperature record gap-filling, the long-term mean monthly temperature was analysed for the six stations from 1991-2005(see Figure 3-9 & Figure 3-10). Gondar and Bahir Dar stations have the highest mean temperature whereas, Debre Tabor has the lowest mean temperature. This shows the inverse relationship between mean temperature and elevation as station Gondar and Bahir Dar has low elevation, whereas Debre Tabor has a higher elevation than the other five stations.

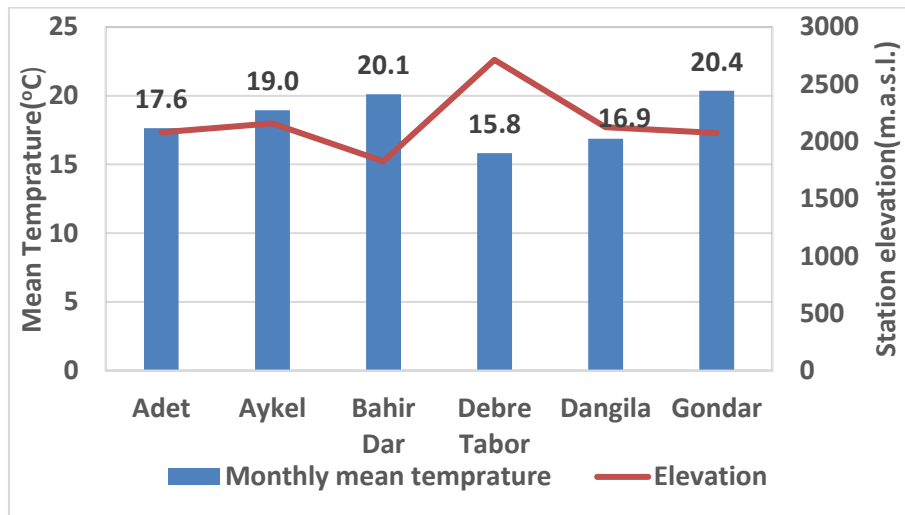


Figure 3-9: Mean monthly temperature with elevation

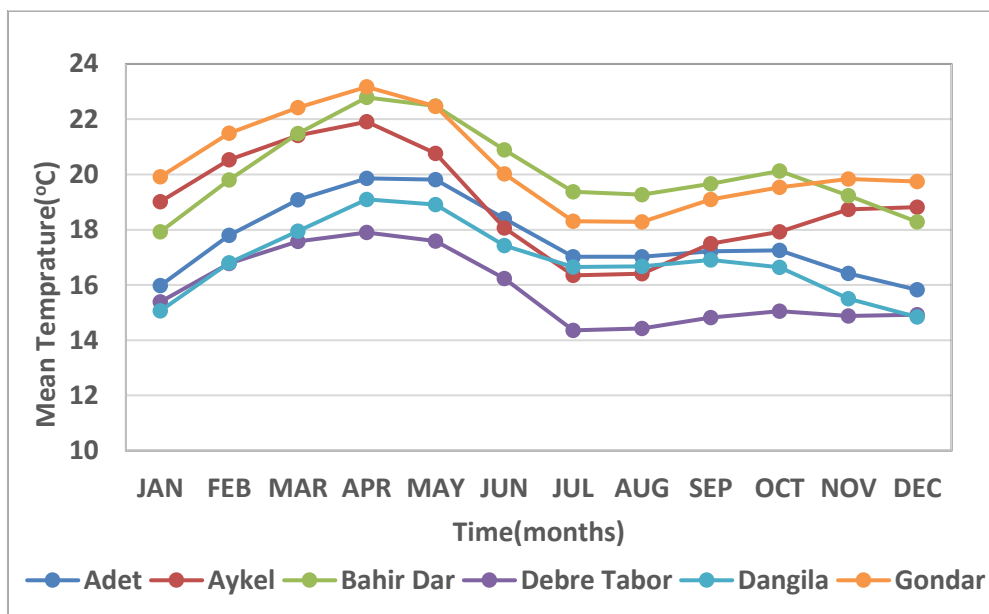


Figure 3-10: Mean monthly temperature of 6 meteorological stations over the period 1991-2005

The annual mean temperature and elevation relationship of 1991-2005 was analysed as shown in the following figures. The analysis results show a general increase in mean annual temperature with a decrease in elevation (see Figure 3-11).

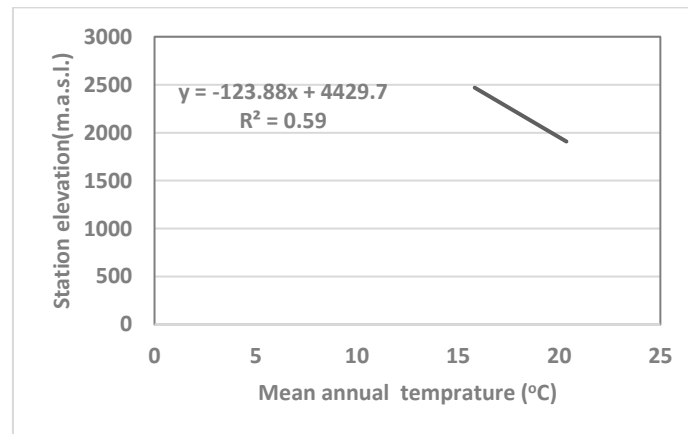


Figure 3-11: Mean annual temperature-elevation relation in Lake Tana sub-basin

### 3.2.2. Regional Circulation Climate Data

For Ethiopia and the Lake Tana basin area, simulated climate data is provided through the Coordinated Regional Climate Downscaling Experiment (CORDEX) program formed within the World Climate Research Programme with a vision of advancing and coordinating the regional climate downscaling application. On a global scale, simulation output of 13 domains is already available, of which the African 'domain' is one. The domain covers the whole of the African continent. For CORDEX, the simulation of RCM grid resolution was set to 0.44 degrees by 0.44 degrees and rotated pole system in which the model operates over an equatorial domain with a quasi-uniform resolution of approximately 50km. There are about 23 confirmed data centres for accessing CORDEX Africa, including many other proposed data from different institutes sponsored by WCRP. At the CORDEX website [Regional Climate Change simulations for CORDEX domains – Cordex](#), an overview is presented on available RCM model output for the African region.

#### 3.2.2.1. RCM Data Selection

The selection of RCM models of the high capability to represent a specific area's climate pattern is essential in reliable climate impact assessment studies. Therefore, selecting RCM models based on their past performance to represent an area's past and future climate is the most practiced approach in several climate impact studies. The selection of RCM models is essential, but obtaining the best performing driving GCMs is also crucial. This is because RCMs depend on the driving GCMs since the GCMs provide time-dependent meteorological conditions and initial and surface boundary conditions to the regional models.

For this study, various studies on climate change assessment in the East Africa area have been assessed in order to select the best performing driving GCMs and RCM models from the CORDEX program. Model outcomes that were proven to provide acceptable simulations results when compared to observed climate data were selected. Thus, NOAA-GFDL-GFDL-ESM2M, GFDL-ESM2M, and HadGEM2-ES are selected as driving GCM models since, according to Endris et al. (2016), those models successfully capture rainfall patterns over the East Africa region for the period between July and September. Also, three different RCMs (RCA4, REMO, and RACMO) are selected. These models were selected because of their performance in capturing climate over the East Africa region. Worku et al. (2018) indicated that the GCMs that were dynamically downscaled through the REMO model performed better in capturing the distribution of rainfall events and the rainfall climatology when evaluated over the Jemma sub-basin. Besides, RCA4 RCMs driven by MPI-ESM-LR and GFDL-ESM2M tend to perform

relatively better than RCMs driven by other CGCMs, when evaluated for the use and analysis of climate change projections over the East Africa region.

Baseline period RCM climate data from 1991-2005 and future RCM data from 2041-2070 have been used to assess climate change and land use intervention impacts on Lake Tana's water balance. The selection of the baseline period RCM data depends on the availability of observed climate data for bias correction. It also depends on the availability of RCM historic data for recent years. The CORDEX program provides historic RCM products from 1950 - 2005. Starting from 2005, RCM products with RCP emission scenarios are available. Minimum temperature, maximum temperature, precipitation, wind speed data is available for the indicated RCMs and driving GCMs. Sunshine hour and relative humidity data are not available for the selected RCMs models and emission scenarios. Figure 3-4 shows selected RCMs and driving GCMs for this study.

Table 3-4: Selected RCMs and driving GCMs for this study

RCM	Driving Model	Institute
RCA4	NOAA-GFDL-GFDL-ESM2M	SMHI (The Swedish Meteorological and Hydrological Institute)
REMO2009	MPI-ESM-LR	Max Planck Institute for Meteorology - Climate Services Centre, Germany
RACMO22T	MOHC-HadGEM2-ES	KNMI (Koninklijk Nederlands Meteorologisch Instituut, Netherlands)

The climate data from the CORDEX program comes in a NetCDF file format. Therefore, changing the file to Tiff file format and extracting the data into excel has been performed using a python script. The climate data for the sub-catchment area were estimated using ArcGIS software to overlay the sub-basins area on the grid cell. Then, each pixel in each catchment was weighted by its contribution to the total area. Figure 3-12 shows the 44 × 44 km grid of RCA4 RCM maximum temperature data on January 1st, 2041, and the location of the meteorological station.

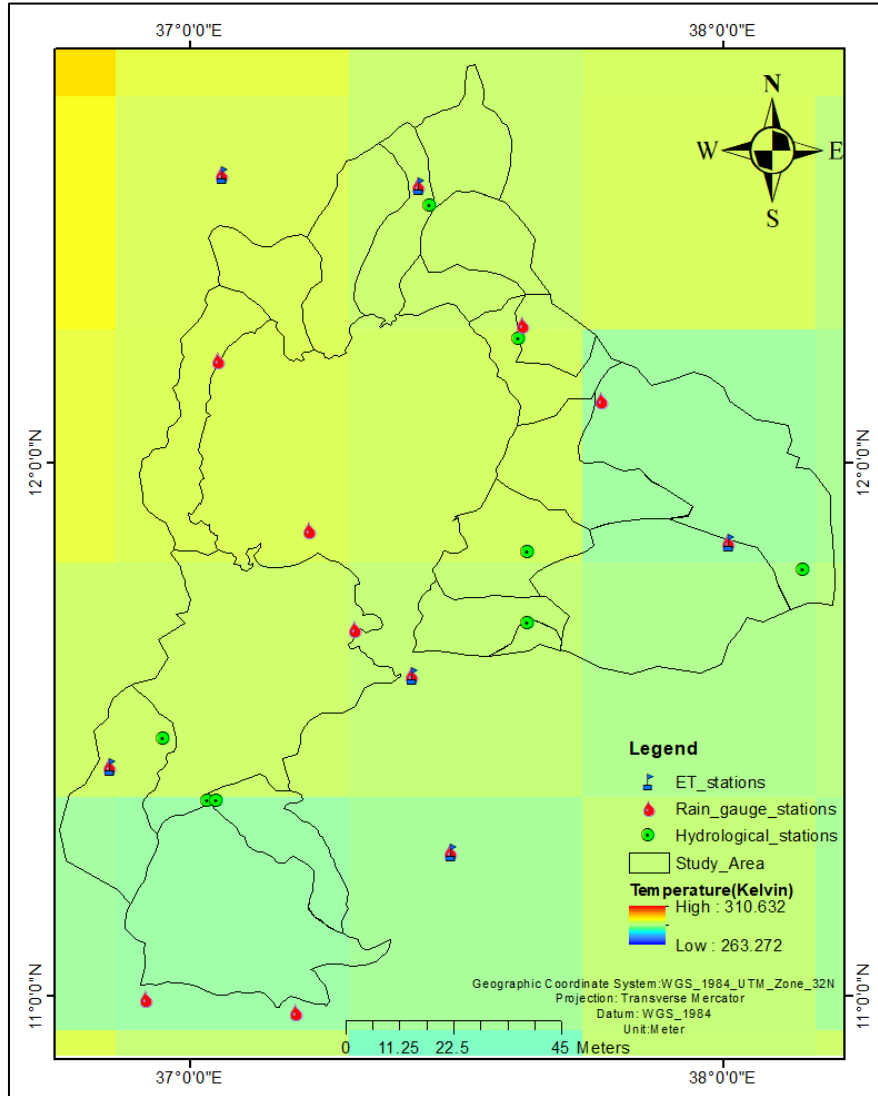


Figure 3-12: Lake Tans basin area overlain by a  $44 \times 44$  km grid showing RCA4 RCM maximum temperature on January 1<sup>st</sup>, 2041. Locations of the meteorological stations are also indicated.

### 3.2.3. Comparison of Observed and RCM Climate Data

Observed precipitation, mean temperature, and windspeed were computed using the inverse distance weighted (IDW) interpolation method. IDW interpolation method is the most widely used method in the Lake Tana sub-basin (Wale et al., 2008; Nigatu et al., 2016). The method uses a nearby meteorology station's weight in the catchment to calculate the target areal climate data. The basic inverse distance weighted interpolation equation reads:

$$\bar{z} = \frac{\sum_{i=1}^n \frac{1}{d_i^m} z_s}{\sum_{i=1}^n \frac{1}{d_i^m}} \quad [3-3]$$

Where,  $z_s$ , is a value of known point,  $d_i$  is the distance to a known point,  $\bar{z}$  is the unknown point,  $n$ , is the number of meteorological stations.

The weight of the stations used, for the computation of observed climate variables is presented in Appendix A.

### 3.2.3.1. Precipitation

Comparison of Observed and RCM data has been performed from 1991 - 2005 for the sub-catchments in the Tana sub-basin. RCM climate data was estimated at the catchment scale and was performed by calculating the area coverage of each pixel that overlay a catchment.

Monthly average RCM precipitation data between the years 1991-2005 was compared with the observed precipitation data. The RCM precipitation data for all the gauged and ungauged catchments was estimated by calculating the area of each pixel that overlays a sub-catchment. Then, a catchment-based comparison of RCM based precipitation records and observed precipitation was performed. The comparison in the major sub-catchments of the basin is shown in Figures 3-13.

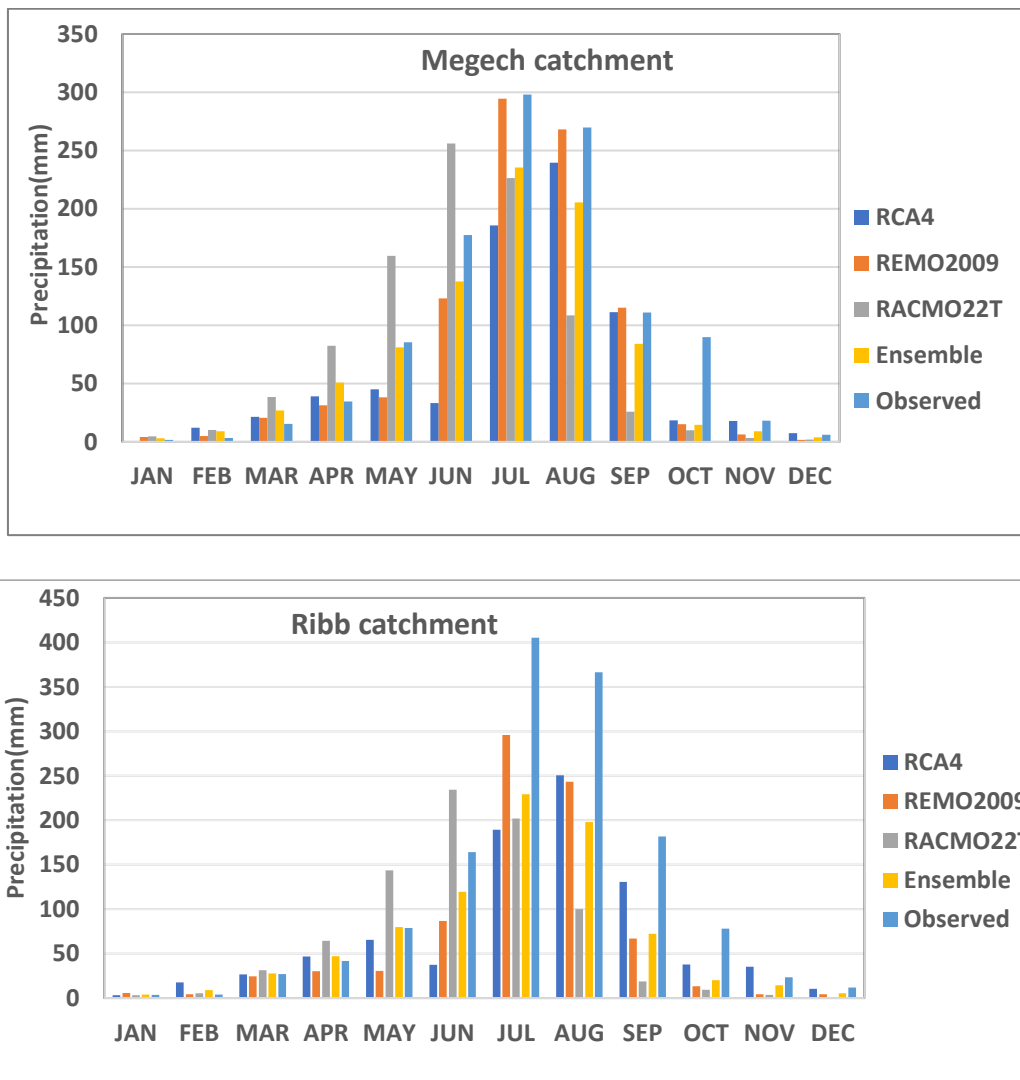


Figure 3-13: Long term monthly mean precipitation comparison of observed and RCM data in Megech, Ribb catchment

When visually inspecting, the above graphs show differences in the amount of precipitation of RCM and observed overall months. In addition, the difference in rainfall amount differs from season to season. For example, REMO2009 has a better match with the observed data during the rainy season. However, the dry season precipitation has been underestimated for most of the dry months. Generally, All RCMs overestimate the dry season precipitation and underestimated the wet season precipitation.

### 3.2.3.2. Mean Temperature

Catchment based comparison of the monthly mean temperature of the observed and RCM data for 1991-2005 was made. Figure 3-14 shows the monthly mean temperature comparison of observed and RCM data in Megech and Ribb catchment. As seen in the figures, there are variations in the monthly mean temperature of the RCMs and the observed data for Megech and Ribb catchments. For Megech catchment, RCMs underestimated the monthly mean temperature. And, for most months, RCMs underestimated the mean temperature in Ribb catchment. This is associated with the location of the catchments in the sub-basin. Megech catchment is located near to Gondar station, which has the highest mean temperature of the 6 meteorological stations (see Figure 3-9). Ribb catchment is located near Debre Tabor station, the station that receives the lowest mean temperature.

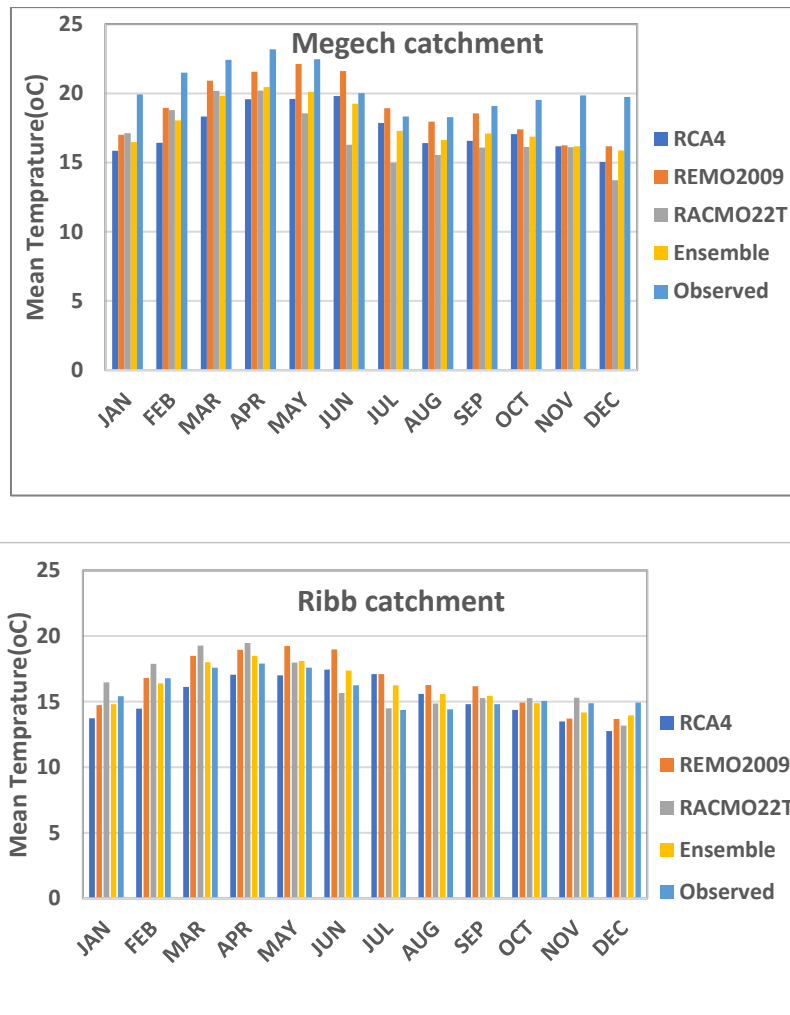


Figure 3-14: Long term monthly mean temperature comparison of observed and RCM data in Megech, Ribb catchment

### 3.2.4. Error Measures

In addition to the visual inspection, statistical analysis has been done to evaluate the performance of the models in simulating rainfall and temperature. Three performance measure criteria were used to evaluate the climate model performance in simulating the catchment rainfall, mean temperature. These metrics are the root mean square error (RMSE), mean absolute error (MAE), and coefficient of determination ( $R^2$ ). These metrics are selected because they are the common error metrics used to evaluate the performance of RCM simulations.

$$MAE = \frac{1}{n} \sum_{i=1}^n |(RCM - Observed)_i| \quad [3-4]$$

$$RMSE = \sqrt{\left(\frac{1}{n} \sum_{i=1}^n (RCM - Observed)_i^2\right)} \quad [3-5]$$

$$R^2 = \frac{\sum(0-s)(s-\infty)}{\sqrt{\sum(0-0)^2} \sqrt{\sum(s-s)^2}} \quad [3-6]$$

Where RCM is the regional circulation model data and n represents the length of the simulation period. RMSE and MAE value close to 0 indicates the good performance of the models whereas  $R^2$  values  $> 0.9$  shows a strong linear relationship of the RCM and in-situ data.

The result of the statistical analysis on precipitation comparison is presented in Table 3-5. REMO2009 has shown better performance in simulating precipitation in Megech and Ribb catchments. The RMSE and  $R^2$  of the RACMO22T indicate the model's poor performance in simulating precipitation over the two catchments. The following table shows the RMSE, MAE,  $R^2$  between observed and RCMs monthly precipitation in Megech and Ribb catchments over 1991-2005.

Table 3-5: RMSE, MAE,  $R^2$  between observed and RCMs monthly precipitation in Megech and Ribb catchments over 1991-2005

RCM	Megech catchment			Ribb catchment		
	RMSE (mm)	MAE (mm)	$R^2$	RMSE (mm)	MAE (mm)	$R^2$
RCA4	90.76	31.57	0.78	127.22	44.50	0.87
REMO2009	46.92	15.61	0.93	103.27	47.95	0.95
RACMO22T	109.16	15.27	0.54	175.32	47.33	0.41
Ensemble	57.48	20.79	0.94	124.03	46.57	0.94

### 3.2.5. Bias Correction

Bias correction of the RCM climate data is common as the RCM data is prone to systematic errors (Muerth et al., 2013). Biases of the RCM models need to be corrected before using them for hydrological analysis. There are a number of bias correction methods available such as power transformation method, linear scaling, distribution mapping/ quantile mapping are commonly applied (Smitha et al., 2018). For this study, a simple Linear scaling bias correction method was applied. The selection of the method is based on reasons of its simplicity and the successful application of the method in previous studies on the Lake Tana basin, e.g., Nigatu (2013), Worqlul et al. (2018). The linear scaling (LS) method is performed with a monthly correction coefficient. The correction coefficient is based on the differences between observed and simulated climate values of the same historic period (Teutschbein & Seibert, 2012). Climate data of observed and baseline RCM from 1991-2005 is used to calculate the bias correction coefficient. The additive bias correction method is applied for minimum and maximum temperature, whereas the multiplicative approach was performed for rainfall and windspeed. The future climate data (precipitation, maximum temperature, minimum temperature, wind speed) has been corrected using the following equations.

$$T_{\text{corr RCM, daily}} = T_{\text{RCM, daily}} + (T_{\text{Obs, M}} - T_{\text{RCM, M}}) \tag{3-7}$$

Where  $T_{\text{RCM, daily}}$  is the daily (for each calendar day) RCM temperature before bias correction,  $T_{\text{Obs, M}}$  is the observed monthly average temperature,  $T_{\text{RCM, M}}$  is monthly average RCM temperature for the baseline period, and  $T_{\text{corr, RCM, daily}}$  is the daily (for each calendar day) corrected RCM temperature.

$$P_{\text{corr RCM, daily}} = P_{\text{RCM, daily}} * (P_{\text{Obs, M}} / P_{\text{RCM, M}}) \tag{3-8}$$

Where  $P_{\text{RCM, daily}}$  is the daily (for each calendar day) RCM precipitation before bias correction,  $P_{\text{Obs, M}}$  is the observed monthly average precipitation,  $P_{\text{RCM, M}}$  is monthly average RCM precipitation for the baseline period,  $P_{\text{corr RCM, daily}}$  is the daily (for each calendar day) corrected RCM precipitation.

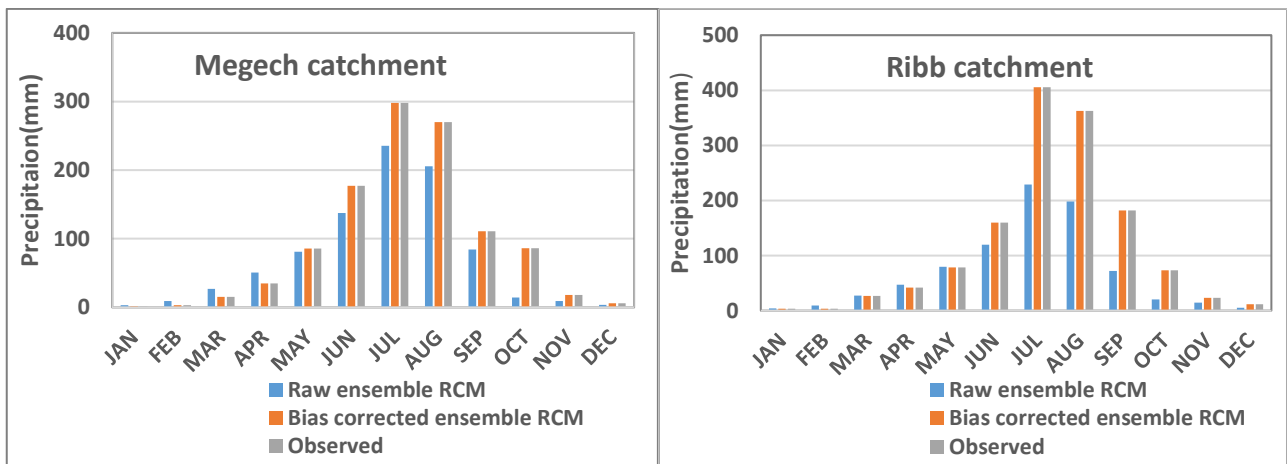


Figure 3-15: Bias corrected precipitation data of ensemble RCMs

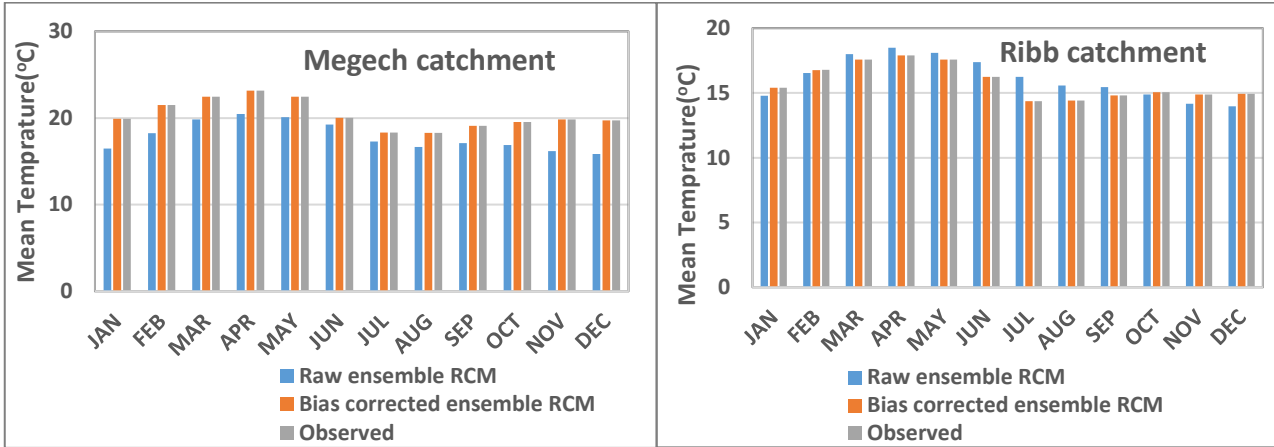


Figure 3-16: Bias corrected mean temperature data of ensemble RCMs

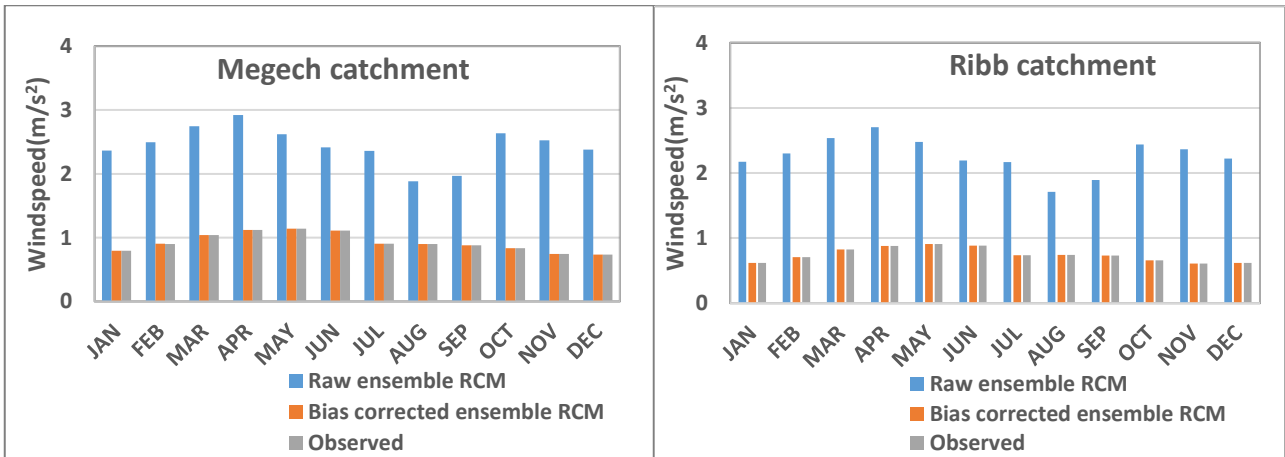


Figure 3-17: Bias corrected wind speed data of ensemble RCMs

Figure 3-15, 3-16, 3-17 shows the bias-corrected RCM precipitation, mean temperature, and windspeed, respectively (for Megech and Ribb catchments). The result of the bias correcting approach shows a perfectly matched bias-corrected ensemble RCM and observed data. These results indicate that the bias-corrected ensemble mean RCM data is of sufficient quality to serve for the HBV, AquaCrop, and WEAP modelling of this study.

## 4. METHODOLOGY

The main objective of this study is to assess the impact of climate change and land use interventions on the water balance of Lake Tana. Impact assessment of climate change and land use interventions on the water balance of Lake Tana was conducted using the water evaluation and planning (WEAP) model. For this study, the WEAP model was used as a tool to compute the water balance of Lake Tana. To assess the lake's water balance change, two-time horizons: baseline period (1991-2005) and future period (2041-2070) and four scenarios were selected. The four scenarios studied are baseline period (1991-2005), baseline with land use interventions, future period 2041-2070, future period with land use interventions 2041-2070. The future period water balance assessment was undertaken for RCP4.5 and RCP8.5 emission scenarios.

HBV rainfall-runoff was used to model streamflow from 19 catchments (gauged and ungauged). The irrigation requirement of the planned irrigation schemes was calculated using the AquaCrop model. The overall methodology adopted in this study is explained in the flowchart presented below.

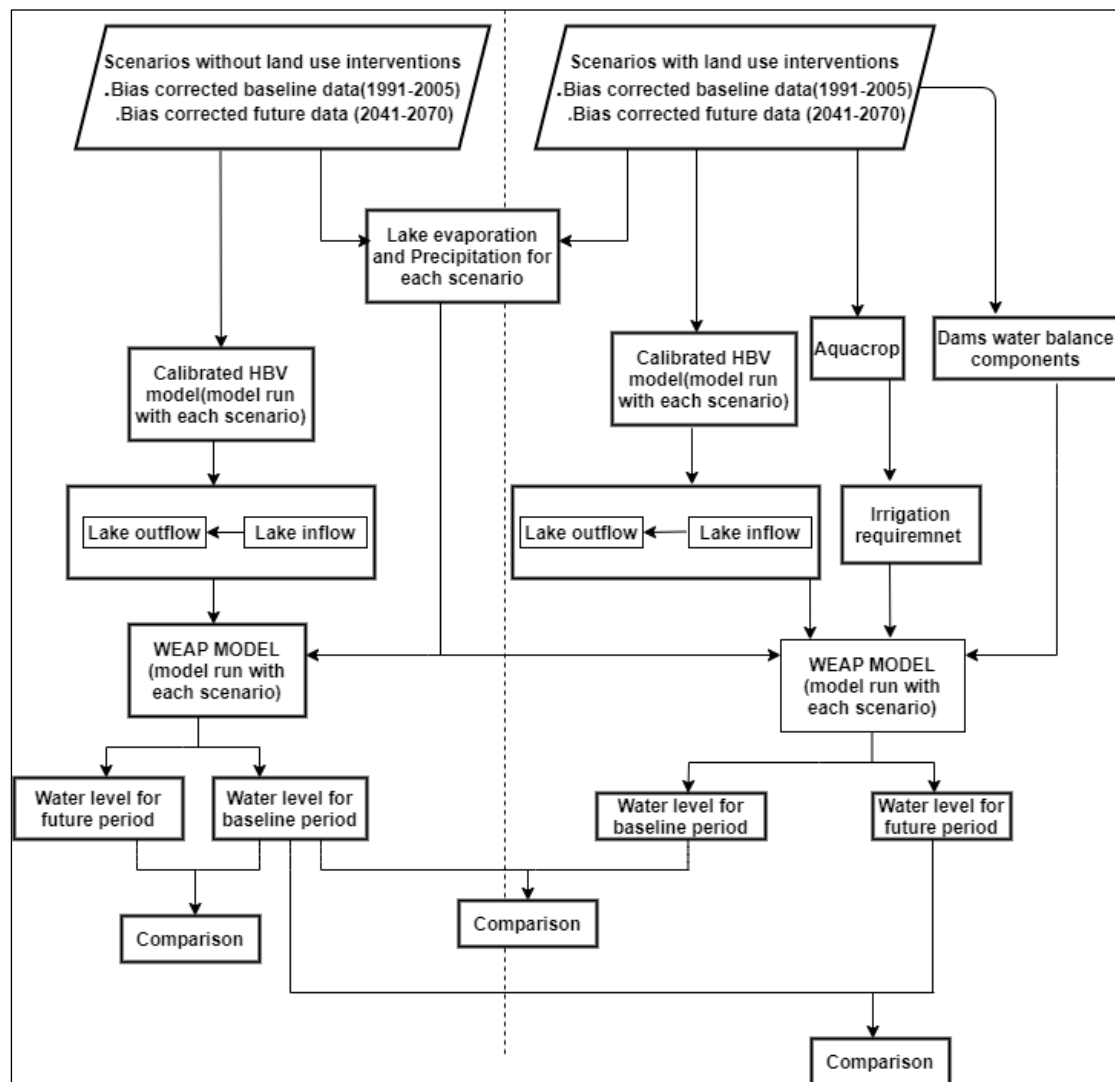


Figure 4-1: Flowchart of the research

## **4.1. WEAP Modelling**

Following the literature review in this study (Chapter 2), the Water Evaluation and Planning (WEAP) model is selected for evaluation and assessing lake water storage subject to simulated inflows and outflows. The model was developed by the Stockholm Environmental Institute (SEI, 2007) and has wide application in its integrated water system simulation and policy-oriented approach. The WEAP model is a water-planning tool with a wide range of applications, e.g., reservoir operation, streamflow simulation, demand allocation, and demand analysis (e.g., agricultural) (SEI 2001). The model operates on the principle of water balance accounting. Building a system that incorporates the water supply and demand represents different catchments, infrastructures, demand nodes, water flows, and interconnected transmissions (Yates et al., 2005). Supply components include streamflow, reservoirs, groundwater, and water transfers and, the demand sides are irrigation, hydropower, industry, and domestic supply.

In essence, WEAP can be employed to determine the impact of land use interventions (such as dam constructions and planned irrigation schemes) and climate change on lake inflows and water levels. To assess the impact of climate change and planned large-scale water projects, two periods were selected. These include a baseline period from 1991- 2005 and a future period 2041-2070. The selection of the simulation period for the baseline period is based on the availability of observed data for calibration, whereas the selection of the future period is based on the assumption of the completion of the proposed dams and irrigation schemes. The Future WEAP modelling was performed for RCP4.5 and RCP8.5 emission scenarios.

### **4.1.1. Scenario Development**

Following the objective of this study, four WEAP scenarios have been developed that target to assess the effects of climate change and land interventions on the Lake Tana water balance. The four WEAP scenarios are developed based on questions such as, what if climate patterns change and large-scale irrigation schemes and irrigation dams are constructed in the Tana sub-basin? Four different development scenarios were developed to simulate water balance and evaluate the sustainability of Lake Tana under climate change and land use interventions. WEAP scenarios undertaken under this study are as discussed under the WEAP schematization.

### **4.1.2. WEAP Schematization**

#### **4.1.2.1. Baseline Period 1991-2005 (scenario 1)**

For this scenario, the WEAP schematization and modelling were for water balance simulation of Lake Tana for the baseline period of 1991 to 2005. The scenario serves as a reference for the remaining scenarios where the effects of land interventions and climate change are assessed. The modelling of WEAP started by setting and linking up a spatial model domain with local (i.e., Site-specific) demand and supply nodes. At these nodes, distribution functions for water demand and supply are entered that are representative for spatial entities such as a township or sub-basin streamflow outflow. Inflows to Lake Tana are natural; flows from 19 sub-catchments as simulated by HBV (gauged and ungauged), stream flows from all the catchments that flow into Lake Tana. Lake Tana has an outlet that flows to the Blue Nile River. The WEAP water balance modelling requires net evaporation data. Thus, net evaporation was calculated pre WEAP modelling and entered as an input to the WEAP model. The net evaporation is computed by subtracting estimated lake evaporation to areal precipitation over the Lake. As it is mentioned earlier, this scenario serves as the reference/ benchmark scenario. Thus, the water balance computed under the other three scenarios was compared with this scenario.

Relative changes in water level due to climate change and land-use interventions were calculated as follows.

$$\Delta LL = LL_1 - LL_{2,3,4} \quad [4-1]$$

Where  $\Delta LL$  is change in annual/monthly lake level,  $LL_1$  is annual/monthly lake level under scenario 1,  $LL_{2,3,4}$  is the annual/monthly lake level under scenario 2, 3, 4.

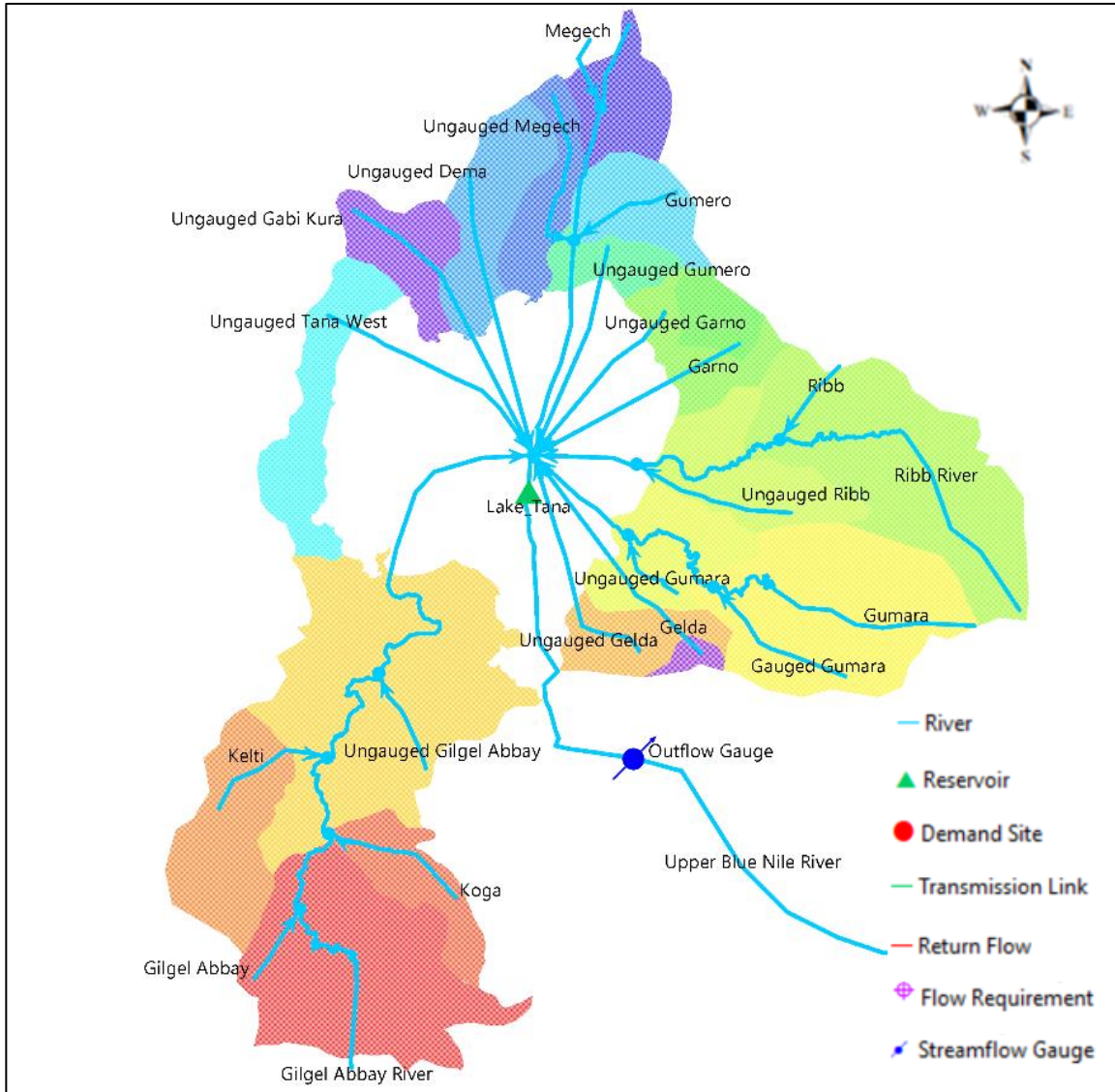


Figure 4-2: WEAP schematization for baseline and future period scenario (scenario 1&3)

#### 4.1.2.2. Baseline Period with Land Use Interventions 1991-2005 (scenario 2)

The water resources developments in the Lake Tana sub-basin include hydropower, large-scale irrigation, and water supply projects. The focus of this study was large-scale irrigation projects and dam constructions. Consequently, the impacts of the hydropower and water supply developments were neglected because of the limited time for the research. This scenario was developed to assess the effects of the planned irrigation schemes and dam constructions under the baseline (1991-2005) climate condition. This scenario incorporates the 19 gauged and ungauged catchments, irrigation demand of the 11 irrigation schemes, and planned dams. Environmental flow requirement downstream of the planned dams and to Tiss Issat Fall is incorporated for the modelling. Parameterisation of HBV and meteorological forcing has remained as used in Scenario 1. However, flows upstream

and downstream of the irrigation dams are simulated independently. The gross irrigation requirement of irrigation schemes is entered into the model. The schematization of the WEAP model under land use intervention is presented in Figure 4-3.

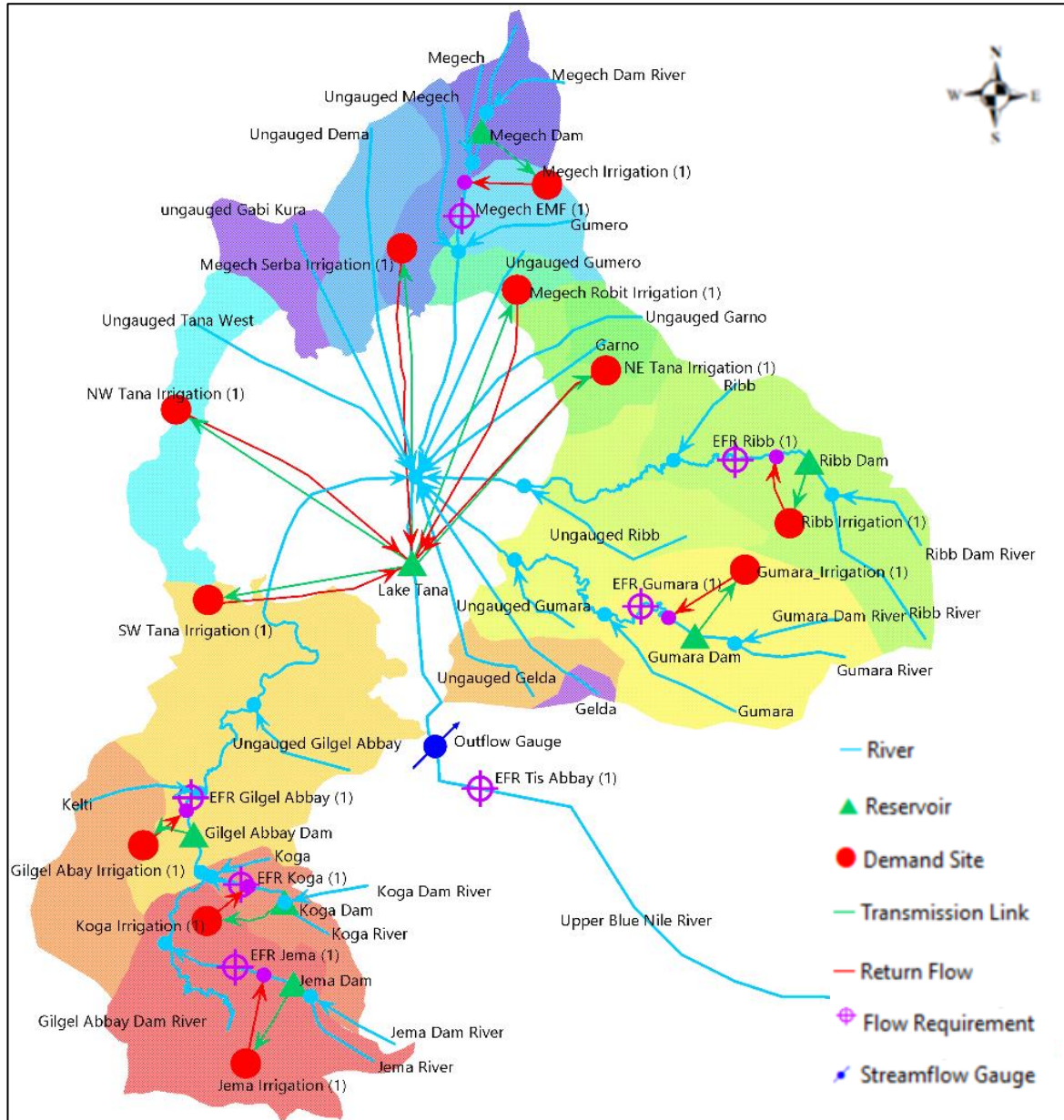


Figure 4-3: WEAP schematization for baseline and future period with land use interventions scenario (scenario 1&3)

#### 4.1.2.3. Future Period 2041-2070 (scenario 3)

This scenario is developed to assess the impact of climate change on the water balance of Lake Tana. In the approach, the models for the baseline period were adopted. Calibrated HBV and WEAP models were used, but baseline meteorological inputs have been replaced by meteorological inputs for the future period 2041-2070. Climate projections for both RCP4.5 and RCP8.5 are considered to evaluate its effect on Lake Tana storage and water levels. As such, inflows to Lake Tana will change subject to projection on climate change. The assumption is that model parameterizations for the baseline period remain valid for the future period. The overall schematization of the WEAP model approach remained the same as applied in the baseline period (scenario 1). In

this scenario, Future period flow data (gauged and ungauged catchments), future net evaporation of lake Tana, future outflow to Blue Nile River are used for the modelling.

#### **4.1.2.4. Future Period with Land Use Interventions 2041-2070 (scenario 4)**

This scenario serves to assess the impacts of climate change and land-use interventions. Whereas parameterization of HBV and AquaCrop models remained as used in Scenario 1, 2, meteorological forcing as applied in Scenario 3 was adopted. And model schematization has remained the same as scenario 2. The schematization of WEAP for scenario 2 was adopted as in that scenario, land interventions were considered. In this scenario, the combined effect of climate change and land use interventions was studied.

#### **4.1.3. WEAP Model Water Balance Computation**

As stated earlier, to facilitate water balance modelling using the WEAP model, the water demand and supply elements in the Tana sub-basin were identified and incorporated. Moreover, the inflows and outflows of the lake were incorporated in the model operations. Thus, the lake rainfall and streamflow from the major tributary rivers (Megech, Gilgel Abay, Ribb, and Gumara) and all the other gauged and ungauged catchments were incorporated in the WEAP modelling. The computation of the water inflow from the gauged and ungauged catchments is explained in the HBV modelling part of the methodology. The outflow components of the water balance, which include net evaporation and outflow from Lake Tana to the Blue Nile River, were also incorporated in the model. Besides the water balance components, demand requirements or water abstractions in the basin were represented by a node. In addition to the specified inputs earlier, the following elements were necessary for the WEAP modelling.

- Environmental flow requirement
- Demand prioritization
- Irrigation demand computation
- Return flow specifications
- Reservoir storage volume versus elevation relationships
- Reservoir operating rules

The computation of the WEAP model is based on the mass balance of water for each node and link. This is done by considering the demand priorities, supply preferences assigned by the modeler.

##### **4.1.3.1. Environmental Flow Requirement**

Environmental flow requirement is the volume of water needed to maintain the natural ecosystem. The term environmental flow can be represented by a variety of terms, such as environmental flow (regime), instream flow, ecological flow requirement, or environmental allocation (Acreman & Dunbar, 2004). Environmental flow requirements are important water demands that have to be incorporated in the WEAP modelling phase of the study. In this study, the baseline and future land use intervention scenarios incorporated the environmental flow requirement downstream of Lake Tana to the Tiss Issat falls. The minimum environmental flow requirement for Tiss Issat fall downstream of Lake Tana was taken as 10m<sup>3</sup>/s and 17m<sup>3</sup>/s for the dry and wet seasons, respectively, as recommended by Salini and Pietrangeli (2006) and SMEC (2008).

In addition to the environmental requirement of Tiss Issat fall, instream flow requirements downstream of the dam sites were included for the WEAP modelling of the land use interventions scenario (scenarios 2 & 4). The following table shows monthly environmental flow requirements obtained from the revised feasibility study and design document of corresponding dams (Halcrow, 2011).

Table 4-1: Environmental flow requirement( $m^3/s$ ) downstream the planned irrigation dams(Halcrow, 2011)

Rivers	Jan	Feb	Mar	Apr	May	Jun	Jul	Aug	Sep	Oct	Nov	Dec
Megech	1.2	0.9	1.2	1.8	0	0	0	0	0	3.055	1.56	1.2
Ribb	0.4	0.4	0.3	0.26	0.3	0	0	0	0	1	0.6	0.3
Gumara	0.228	0.2	0.23	0.228	0.23	0.228	0.23	0.23	0.23	0.228	0.228	0.2
Koga	0.399	0.4	0.3	0.258	0.3	0	0	0	0	1.001	0.602	0.3
G/Abay	5.49	2.8	3.02	2.7	6.2	0	0	0	0	23.41	7.95	4
Jema	1.24	0.9	1.04	1.24	1.87	0	0	0	0	3.17	1.62	1.2

#### 4.1.3.2. Demand Prioritization

Once the demands were specified, water demand priorities were assigned for each node in the model. Demand prioritization is very important for a period of peak demand and shortage. Prioritization of demand nodes was essential since it enabled the model to supply water according to the specified priority. Thus, demand sites with higher priorities are processed first before the ones with lower priorities. For this study, the highest priority of 1 was given for the irrigation schemes, instream flow requirement nodes, and a demand priority of 99 (Default) was assigned for the proposed dams and Lake Tana. This meant that the dams had to be filled before all the demands were met.

Ethiopia's water resources management policy recognizes minimum flow requirements as basic human and livestock needs and recommends the highest priority for minimum flow requirements in any water allocations (MOWR, 1999). Consequently, the highest demand priority was assigned for the environmental flow requirements.

Table 4-2: Demand prioritization

Demand Nodes	Priority
Irrigation Schemes	1
Minimum Environmental flow requirement (MEFR)	1
Proposed dams	99
Lake Tana	99

#### 4.1.3.3. Irrigation Water Demand Computation

The irrigation requirement is one of the main inputs to the WEAP model for the assessment of the impact of land use interventions in Lake Tana. For this study, irrigation water demand in each irrigation node was calculated using the AquaCrop model (see section 4.4). As discussed earlier, the WEAP model performs its computation using the mass balance equation in each node. According to the priority assigned for the demand sites, the WEAP model will allocate water for each demand node. In case of inadequate water supply for each demand node, unmet demand will occur. Unmet demand is the difference between the demand requirement and supply delivered to the demand node.

#### 4.1.3.4. Return Flow Specifications

According to WEAP, water that is not consumed in the demand site can re-enter one or more demand sites, wastewater treatment plants, surface, or groundwater nodes. The return flow is specified as a percentage of water lost as outflow. According to BCEOM (1998), for the planned irrigation projects, an average of approximately 20% of the irrigation water supplied to the projects will eventually be returned as drainage water. The percentage of return flows recommended by BCEOM (1998) were adapted for this study. Thus, return flows from planned irrigation schemes were modelled with an assumption of 20%, where 80% is assumed to be lost from the system.

#### 4.1.3.5. Reservoir Storage Volume versus Elevation Relationship

The WEAP model needs volume elevation relationship of Lake Tana. So, the model can compute elevation change as a function of evaporation and compute the water level based on the changes in the water balance. Therefore, Bathymetry survey data of Lake Tana, available from Wale (2008) as a function of Elevation Volume relationship, was used for this study. The following equation shows the elevation volume relationship of Lake Tana by Wale (2008): -

$$E = 1.21 * 10^{-13} (V)^3 - 1.02 * 10^{-8} (V)^2 + 6.20 * 10^{-4} (V) + 1774.63 \quad [4-2]$$

#### 4.1.3.6. Reservoir Operating Rules

After input data were entered into the model and the demand priorities were assigned, the WEAP simulation started by specifying the simulation period. The model divides the modelling period into two periods, the current account and the reference account. The current account is the first year of the simulation period, where model parameters were entered, and model initialization takes place. Whereas the reference account is dependent on the current account and inherits the information of the base year unless specified by the modeler.

In the WEAP modelling, data such as initial storage, the reservoir's storage capacity (i.e., Lake Tana) were entered into the model. The storage capacity represents the total reservoir capacity, whilst the initial storage is the amount of water initially stored at the beginning of the first month of the current account's year. The model maintains a mass balance of monthly inflows and outflows to track the monthly storage volume. Storage capacity of 32,029 Mm<sup>3</sup> and initial storage of 26,055 Mm<sup>3</sup>, a volume which corresponds to 1788 m.a.s.l. and 1786 m.a.s.l. Water levels respectively were set to the model. The initial storage was the previous month's elevation-volume data of the current account. The storage capacity for this study was fixed after evaluating the maximum water level of the baseline period (1991-2005). Thus, throughout the baseline simulation period, the maximum water level was during September 1998, having a water level of 1788.

According to WEAP, reservoir operation rules are defined in water level-related layers. These layers represent the amount of water to be released from the reservoir and the amount of water to be stored in the reservoir. The upper layer of the reservoir is the flood zone. In this zone, the water level is lying above the full supply level. So, the water in the flood zone cannot be stored in the reservoir. The zone right below the flood zone is the Conservation Zone. Free release of water is allowed in the conservation zone since water is used as required to meet demands. In the Buffer Zone, which is the layer at the bottom, some restrictions are applied so that the water is not used too quickly (Sieber, 2005). The buffer coefficient controls the release of water in the buffer zone. The buffer coefficient value ranges from 1 to 0. A value close to 1 will cause demand to be fully met while emptying the buffer zone. A value close to 0 will preserve the buffer zone storage while keeping the demand unmet. The following figure shows the different zones of the reservoir.

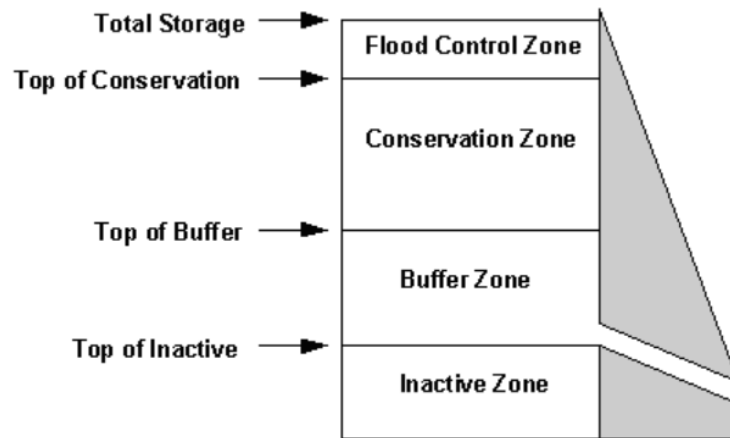


Figure 4-4: Reservoir storage zones (Source: Sieber (2005))

The amount of water available to be released from the reservoir is stored in the conservation zone and flood control zones and a fraction of water in the buffer zone (Yates et al., 2005). The following equation shows the calculation for the amount of water available to be released from the reservoir.

$$SR = SC + SF + (BC * SB) \quad [4-3]$$

Where,

SC - the storage in the conservation zone,

SF - the storage in the flood zone,

BC - Buffer coefficient,

SB - buffer storage.

The reservoir operation data was not incorporated for the lake since the lake was entirely natural before the construction of the Chara Chara weir. The lake operation data after the construction of the weir is unavailable. Thus, no reservoir operation rules are not incorporated for Lake Tana. However, a buffer coefficient of 1 is entered into the WEAP model so that the water demand by the irrigation schemes and environmental flow requirements is fully met.

Reservoir operation data of the planned irrigation dams is incorporated in the WEAP modeling of scenarios 2 and 4. Data of the reservoir operation was obtained from the design report of the respective irrigation scheme (see Table 4-3).

Table 4-3: Reservoir operation data for the planned dams

Dam	Bottom Level (m.a.s.l.)	Top of Dead (m.a.s.l.)	Normal water level (m.a.s.l.)	Spillway (m.a.s.l.)	Sources
Megech	1877.00	1906.37	1947.10	1948.39	Detail Design by WWDSE,2009
Ribb	1877.00	1901.43	1928.00	1930.50	Detail Design by WWDSE,2008
Gumara	1892.00	1922.11	1928.23	1930.00	Detail Design by WWDSE,2010
Jema	2055.00	2090.40	2127.59	2130.00	Detail Design by WWDSE,2010
Koga	2004.00	2005.40	2015.25	2015.25	Final Design by WWDSE & Mott MacDonald (2006)
Gilgel Abay	1840.00	1862.39	1891.80	1892.00	Detail Design by WWDSE,2010

#### 4.1.4. Comparison of the Simulated and Observed

Before WEAP modeling of the four scenarios was performed, the WEAP model was simulated for the period 1991-1995. Then, the simulated water levels were compared with the observed water levels. The period between 1991-1995 was selected for the comparison purpose because 1991-1995 is the period before the construction of the Chara Chara weir. Thus, it shows the natural condition of the lake.

##### 4.1.4.1. Objective Functions

The fitness of the observed and simulated result is usually evaluated using visual inspection and objective functions. The evaluation based on objective function uses statistical parameters to measure the modeling error. WEAP model performance was assessed by the objective functions of NSE (Nash Sutcliffe) and the regression coefficient ( $R^2$ ).

$$NSE = 1 - \frac{\sum_{i=1}^n (S - O)_i^2}{\sum_{i=1}^n (O - \bar{O})^2} \quad [4-4]$$

$$R^2 = \frac{\sum (O_i - O_{av})(S_i - S_{av})}{\sqrt{\sum (O_i - O_{av})^2} \sqrt{\sum (S_i - S_{av})^2}} \quad [4-5]$$

Where,

- $O_i$  - Observed lake level (m),
- $O_{av}$  - average observed lake level (m),
- $S_i$  - simulated Lake level (m)
- $S_{av}$  - average simulated Lake level (m),
- $I$  - the time step (i) and
- $n$  - number of samples or total observed data.

## 4.2. Water Balance Components of Lake Tana

The definition of the water balance is based on the principle of conservation of mass in which water input to any hydrological system, output, and changes in storage over a specific period is balanced. There are different processes that account for the water balance of Lake Tana. The water balance of the lake has inflow and outflow components. The inflow component constitutes lake area precipitation, streamflow from the gauged and ungauged catchments. And the outflow component of the water balance is the sum of the lake outflow and open water evaporation.

In order to allow computation of water balance using the WEAP model, the water balance components of the lake were calculated for the baseline period from 1991 to 2005 and the future period of 2041-2070. The following equation generally expresses the water balance: -

$$\frac{\Delta S}{\Delta T} = Inflow - Outflow \quad [4-6]$$

Where  $\Delta S(m^3)$  is the change in storage for a selected time  $\Delta T$ . The general equation representing the water balance of a lake can be presented as: -

$$\frac{\Delta S}{\Delta T} = (P + Qinflow + GWin) - (E + Qout + GWo) \quad [4-7]$$

Where  $\Delta S(m^3)$  is the change in storage for a selected time  $\Delta T$ ,  $P(m^3)$  is lake area rainfall,  $Qinflow(m^3)$  is the flow from all catchments (gauged and ungauged),  $GWin(m^3)$  is the groundwater flow into the lake,  $E(m^3)$  is evaporation from the lake surface,  $Qout$  is lake surface outflow,  $GWo(m^3)$  is groundwater outflow.

Several studies have been performed to study the water balance of Lake Tana (Wale et al., 2008; Nigatu et al., 2016). Based on Rientjes et al. (2011b), the most dominant water balance components of Lake Tana are evaporation, surface runoff, and the outflow to the Blue Nile River. The groundwater component is ignored for this study since there is no groundwater monitoring in the lake area.

### 4.2.1. Over Lake Precipitation

The precipitation data for the lake area was estimated using ArcGIS software to overlay the lake area on the grid cell. It was estimated by computing the area coverage of each pixel covering the lake area. Then, after bias correcting the precipitation of The RCM data, the lake area precipitation for the baseline period (1991-2005) and future period (2041-2070) was used for the water balance simulation of the WEAP model.

### 4.2.2. Open Water Evaporation

The estimation of the open water evaporation was performed using the Penman combination equation (Maidment, 2010). This method is a widely used method that combines remote sensing and in-situ climate data. The bias-corrected climate data are used to calculate the baseline and future period open water evaporation of Lake Tana. The Penman combination (Maidment, 2010) method uses the following equation: -

$$E_p = \frac{\Delta}{\Delta + \gamma} (R_n + A_h) + \frac{\gamma}{\Delta + \gamma} \left( \frac{6.43 (1 + 0.536 U_2) D}{\gamma} \right) \quad [4-8]$$

Where,  $E_p$  is open water evaporation that occurs from free water evaporation [mm day<sup>-1</sup>],  $R_n$  = net radiation exchange for the free water surface [mm day<sup>-1</sup>],  $A_h$  = energy advected to the water body [mm day<sup>-1</sup>],  $U_2$  = wind speed measured at 2m [m s<sup>-1</sup>],  $D$  = average vapor pressure deficit, [kPa],  $\lambda$  = latent heat of vaporization [MJ kg<sup>-1</sup>],

$\gamma$  = psychrometric constant [kPa °C<sup>-1</sup>],  $\Delta$  = is slope of saturation vapor pressure curve at air temperature [kPa °C<sup>-1</sup>](Maidment, 1993).

The net radiation ( $R_n$ ) is the difference between the short and long waves' downward and upward radiation fluxes. It is calculated as:

$$R_n = R_s(1 - \alpha) - R_l \quad [4-9]$$

Where  $R_n$  is short wave radiation,  $\alpha$  is surface Albedo and  $R_l$ : is longwave radiation

$$R_s = (0.25 + \frac{0.5n}{N})R_a \quad [4-10]$$

$N$  is the maximum possible duration of sunshine hours(hour),  $n$  is the actual duration of sunshine(hour), and  $R_a$  is extra-terrestrial radiation (MJ m<sup>-2</sup> day<sup>-1</sup>).

Albedo is the fraction of the incident light or incoming radiation that is reflected back to the atmosphere. Albedo indicates how well the earth's surface reflects solar energy. Water contents affect the reflectivity of solar energy. If a lot of water is available, there will be higher solar radiation absorbed by the water. The value of Albedo ranges from 0 to 1. A value of 0 indicates the surface is a perfect absorber, and a value of 1 indicates the surface is a perfect reflector.

Albedo can be obtained from remote sensing products. Wale (2008) used Landsat ETM+ images of 10/23/1999, 09/12/1999, and 11/15/1999 to estimate the albedo of the lake and estimated an albedo value ranging from 0.05 to 0.062. Whereas Perera (2009) used MODIS Level 1 product for 2000 and 2002 and estimated a value between 0.08 and 0.16. An albedo value used by Perera (2009) was used for this study for the computation of lake evaporation of the baseline and future period.

#### 4.2.3. Lake Inflow

The inflow to the lake consists of the flows coming from the major rivers, streams and direct overland flow. According to Kebede et al. (2006), more than 40 rivers and streams feed lake Tana. The main rivers contributing to the inflow of lake Tana are Gilgel Abay, Ribb, Gumara, and Megech. The inflow to Lake Tana includes runoff from gauged and ungauged catchments. HBV model is used to model the inflow to Lake Tana from all the gauged and ungauged catchments.

### 4.3. HBV Modelling

The HBV model is a semi-distributed conceptual model for continuous runoff calculation. It was originally developed at the Swedish Meteorological and Hydrological Institute (SMHI, 2006). The model simulates daily discharge using daily precipitation, daily mean temperature, and potential evapotranspiration as input to the model. The model also uses observed discharge data for calibration purposes. The model consists of three subroutines: precipitation and snow accumulation, soil moisture, and runoff generation routines.

The general water balance of the HBV model is described as:

$$P - Q - E = \frac{d}{dt}(SP + SM + UZ + Lake) + ss \quad [4-11]$$

Where P is precipitation

Q is runoff

E is evapotranspiration

SP is snowpack

UZ is the upper groundwater zone

LZ is a lower groundwater zone

Lake is the volume of the lake

Ss is sink or source

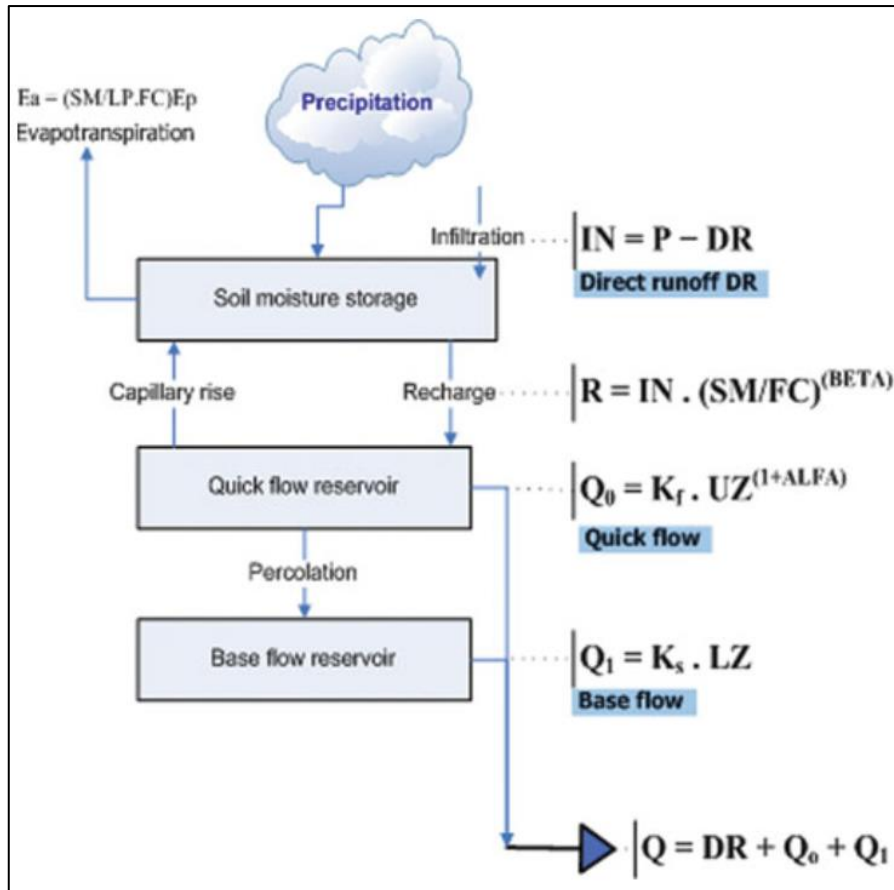


Figure 4-5: Schematic representation of HBV model (IHMS, 2006), modified by (Perera, 2009)

The computation of precipitation is performed separately for each vegetation zones/ elevation zone within a sub-basin. Soil moisture accounting is based on three parameters named BETA, the limit for potential evaporation (LP), and field capacity (FC). The parameter BETA controls the increase of soil moisture storage ( $1 - \Delta Q / \Delta P$ ) from each snowmelt or millimeter of rainfall. LP is the value of soil moisture above which evapotranspiration

reaches its potential value. Field capacity (FC) is the maximum soil moisture storage(mm). Excess water is transformed from the soil moisture zone to runoff by the response function of the runoff generation zone. The response function is composed of linear lower and nonlinear upper reservoirs. The response routine consists of upper and lower linear reservoirs. The upper reservoir is attached to the soil moisture zone by capillary rise. Once seepage from the soil moisture routine exceeds the percolation threshold, the upper reservoir starts to fill, and simultaneously the water will percolate to the lower reservoir. The percolation of water to the lower reservoir is controlled by the percolation parameter (PERC).  $\beta$  is the parameter that determines the non-linearity of flow in the upper reservoir. The lower reservoir characterizes the groundwater storage of the catchments, which contributes to the baseflow as a function of Ks (recession coefficient for baseflow routine). For this study, model parameters are selected from a previous study by Perera (2009). Accordingly, the eight most sensitive model parameters, FC, BETA, LP, ALFA, Ks, Kf, PERC, and CFLUX, were selected for the calibration of the model.

The model has been widely used in Lake Tana sub-basin for water balance and climate impact studies: Wale et al. (2009), Abdo et al. (2009), Gebremariam (2009), Rientjes et al. (2011), and Nigatu (2013) used the model to compute streamflow in the area. Accordingly, streamflow from the gauged and ungauged catchments is estimated using the HBV hydrological model for this study. The FORTRAN code has been developed previously by Booiij (2005) for the Meuse basin. For Tana sub-basin hydrological modelling, the code developed by Booiij (2005) has been used by Perera (2009) and Nigatu (2013). For this study, the FORTRAN HBV model code has been translated to a Python code based on the HBV version of the Fortran model.

#### 4.3.1. Inputs to HBV Model

As discussed earlier, HBV simulates runoff from daily precipitation, daily temperature, and daily potential evapotranspiration data. The bias-corrected daily precipitation, mean temperature, and PET data extracted for the catchment area were used as an input to the HBV model to model the baseline and future period streamflow in the Lake Tana sub-basin.

##### 4.3.1.1. Catchment Potential Evapotranspiration

Potential evapotranspiration is one of the main input data into the HBV model. The most widely used method to calculate potential evapotranspiration is the Penman-Monteith equation. For this study, daily catchment potential evapotranspiration is calculated using the Penman-Monteith equation (FAO-56, 2007). Climate data such as temperature, relative humidity, sunshine hour, and wind speed were used as a basic input for the formula.

$$ET_0 = \frac{0.408\Delta(R_n - G) + \gamma \frac{900}{T + 273} u_2 (e_s - e_a)}{\Delta + \gamma(1 + 0.34u_2)} \quad [4-12]$$

Where  $ET_0$  - reference evapotranspiration(mm/day)

$R_n$  - Net radiation at the crop surface ( $MJ m^{-2} day^{-1}$ )

$G$  - Soil heat flux density ( $MJ m^{-2} day^{-1}$ )

$T$  - Mean daily air temperature at 2m height( $^{\circ}C$ )

$U_2$  - Wind speed at 2m height ( $m s^{-1}$ )

$e_s$  - Saturation vapour pressure(kPa)

$e_a$  - Actual vapour pressure(kPa)

$\Delta$  - Slope vapour pressure ( $kPa ^{\circ}C^{-1}$ )

$\gamma$  - Psychrometric constant ( $kPa ^{\circ}C^{-1}$ )

### 4.3.2. Model Calibration

Every hydrological model needs parameter adjustment to minimize the difference between simulated and observed data to assure the model's reliability. Rientjes (2007) indicated that adjusting model parameters is very important to match the model output with measured data for the selected period. The purpose of the calibration of HBV is to find the best set of parameters that can give a good fit between observed and simulated discharge. The goodness of fit between the modelled and observed discharge can be evaluated by objective functions (Booij et al., 2007). The HBV model is mostly calibrated using two dimensionless objective functions when evaluating the aspect of a good fit of water balance and a good overall agreement of the hydrograph shape; relative volume error (RVE) and the Nash Sutcliffe coefficient (NS). The NS measures the overall agreement of the shape of the hydrograph. Whereas the RVE measures the error in the simulated streamflow volume when compared to the observed streamflow. NS coefficient can be explained with the following equation.

$$NS = 1 - \frac{\sum_{i=1}^n (Q_{sim,i} - Q_{obs,i})^2}{\sum_{i=1}^n (Q_{obs,i} - \overline{Q_{obs}})^2} \quad [4-13]$$

Where,  $Q_{sim,i}$  – simulated flow,  $Q_{obs,i}$  – observed flow,  $\overline{Q_{obs}}$  - mean observed flow,  $n$  – number of time steps used during calibration,

The value of NS ranges between  $-\infty$  to 1. A value of 1 indicates a perfect fit (shows a perfect match between the modelled and observed discharge), NS value of 0.9 to 1 indicates that the model performs extremely well. A value from 0.8-0.9 indicates the model performs very well. And 0.6-0.8 NS value shows that the model performs reasonably well. NS value 0 indicates model prediction is as accurate as of the observed data. NS value less than 0 indicates that observed mean discharge is a better predictor than the model (Deckers, 2006).

The relative volumetric error (RVE) is explained with the following equation:

$$RVE = \left[ \frac{\sum_{i=1}^n (Q_{obs,i} - Q_{sim,i})}{\sum_{i=1}^n Q_{obs,i}} \right] \times 100\% \quad [4-14]$$

Where,  $Q_{sim,i}$  – simulated flow,  $Q_{obs,i}$  – observed flow,  $n$  - number of the simulation period.

A relative volume error value between +5% and -5% shows that the model performs well, while RVE from +5% to +10% and -5% to -10% indicates a reasonable performance of the model.

For this study, calibrated HBV parameters sets are obtained from Perera (2009), who calibrated the model from 1994-2000 and validated it from 2001 to 2003. The calibrated HBV parameters have been evaluated whether they successfully simulate the streamflow for an extended period from 1997-2005. To evaluate the HBV model parameters performance, simulation of HBV model was performed using observed precipitation, observed mean temperature, and observed evapotranspiration data. For the catchments in which the objective functions did not show a reasonable result, recalibration of the model parameters has been performed for the period between 1997-2003. Manual model calibration was done following the sensitivity analysis performed by Perera (2009). The calibration is done by adjusting in order of the most sensitive parameters to the objective functions, NS and RVE. According to Perera (2009), the most sensitive parameters for the RVE error in Gilgel Abay and Gumara catchments are FC, Beta, LP. Major parameter adjustments have been undertaken to those parameters. The following table shows the calibrated model parameters for gauged catchments by Perera (2009).

Table 4-4: Calibrated model parameters for gauged catchment 1991-2000 (Perera, 2009)

HBV parameters	Ribb	Gilgel Abay	Gumara	Megech	Koga	Kelti	Gumero	Garno	Gelda
FC	309.03	434.39	349.86	193.04	730.05	196.62	469.23	221.25	141.14
BETA	1.23	2.08	1.31	1.56	1.34	1.60	1.10	2.58	1.20
LP	0.73	0.63	0.87	0.71	0.42	0.62	0.26	0.23	0.86
ALFA	0.31	0.24	0.25	0.29	0.41	0.28	1.08	0.27	0.51
KF	0.07	0.08	0.03	0.03	0.07	0.03	0.03	0.10	0.00
KS	0.10	0.09	0.07	0.09	0.05	0.10	0.13	0.11	0.15
PERC	1.09	1.02	1.44	1.47	1.63	1.53	2.32	1.61	1.41
CFLUX	0.60	1.09	0.72	0.79	0.74	0.83	0.39	1.35	1.00
NS	0.78	0.85	0.72	0.61	0.67	0.66	0.16	0.33	0.41
RVE%	-1.61	-0.35	-2.44	2.91	-0.06	-2.00	0.01	0.00	-0.06

#### 4.3.3. Model Validation

Since the world is very complex, representing it by a model approach and sets of parameters may not be accurate. As a result, models are uncertain and cannot be reliable when only one field situation is simulated. Thus, calibrated model parameters might not accurately represent the real-world system behaviour under different hydrological stress conditions (Rientjes, 2007). Therefore, model parameters should be validated with another set of stress conditions. If the calibrated model parameters failed during the validation period, the model should be recalibrated with new sets of model parameters until it satisfies the calibration target.

For this study, calibrated gauged catchments (Gilgel Abay and Gumara), were calibrated for the period between 2004-2005. And objective functions NS and RVE were computed to evaluate the performance of the model parameters.

#### 4.3.4. Flow from Ungauged Catchments

##### 4.3.4.1. Regionalization

For catchments with limited or no observed/gauge streamflow data, rainfall-runoff model parameters cannot be obtained through calibration of the models. Therefore, runoff from ungauged catchments is usually obtained by other methods, such as the regionalization method. According to Blöschl and Sivapalan (1995), regionalization is a method of deriving information to catchment of interest from a comparable catchment. Spatial proximity is a type of regionalization technique in which runoff from ungauged catchments is generated from nearby gauged catchments. The method assumes closer catchments would likely have similar catchment regimes since climate and catchment conditions will mostly be the same. Another common regionalization method is a technique of estimating flow from the ungauged catchments by establishing a relationship between the calibrated model parameter of gauged catchments with their physical characteristics. For further details on the regionalization approach and the regional model, reference is made to (Perera, 2009 and Rientjes et al., 2011).

The regionalization method performed by Perera (2009) gave an excellent lake-level simulation result. However, parameter values for two (Gilgel Abay & Gumara) catchments changed; as a consequence, regionalization relations

based on catchments should be updated, and this updating has been carried out by adapting the same regionalization procedures followed by Perera (2009).

Table 4-5: Physical catchment characteristics for regionalization method (Perera, 2009).

Group	Parameter	PCC and Unit
Geography and physiography	<i>AREA</i>	Catchment area [km <sup>2</sup> ]
	<i>LFP</i>	Longest flow path [km]
	<i>MDEM</i>	DEM mean [m]
	<i>HI</i>	Hypsometric integral [-]
	<i>AVGSLOPE</i>	Average slope of catchment [%]
	<i>SHAPE</i>	Catchment shape [-]
	<i>CI</i>	Circularity index [-]
	<i>EL</i>	Elongation ratio [-]
	<i>DD</i>	Drainage Density[m/km <sup>2</sup> ]
	Land use	<i>CROPD</i>
<i>CROPM</i>		Cultivated Moderately[%]
<i>GL</i>		Grassland[%]
<i>URBAN</i>		Urban[%]
<i>FOREST</i>		Forest[%]
Geology and soil	<i>LEP</i>	Leptosol area [%]
	<i>NIT</i>	Nitosol area [%]
	<i>VER</i>	Vertisol area [%]
	<i>LUV</i>	Luvisol area [%]
Climate	<i>SAAR</i>	Standard annual average rainfall [mm]
	<i>PWET</i>	Mean precipitation wet season (Jun. to Sep.) [mm]
	<i>PDRY</i>	Mean precipitation dry season (Oct. to May) [mm]
	<i>PET</i>	Mean annual evapotranspiration [mm]

#### 4.3.4.2. Multiple Regression

The study by Perera (2009) evaluated different regionalization methods such as multiple regression, spatial proximity, and area ratios if they gave satisfactory lake level simulation results. The result from the regression method gave an excellent lake-level simulation. Thus, the relationship between the physical catchment characteristics and HBV model parameters. Procedures of the regionalization approach are adapted from the study of Perera (2009).

Multiple regression is a statistical analysis for determining a relationship between a dependent variable and a set of independent variables. The unknown variable that has to be determined is the dependent variable. Whereas the other variable that does not depend on other variables is the independent variable. For this study, model parameters were considered dependent variables (MPs) and the physical catchment characteristics (PCCs) as independent variables. The general equation of the multiple regression approach is shown in the equation.

$$Y' = \beta_0 + \beta_1 X_1 + \beta_2 X_2 + \beta_3 X_3 + \dots + \beta_n X_n \quad [4-15]$$

Where,

$Y'$  - Estimated dependent variable (model parameters)

$\beta_0$  - Intercept of the regression line

$\beta_1, \beta_2, \beta_3 \dots \beta_n$  - Regression coefficients

$X_1, X_2, X_3 \dots X_n$  - Independent variable (catchment characteristics)

After establishing the regional model for the ungauged catchment, the regional model is validated by comparing the simulated and observed flow of the gauged catchments.

#### 4.3.5. Lake Outflow

Some studies indicated that the outflow data of Lake Tana could be uncertain. (Duan, Gao, & Ke, 2018) Suggested that the measured outflow is not certain because of the fact that responsible agencies are not keen to share the data in a transparent way. The study further explained that, since the outflow from Lake Tana is the source for the Blue Nile River, the water uses and management downstream depends on the release of water from the Lake. Besides, different traditional irrigation(unmeasured) taking place around the lake, which accounts for the outflow components of Lake Tana water balance.

For this study, given the fact the outflow from Lake Tana could be uncertain, computation of Lake Tana outflow was performed. The calculation is performed by assuming the outflow is linearly correlated with the total inflow. And a linear relationship was established between the inflow data and the outflow. A coefficient *Beta* is used to calculate the outflow ( $\text{Outflow} = \text{Beta} \times \text{inflow}$ ). Then, the coefficient is calibrated for different values starting from 0.5 to 0.9. For each *Beta* value, the simulated lake level is compared with the observed one, and the objective function of NSE and  $R^2$  is calculated. The NSE and  $R^2$  are calculated using equations [4-5] and [4-6]. Observed lake level from 1991-1999 was used for the comparison purpose.

#### 4.3.6. Streamflow Upstream of Planned Irrigation Dams

Water balance simulation under land use interventions incorporates the six planned dams. The streamflow upstream of the dams does not directly contribute to the lake inflow; instead, it flows to the irrigation dams. This has an impact on the water balance of the lake by reducing the inflow to the lake. Thus, streamflow upstream of the irrigation dams should be modelled independently for the WEAP simulations under land use intervention scenarios. Consequently, the streamflow upstream of the dams was modelled separately and included in the WEAP simulation under the land use interventions. The streamflow upstream of the dams was computed by relating the upstream catchment area to that of the downstream catchment and the amount of streamflow it generates. This was performed by using the ratio and proportions.

Table 4-6: Catchment area upstream proposed irrigation dams

Dams	Upstream Area (Km <sup>2</sup> )
Gilgel Abay	1522
Megech	427
Ribb	682
Gumara	377
Koga	213
Jema	221

#### 4.3.7. Dam Precipitation and Evaporation

For the water balance simulation of land use intervention scenarios, the water balance components of the planned dams are incorporated. Thus, the inflow and outflow components of the planned are calculated for the baseline and future scenarios. The dam precipitation and evaporation were calculated the same way the lake precipitation and evaporation were calculated. Bias corrected RCM climate data were used for the computation. Methods applied to compute the lake precipitation, and lake evaporation are adopted to the precipitation and evaporation computation of the irrigation dams.

#### 4.4. AquaCrop Modelling

AquaCrop model is a water-driven model with relatively low input data demand and parameters to model the yield response to water of the major field and vegetable crops cultivated worldwide (Steduto et al., 2003). The AquaCrop model was developed by the Food and Agricultural Organization (FAO), based on the soil water balance method. It has been used to model crop water needs in different parts of the world, with different climatic and agro-ecological conditions using a relatively small number of input variables and crop parameters (Vanuytrecht et al., 2014). AquaCrop is the updated version of the CropWat model, which was initially released in January 2009. The model simulates net irrigation requirements based on the climate information (rainfall, reference evapotranspiration), CO<sub>2</sub> concentration in the atmosphere, crop information, soil characteristics, and field management information.

For this study, the AquaCrop model was used to simulate the net irrigation requirement (NIR) of the planned irrigation schemes in the Tana sub-basin. The selection of the model is mainly because of the fact that the AquaCrop model integrates projected future climate data in combination with projected CO<sub>2</sub>. This makes the model very essential for climate change studies. The other selection criteria is based on the capability of the model to simulate using time series data. Flowchart for the computation of the net irrigation requirement is presented below.

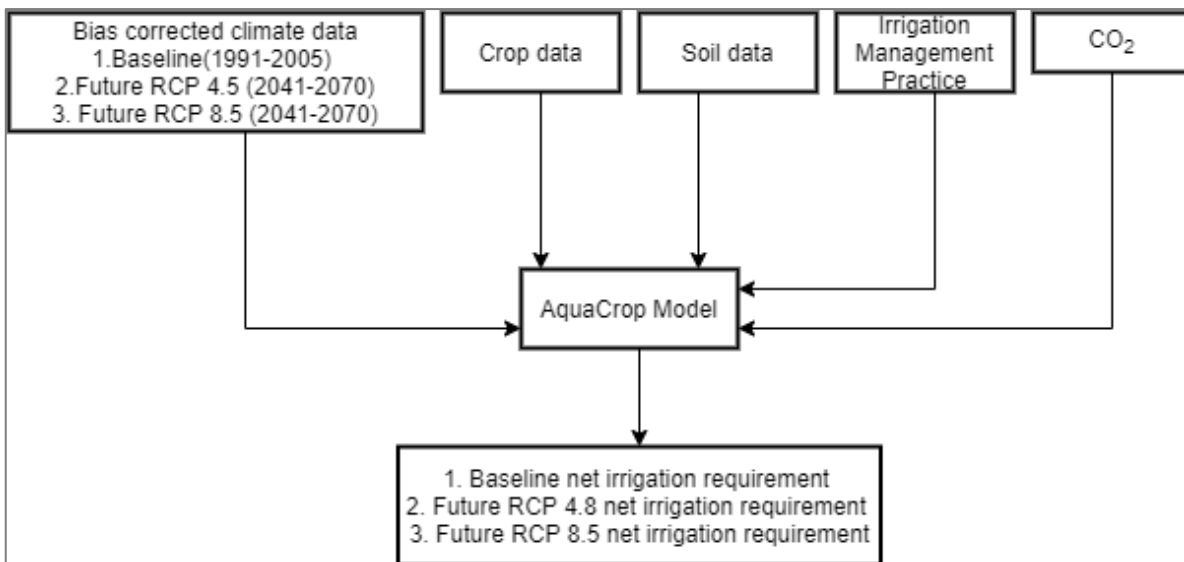


Figure 4-6: Flowchart on AquaCrop modelling

##### 4.4.1. Climate Data

As mentioned earlier, climate data of rainfall and reference evapotranspiration are some of the main input data to the model. Bias corrected RCM rainfall data was used for the baseline and future (scenarios 3 & 4) net irrigation requirement simulations. AquaCrop model uses the Penman-Monteith equation to compute reference evapotranspiration. The climate data needed by the AquaCrop model to calculate the reference evapotranspiration are daily data of maximum and minimum temperature, wind speed, relative humidity, sunshine hour, solar radiation. For this study, bias-corrected maximum and minimum temperature and wind speed data are used as input to simulate the reference evapotranspiration for the baseline and future period. Other missing climate data (relative humidity, solar radiation) are computed by the model from the available temperature data and the information about the locations of the meteorological stations. The computation is performed based on calculation procedures outlined by FAO Irrigation and Drainage NR.56. According to the FAO recommendations, the relative

humidity data for humid and sub-humid locations can be computed by assuming that dewpoint temperature ( $T_{dew}$ ) is near the daily minimum temperature ( $T_{min}$ ). The air might not be saturated when the temperature is at a minimum; the  $T_{dew}$  is approximated by subtracting 2 °C to 3 °C from the minimum temperature, For Arid regions, since. In the absence of solar radiation data, the model uses the temperature difference method to compute the solar radiation data. Based on the FAO recommendation, the temperature difference is associated with the degree of cloud cover in a specific location. Therefore, the temperature difference ( $T_{max}-T_{min}$ ) can be used to indicate the fraction of the extra-terrestrial radiation that reaches the earth's surface.

#### 4.4.2. Atmospheric Carbon Dioxide Concentration

Increased CO<sub>2</sub> concentration in the atmosphere will affect the future climate and crop production. AquaCrop can simulate projected future climate data in combination with projected CO<sub>2</sub> levels for different climate scenarios. The model integrates different future CO<sub>2</sub> emission scenarios. This makes the model very important for future water demand assessment. For baseline period simulation, AquaCrop integrated the MaunaLoa.CO<sub>2</sub> file., the atmospheric concentrations at Mauna Loa (Hawaii). The file contains the mean annual atmospheric CO<sub>2</sub> concentration measured at Mauna Loa Observatory since 1958. For future period modelling, AquaCrop contains CO<sub>2</sub> files from SRES (Special Report on Emissions Scenarios), including data derived from emissions scenarios are available in the database of AquaCrop. Also, four different RCP's (RCP2-6.CO<sub>2</sub>, etc.) are available in the database of AquaCrop. For this study, the MaunaLoa.CO<sub>2</sub> file for the baseline period simulation and RCP4-5.CO<sub>2</sub> and RCP8-5.CO<sub>2</sub> is used for the RCP4.5 and RCP8.5 future period irrigation requirement modelling.

#### 4.4.3. Crop Data

Calibrated crop parameters for major crops are provided by FAO and are incorporated as default values in the AquaCrop model (Steduto et al., 2012). The model has two types of crop parameters, the conservative and non-conservative crop parameters. The conservative crop parameters are parameters that do not change due to location, time, and management practice. Therefore, they do not need adjustments to the localized environment. Canopy growth, stomatal closure, and soil water extraction patterns are some of the examples of conservative parameters. The non-conservative parameters are user-specific and might need an adjustment since they might be affected by the weather conditions, field management (e.g., sowing date, maximum rooting depth, and maturity date). For this study, default non-conservative crop parameters were used for the specific crops selected for the net irrigation simulation.

Based on BCEOM (1998) design document, two irrigation patterns named CP1 and CP6 are proposed for the planned irrigation schemes in the Lake Tana sub-basin. In which maize, wheat, barley, and sugarcane are the major irrigated crops under the CP1 cropping pattern. Whereas the major irrigated crop under CP6 cropping pattern is rice. However, according to a recent study performed by (Asmamaw et al., 2021), conducted in the currently operational Koga scheme, major crops practiced are maize, wheat, potato, onion, cabbage. Asres (2016) also indicated that wheat, barley, bean, maize, cabbage, potato, tomato, onion, shallot, and pepper are significant crops in the area. According to FAO (2020), wheat occupies almost 70 percent of cropped area in the Koga irrigation scheme. Thus, wheat and maize are selected purposely to model the irrigation requirement in the Lake Tana sub-basin because they are the most practiced crops in the area. Due to limited amount of time to model different types of crops in each irrigation schemes, wheat and maize are assumed to be representative crops for all irrigation schemes. Subsequently, calibrated crop non-conservative parameters (e.g., planting date and harvesting date) for wheat and maize are obtained from the AquaCrop database.

In the AquaCrop model, the crop growth period can be described as *calendar* or *thermal* time. AquaCrop uses thermal time as default. It also allows the user to choose calendar time as an alternative crop growth period. The

model uses Growing Degree Days (GDD) to compute thermal time. Growing degree days are a measure of heat accumulation, and they are used to estimate the development and growth of certain crops during the growing season. GDD is an accumulation of average daily temperature, which is computed using the below equation.

$$GDD = \frac{(T_{max} + T_{min})}{2} - T_{base} \quad [4-16]$$

Where  $GDD$  is the number of degrees which determines a proportional crop growth and development,  $T_{max}$  is daily maximum air temperature,  $T_{min}$  is the daily minimum air temperature and  $T_{base}$  is the temperature below which crop development stops.

#### 4.4.4. Soil Characteristics

Soil characteristics such as Field capacity ( $\theta_{FC}$ ), water retention in the fine soil fraction at saturation ( $\theta_{sat}$ ), permanent wilting point ( $\theta_{PWP}$ ), and hydraulic conductivity of the soil at saturation ( $K_{sat}$ ) are also locally incorporated in the model for different soil types. Soil type classification of Tana sub-basin is obtained from Perera (2009), which was initially collected from the GIS department of EMWR (see Appendix B). According to the data, dominant soil types in the area are silty clay, silty clay loam, clay loam, and clay. Default soil parameters of AquaCrop for each soil type in the Lake Tana sub-basin is presented in Figure 4-7.

The AquaCrop model has an option of defining the profile of the soil by incorporating up to five horizons of variable textural composition and depth in the root zone. This can be achieved by conducting field measurements (profile pile excavation). For this study, no field sampling has taken place; therefore, a single soil layer was assumed for AquaCrop modelling.

Table 4-7: Default soil parameters of AquaCrop model

Soil Texture	TAW (Total available water) (mm/m)	PWP(Vol%)	FC(Vol%)	SAT	Hydraulic conductivity Ksat(mm/day)
Silty clay	180	32	50	54	100
Silt clay loam	210	23	44	52	150
Clay loam	160	23	39	50	125
Clay	150	39	54	55	35

#### 4.4.5. Irrigation and Field Management Practices

The management practices of the AquaCrop comprises irrigation scheduling, irrigation techniques, and mulching practices. These components are discussed as follows: -

##### 4.4.5.1. Irrigation Techniques

Different criteria are used to classify irrigation techniques, such as energy or pressure required and where and how irrigation water is applied (Ali, 2011). Based on the criteria of the wetted area by irrigation, irrigation techniques can be classified as flood irrigation, trickle, and sprinkler irrigation. Flood irrigation consists of the furrow, basin, and border irrigation. The technique of trickle irrigation comprises drip and subsurface drip irrigation. AquaCrop has integrated the selection of irrigation technique options; thus, the user can choose from sprinkler, drip, and furrow irrigation types. Based on the existing irrigation practices in the Lake Tana area, furrow irrigation is used to simulate the NIR of the different irrigation schemes. Following default settings of the model, 80% wetting

percentage is assumed to be representative of the furrow irrigation technique. The assumption was based on the AquaCrop manual of an indicative range of 60-100% wetting percentage for furrow irrigation (Raes et al., 2013).

#### **4.4.5.2. Irrigation Strategies**

Irrigation strategy is an irrigation management practice that concerns the time and volume of soil water application (Chukalla et al., 2015). Based on the criteria of when to irrigate, irrigation strategies are defined as full irrigation, deficit irrigation, supplementary irrigation. In full irrigation, the soil moisture is kept constantly at field capacity (no stress condition). It is an irrigation strategy that assures the fulfillment of the full evaporative demand, aiming to maximize the crop yield. At the same time, deficit irrigation is when the soil moisture is under different deficit conditions. It is the application of water below evapotranspiration requirements by limiting water application, particularly during less drought-sensitive plant development stages (English, 1990). The supplementary irrigation strategy applies a limited amount of water when rainfall fails to provide enough water for the plant development (Oweis et al., 1999). Full irrigation strategy is used for the net irrigation requirement modelling of planned irrigation schemes in the Lake Tana sub-basin. The irrigation season is fixed between October to May. The selection of the irrigation season is because the dry season from October- May is considered an irrigation season since the rainy period is a rainfed season with some supplementary irrigation in the area. Also, 100% irrigation intensity is assumed. Irrigation intensity is the percentage of the net irrigable area from the total irrigable area.

In the AquaCrop model, the root zone water depletion/readily available water (RAW) is the stress indicator for soil stress, expressed as a fraction of total available water TAW in the soil (Raes et al., 2018). RAW is the percentage of available soil water that can be depleted between irrigations without series water stress. FAO 33 recommended an average level of 50% RAW. Also, in supplementary irrigation, water refilling of the root zone is a one-time process that takes place when 100% RAW is depleted (Chukalla et al., 2015).

The application of irrigation amount also depends on the type of crop and growth stage of crops. Asmamaw et al. (2021) indicated that farmers in the Koga irrigation scheme apply the same amount of water for every crop type and growth stage. Thus, the irrigation threshold is entered into the model by fixing the root zone depletion based on FAO recommendations. FAO recommended 50% of RAW for deep-rooted crops of no-stress condition. The selection of %RAW determines the minimum amount of water that must remain in the root zone throughout the crop growing cycle. Thus, an average of 50% RAW is assumed for this study's AquaCrop modelling of wheat and maize. In addition to this, AquaCrop allows specifying the initial condition of the soil at the start of the simulation period. Since the irrigation season for AquaCrop modelling starts after a long rainy season (i.e., October), the initial condition is assumed as the soil water content is at Field capacity (FC).

#### **4.4.5.3. Mulching Practices**

Mulching practice is a field management practice that involves using organic and inorganic materials in order to cover the cropped surface (Chukalla et al., 2015). There is no awareness of whether such practices are experienced in the area or not. Therefore, moderate application practice of weed management, soil fertility level, and pest was assumed for this study.

#### **4.4.6. Calculation of Gross Irrigation Requirement**

After the AquaCrop simulation of the net irrigation requirement of the crop, the gross irrigation requirement is calculated because the WEAP model needs the gross water requirement of irrigation. The computation of the gross irrigation requirement was performed in the post AquaCrop modelling of the net irrigation requirement, using an excel spreadsheet.

The total amount of water applied by irrigation is called as 'gross irrigation requirement.' In other words, it is the net irrigation requirement plus losses in water application and other losses. The gross irrigation requirement has been computed by applying an Irrigation efficiency. The irrigation efficiency accounts for the losses like conveyance loss, application loss, and distribution loss. It is included in the post AquaCrop modelling of the net irrigation requirement. The gross irrigation requirement is computed by applying 50% irrigation efficiency since AquaCrop does not consider the conveyance and field application losses; instead, it only calculates the water requirement consumed by the crop. The computation of gross irrigation requirement is performed using the following equation.

$$GIR = \frac{NIR}{E} \quad [4-17]$$

Where, *GIR* is gross irrigation requirement, *NIR*, is net irrigation requirement and *E* is irrigation efficiency.

.

## 5. RESULTS

### 5.1. Climate Projections

This section represents the results of baseline and projected climate variables with regard to objective one of the thesis. Results and findings are given on to how extent the climate would change for the future period (2041-2070).

#### 5.1.1. Projected Change in Mean Temperature of Lake Tana

The projected mean annual temperature for RCP4.5 and RCP8.5 emission scenarios shows an overall increasing pattern for the future period. Results on the projected mean annual temperature indicate the future period mean annual temperature of Lake Tana may increase by 1.26 °C and 3.84 °C for RCP4.5 and RCP8.5 emission scenarios, respectively (see Figure 5-1). The mean temperature under the RCP8.5 emission scenario shows a rising pattern over the years.

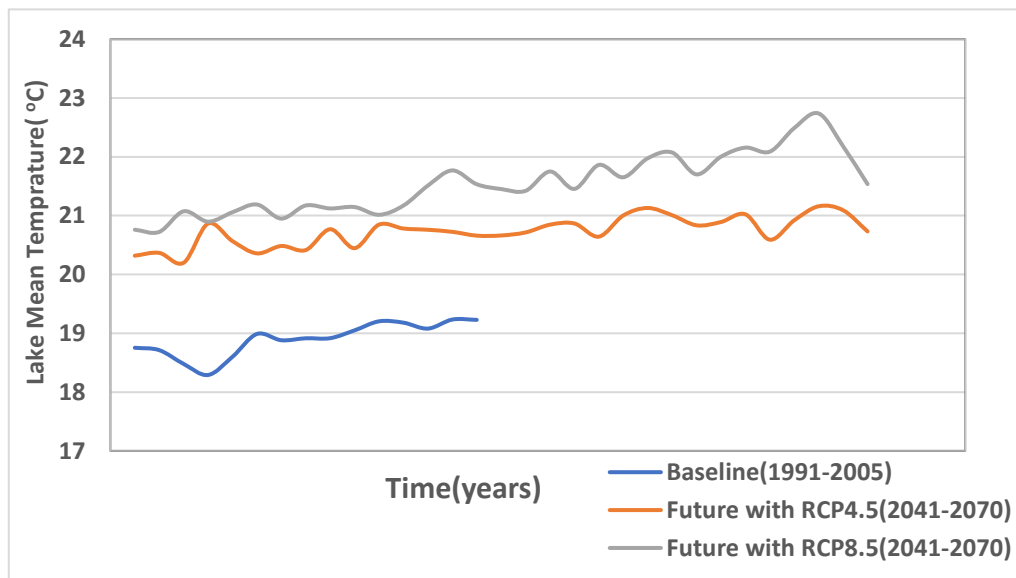


Figure 5-1: Annual temperature of Lake Tana for baseline and future period under RCP4.5 and RCP8.5 emission scenario

Figure 5-2 shows the change in the monthly mean temperature of the RCP4.5 and RCP8.5 emission scenarios. Findings on the average monthly mean temperature of RCP4.5 and RCP8.5 scenarios indicate that the mean monthly temperature will increase for the future period. Projected changes reveal that Lake Tana's mean temperature will likely increase for all months of the year. Changes for the RCP4.5 scenario show that the largest increment will be expected from July to August, reaching 11.4% in July. The largest temperature increases for the RCP8.5 emission scenario will be expected from July to January, reaching 15% in November.

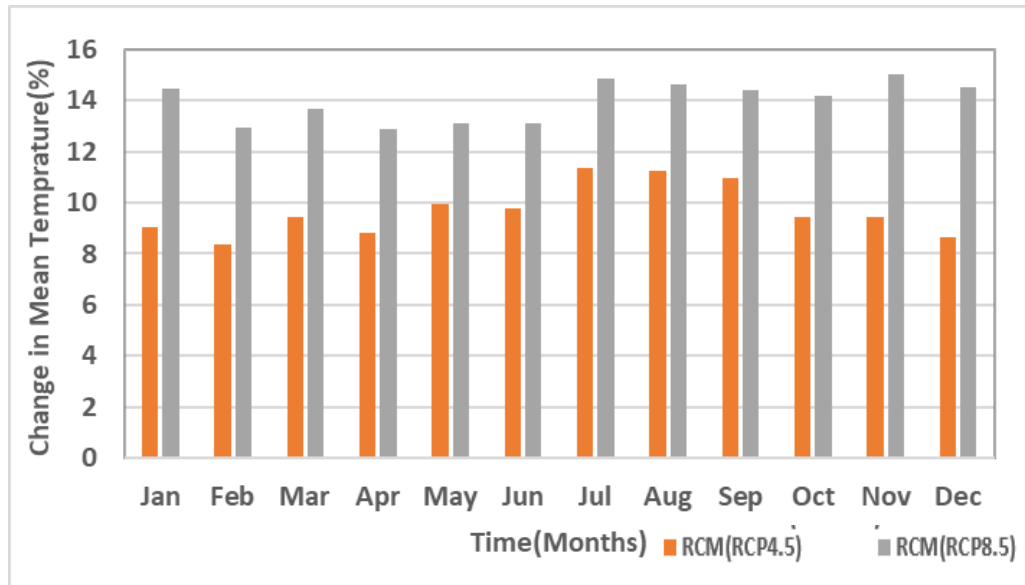


Figure 5-2: Projected monthly changes of Lake Tana mean temperature for the future period under RCP4.5 and RCP8.5 emission scenarios

### 5.1.2. Projected Change in Catchment Mean Temperature

Figure 5-3 contains the graphical representation of the baseline and projected period mean annual catchment temperature for the future period. Results of the catchment mean annual temperature has similar nature to the mean annual temperature of Lake Tana. The catchment mean annual temperature also shows an increasing pattern under the RCP4.5 and RCP8.5 scenarios. The mean annual temperature of the catchment may increase by 1.1 °C and 2.8 °C for RCP4.5 and RCP8.5 emission scenarios, respectively (see Figure 5-3).

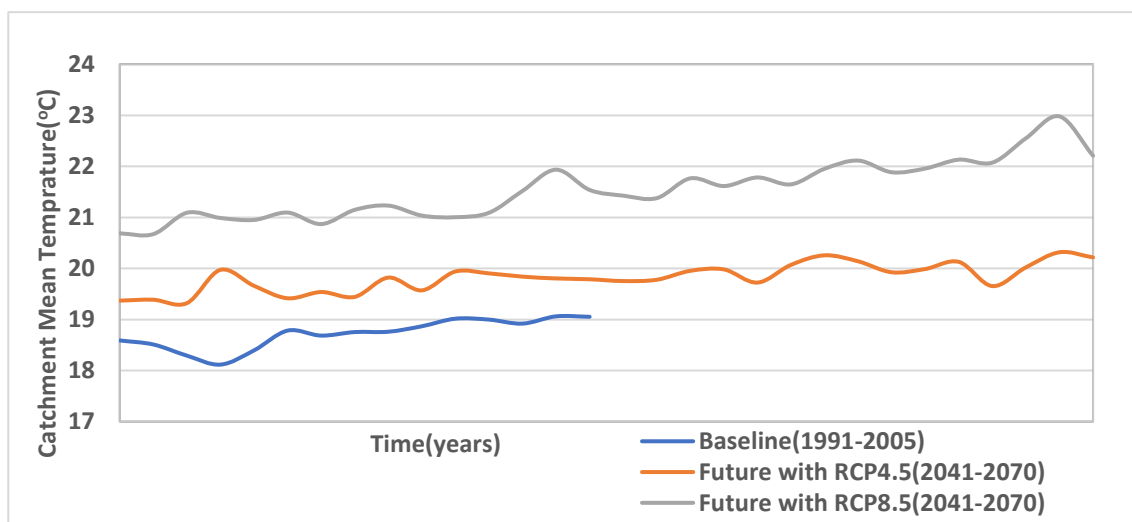


Figure 5-3: Annual mean temperature of catchments for baseline and future period under RCP4.5 and RCP8.5 emission scenario

Projected changes in monthly catchment mean temperature shows an overall increasing pattern for RCP4.5 and RCP8.5 scenarios (see Figure 5-4). According to the ensemble mean RCM products, the future catchment mean temperature will likely increase for all months of the year. The largest increment under the RCP4.5 scenario will be expected from June to July, reaching 10.2 % in July. A higher change in monthly catchment mean temperature

is shown under RCP8.5 than in the RCP4.5 emission scenario. Projected changes for the RCP8.5 scenario indicate that the largest temperature increment will be expected from July to January, reaching 16.5 % in November.

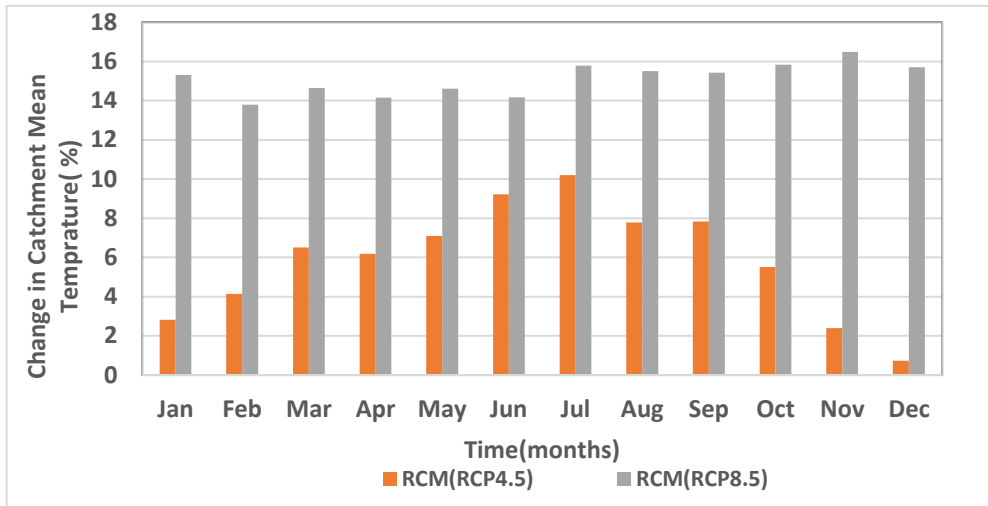


Figure 5-4: Projected monthly changes catchment mean temperature for the future period under RCP4.5 and RCP8.5 emission scenarios.

### 5.1.3. Projected Change in Catchment Precipitation

Figure 5-5 shows the annual catchment precipitation for the baseline and future period under RCP4.5 and RCP8.5 emission scenarios. As seen in the figure, the results of the catchment precipitation show an increasing pattern over the years. Results of the model’s output reveal that catchment annual mean precipitation for the baseline period is 1305 mm/year. The future period catchment annual mean precipitation will likely be 1411 mm/year and 1384 mm/year for RCP4.5 and RCP8.5 emission scenarios, respectively. This change corresponds to an increase of 8.1% and 6.07% future annual rainfall under RCP4.5 and RCP8.5 emission scenarios, respectively.

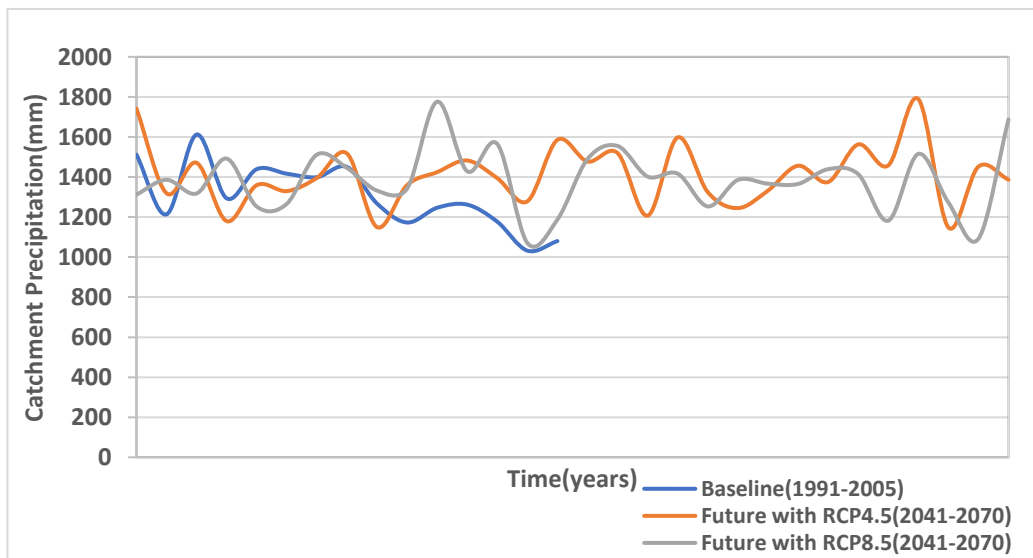


Figure 5-5: Annual catchment precipitation for baseline and future period under RCP4.5 and RCP8.5 emission scenario

Figure 5-6 shows projected change in monthly catchment precipitation for the future period. Unlike the mean temperature, the projections monthly rainfall does not show a consistent increase throughout the months. The corrected RCM ensemble indicates that future catchment precipitation will likely decrease between January and July and increase from August to December. The possible decrement is between 5.3% to 56% for the RCP4.5 scenario and 6.6% to 56.8% for the RCP8.5 scenario. The change in monthly catchment precipitation of the RCP4.5 is greater for the period from August to November. The decrease in the amount of rainfall in June and July (major rainy months) and the extended increase in precipitation until December suggest a shift of rainfall pattern due to climate change.

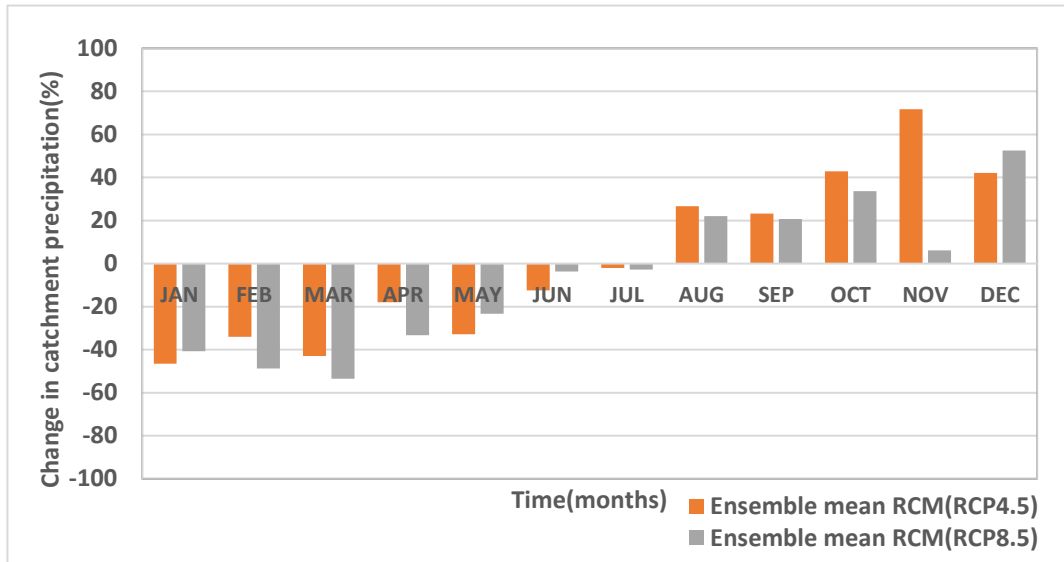


Figure 5-6: Projected changes in monthly mean precipitation of catchments for the future period under RCP4.5 and RCP8.5 emission scenarios

#### 5.1.4. Projected Change in Catchment Potential Evaporation

The change in catchment potential evapotranspiration results presented below is the average PET of the gauged and ungauged catchments calculated using the Penman-Monteith equation. The average annual projected PET was estimated to be 1431 mm/year and 1458 mm/year for the RCP 4.5 and RCP8.5 emission scenarios, respectively, while the baseline period PET is 1376 mm/year. This shows that future catchment evapotranspiration will possibly increase by 4% and 6% under the RCP4.5 and RCP8.5 emission scenarios. The baseline and future period annual PET of the catchment is presented in Figure 5-7.

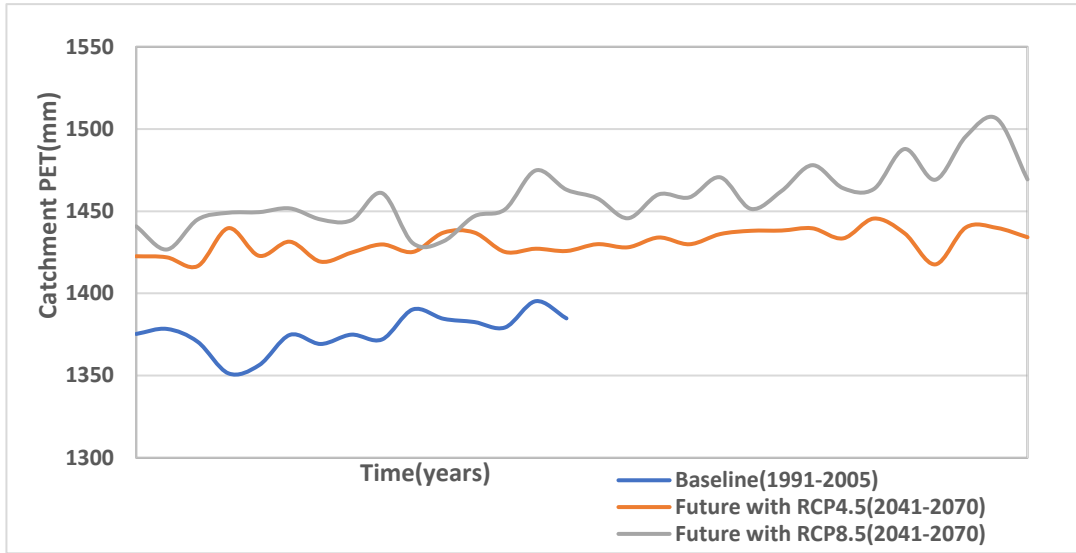


Figure 5-7: Annual catchment PET for baseline and future period under RCP4.5 and RCP8.5 emission scenario

Projected changes in monthly PET by the ensemble RCM indicates that PET will increase for the future period under RCP4.5 and RCP8.5 scenario. The increase in the monthly PET for RCP4.5 and RCP8.5 scenarios shows a consistent pattern (see Figure 5-8). The result indicated that the catchment potential evapotranspiration will increase for all months. According to the result, catchments in the Lake Tana sub-basin will experience the largest PET increment in July and August. Under both scenarios, the maximum PET increment will likely occur in July and August, with the largest increment of 5.2% and 6.6% in July for RCP4.5 and RCP8.5 emission scenarios, respectively.

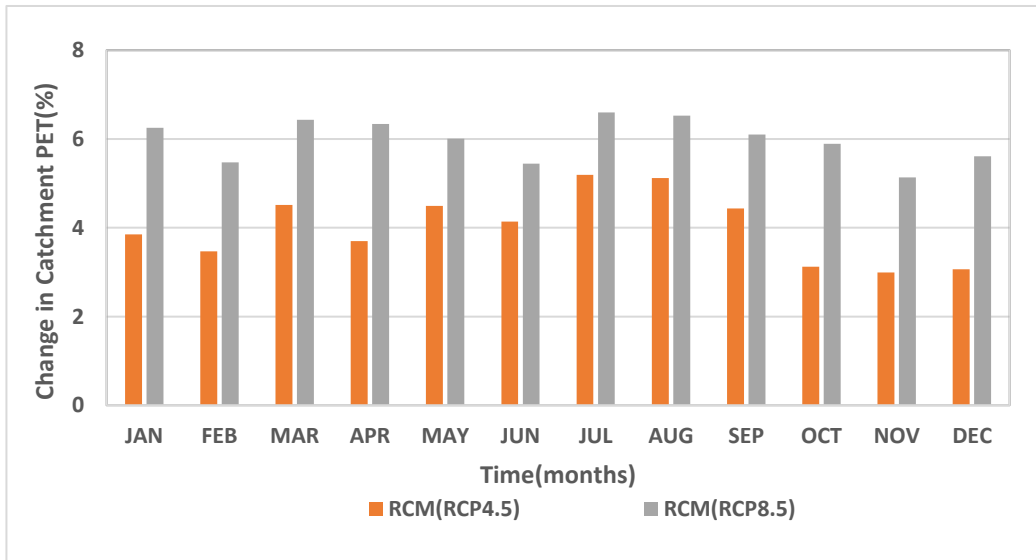


Figure 5-8: Projected changes in monthly catchment PET for the future period under RCP4.5 and RCP8.5 emission scenario

## 5.2. Lake Water Balance Components

The findings presented under this section are the result of the water balance components. The results presented here are based on objective two of the study.

### 5.2.1. HBV Model Result

The evaluation result of previously calibrated HBV parameters by Perera (2009) for an extended period from 1997-2005 is presented in Table 5-1. The evaluation has been performed in five gauged catchments of the sub-basin: Ribb, Gumara, Koga, Megech, Gilgel Abay. The results for the evaluation of previously set parameters showed satisfactory results for most catchments. However, it resulted in a large RVE (the relative volume error) for Gilgel Abay and Gumara catchment. This might be because of the extended period for evaluation and the use of the automated calibration approach by Perera (2009). Thus, recalibration of the HBV parameter set for Gilgel Abay and Gumara catchments has been done by following the sensitivity analysis performed by Perera (2009) and adjusting the most sensitive parameter to the NS and RVE error.

Table 5-1: Evaluation of Previously calibrated parameters

Catchments	NS	RVE (%)	Simulation period
Gilgel Abay	0.75	8.55	1997-2005
Gumara	0.76	-10.91	1997-2005
Koga	0.6	-0.59	1997-2005
Ribb	0.82	1.14	1997-2005
Megech	0.58	0.98	1997-2005

#### 5.2.1.1. Model Calibration Result

According to the study by Perera (2009), the most sensitive parameters for the RVE error in Gilgel Abay and Gumara catchments are FC, Beta, LP. Major parameter adjustments have been undertaken to those parameters. No major adjustment was made to the parameters, which does not significantly affect the model performance with respect to the RVE error. These parameters are KS, PERC, CFLUX.

The following table shows the calibrated parameters for the Gilgel Abay and Gumara catchments and Nash Sutcliffe (NSE) and Relative Volume Error (RVE) values.

Table 5-2: Calibrated model parameters for Gilgel Abay and Gumara catchment

HBV parameters	Gilgel Abay	Gumara
FC (mm)	500	265
BETA (-)	2.3	1.25
LP (-)	0.66	0.93
ALFA (-)	0.24	0.25
KF(1/d)	0.1	0.03
KS(1/d)	0.09	0.07
PERC (mm/d)	1.2	1.44
CFLUX (mm/d)	1.1	0.7
NS (-)	0.76	0.76
RVE (%)	4.54	-2.74

Figure 5-9 shows the simulated and observed streamflow for the calibration period (1997-2003) at Gilgel Abay and Gumara catchments. As seen in the figures, the HBV model has well captured the overall pattern of the observed hydrograph. Also, the NSE and RVE values reveal that the simulated streamflow for Gilgel Abay and Gumara catchments captured the observed discharge well.

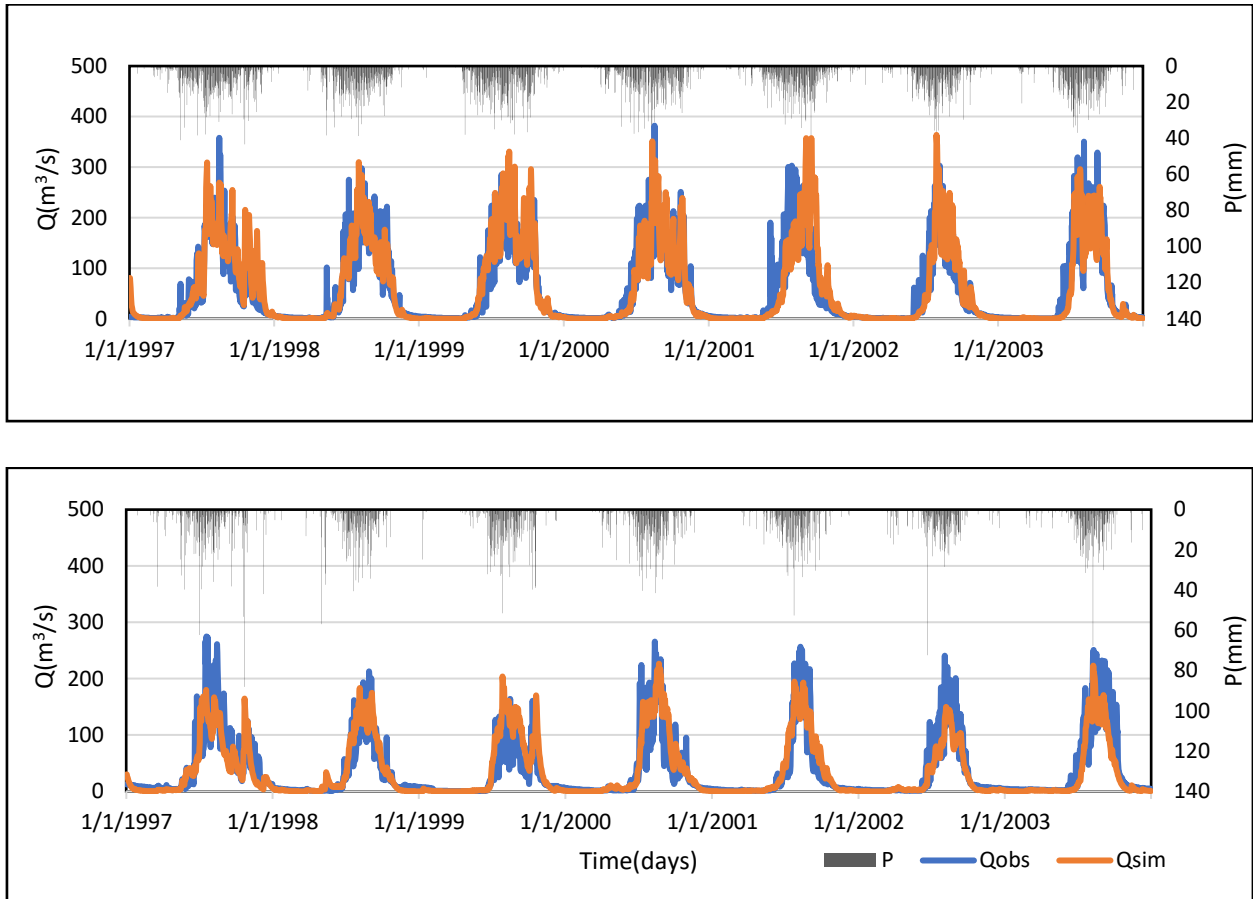


Figure 5-9 Model calibration results of Gilgel Abay and Gumara catchment

Table 5-3 shows the model parameters used for the simulation of gauged catchments in this study. The table contains the calibrated model parameters for Gilgel Abay & Gumara catchments and model parameters for gauged catchments obtained from Perera (2009).

Table 5-3: HBV model parameters for gauged catchments

Gauged Catchments	FC (mm)	BETA (-)	LP (-)	ALFA (-)	KF(1/d)	KS(1/d)	PERC (mm/d)	CFLUX (mm/d)
Ribb	309	1.23	0.73	0.31	0.07	0.1	1.09	0.6
Gilgel Abay	500	2.3	0.66	0.24	0.1	0.09	1.2	1.1
Gumara	265	1.25	0.93	0.25	0.03	0.07	1.44	0.7
Megech	193	1.56	0.71	0.29	0.03	0.09	1.47	0.79
Koga	730.	1.34	0.42	0.41	0.07	0.05	1.63	0.74
Kelti	219	2.43	0.72	0.41	0.09	0.06	1.29	1.07

**5.2.1.2. Model Validation Result**

Table 5-4 shows the result of model validation for Gilgel Abay and Gumara catchments. The model validation of Gumara catchment showed a better performance than the model calibration, with improved NS and RVE values of 0.78 and 1.1%, respectively. Model validation result for Gilgel Abay catchment showed an NS value of 0.73 and an improved relative volumetric error of 2.61% than the model calibration result.

Table 5-4: HBV model validation result for Gilgel Abay and Gumara catchments from 2004-2005

Catchments	Gilgel Abay	Gumara
NS (-)	0.73	0.78
RVE (%)	2.61	1.1

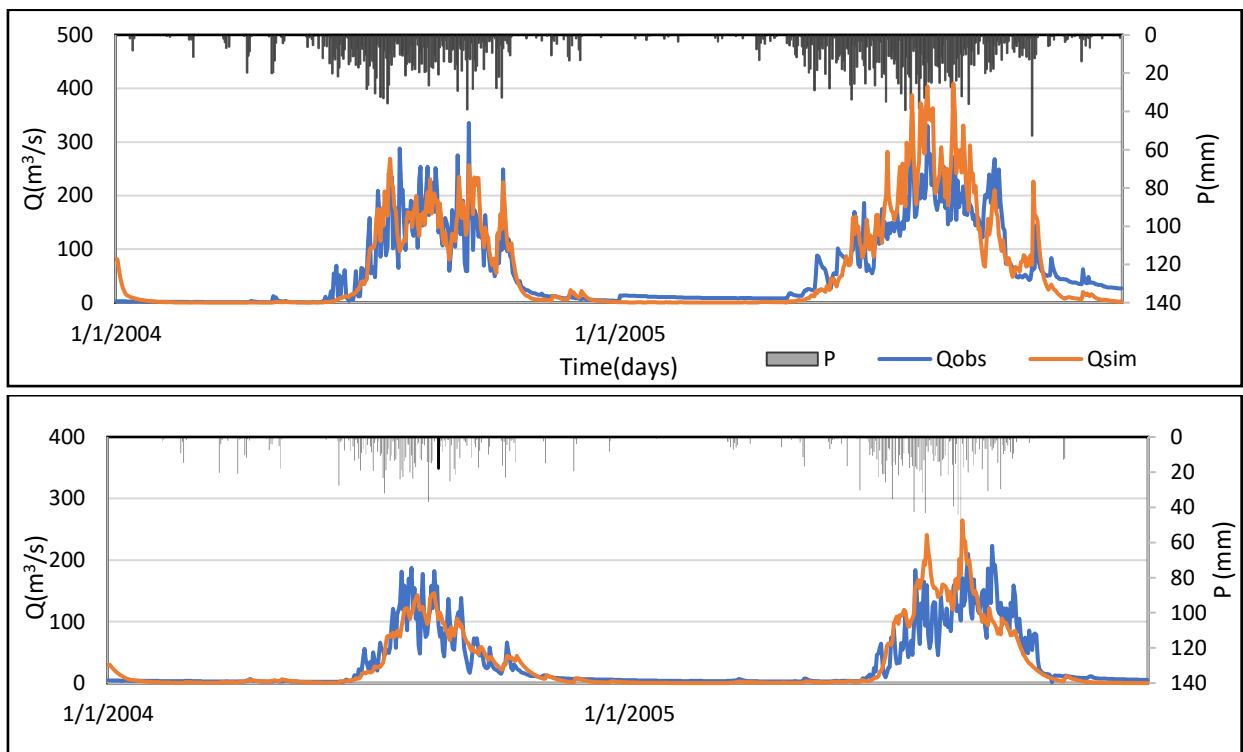


Figure 5-10: Model validation result of Gilgel Abay and Gumara catchment from 2004-2005

### 5.2.1.3. Result of Regionalization

The regionalization approach presented below was achieved after the evaluation of HBV model performance to represent the gauged catchments. The results of the multiple regression approach performed are shown in Table 5-5.

Table 5-5: Developed Regional model equation

Model parameters	$\beta_0$	$\beta_1$	$\beta_2$	$\beta_3$	R <sup>2</sup> (%)
$FC = \beta_0 + \beta_1 * HI$	3591.46	-6807.1			62
$BETA = \beta_0 + \beta_1 * SHAPE + \beta_2 * HI$	7.88	-0.039	-8.902		90
$LP = \beta_0 + \beta_1 * HI + \beta_2 * LUV$	-2.4967	6.3813	0.0032		91
$ALFA = \beta_0 + \beta_1 * AREA + \beta_2 * URBAN$	0.45215	-0.00009	-0.73563		92.73
$KF = \beta_0 + \beta_1 * SAAR$	-0.0701	0.00009			59.03
$KS = \beta_0 + \beta_1 * AVGSLOPE$	0.0183	0.0018			84.72
$PERC = \beta_0 + \beta_1 * DD + \beta_2 * SAAR$	6.8784	-0.012	-0.0003		96.8
$CFLUX = \beta_0 + \beta_1 * SHAPE + \beta_2 * PDRY + \beta_3 * PET$	-0.3834	-0.0082	0.405	0.0008	99.97

### 5.2.1.4. Validation of Regional Model

Table 5-6 shows the validation result of the regional model on the gauge catchment (2003-2005). The developed regional model performed well when evaluated on the gauged catchments. The validation result indicates a fair performance of the regional model in simulating the gauged catchments inflow.

Table 5-6: Validation of a regional model of the gauged catchment from 2003-2005

Gauged Catchments	FC	BETA	LP	ALFA	KF	KS	PERC	CFLUX	NS	RVE	Validation period
Ribb	294	1.16	0.71	0.29	0.06	0.1	1.13	0.6	0.79	-0.68	2003-2005
Gilgel Abay	329	2.04	0.74	0.25	0.1	0.08	1.22	1.11	0.54	5	2003-2005
Gumara	302	1.5	0.86	0.28	0.06	0.08	1.41	0.7	0.72	-4.91	2003-2005
Megech	194	1.56	0.7	0.29	0.03	0.09	1.47	0.79	0.5	-10	2003-2005
Koga	663	1.31	0.4	0.43	0.07	0.06	1.65	0.74	0.77	7.36	2003-2005

### 5.2.2. Lake Precipitation

Results of the future period annual mean precipitation of Lake Tana shows that Lake Tana is likely to experience an increase in mean annual precipitation for the period of 2041-2070 under both RCP4.5 and RCP8.5 emission scenario (see Figure 5-11). The baseline mean annual precipitation of the lake is 1438 mm/year. The climate model projection indicates that the long-term annual mean precipitation of the future period will be 1498 mm/year and 1442 mm/year for RCP4.5 and RCP8.5 emission scenarios, respectively. The change in the precipitation will be 4.2 % and 0.3 % for RCP4.5 and RCP8.5 scenarios, respectively.

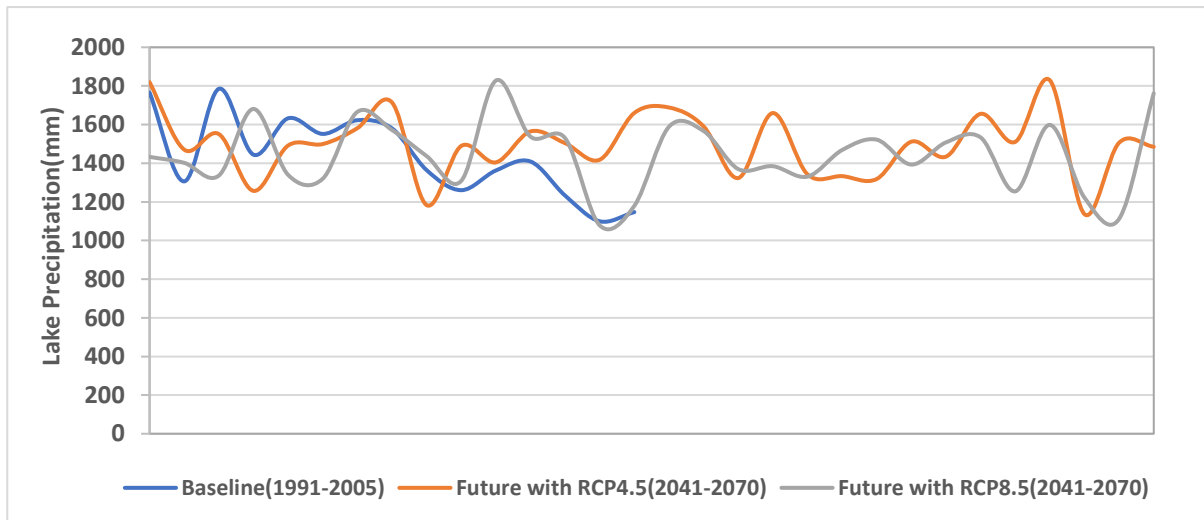


Figure 5-11: Lake Tana's annual precipitation for baseline and future period under RCP4.5 and RCP8.5 emission scenario

According to the ensemble of the model's output, there will be a possibility of increment in the future precipitation from August to December (See figure 5-12). The increase in the precipitation is higher for the RCP4.5 scenario than the RCP8.5 scenario. The increase in precipitation would possibly propagate up to the maximum of 80% and 37% for the RCM model under RCP4.5 and RCP8.5 emission scenarios, respectively. Projected change in lake area precipitation shows a decreasing pattern during the dry season. The decrement of precipitation for the dry season is expected to be a maximum of 56% and 61% for RCP4.5 and RCP8.5, respectively.

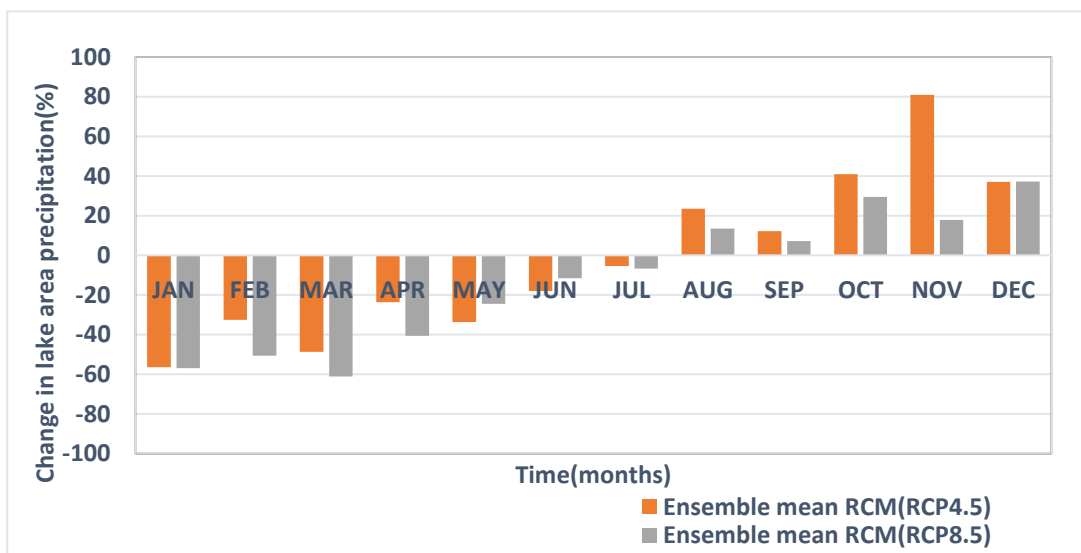


Figure 5-12: Projected changes in monthly Lake precipitation for the future period under RCP4.5 and RCP8.5 emission scenario

### 5.2.3. Lake Evaporation

The open water estimation results show Lake Tana’s annual mean evaporation for the baseline period is 1845 mm/year, 1896 mm/year, and 1922 mm/year for the future period under RCP4.5 and RCP8.5 emission scenarios, respectively. This shows a 2.76% and 4.17% increase of lake evaporation under RCP4.5 and RCP8.5, respectively (see Figure 5-13).

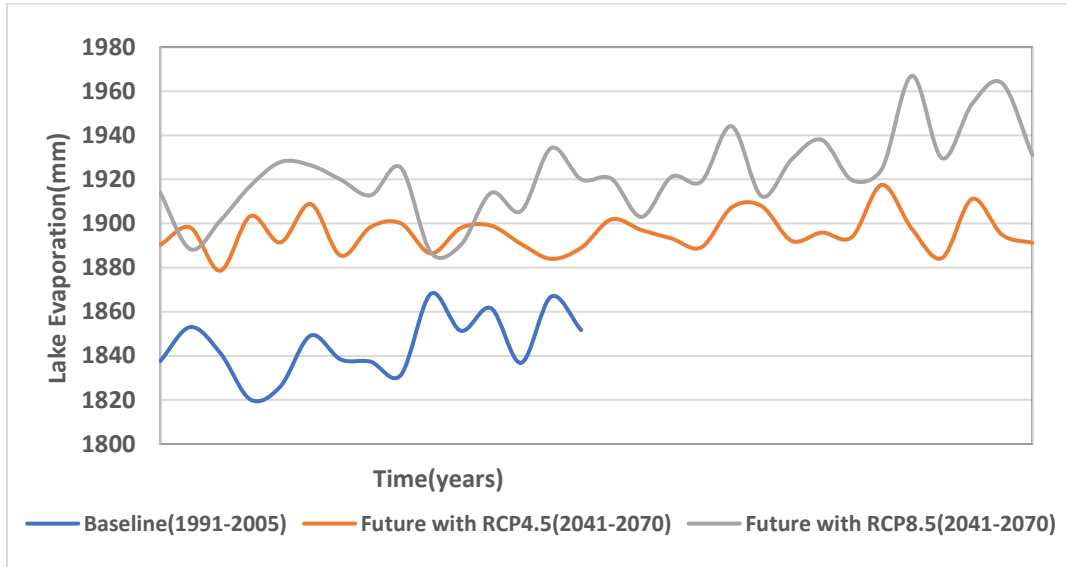


Figure 5-13: Lake Tana's annual evaporation for baseline and future period under RCP4.5 and RCP8.5 emission scenario

The monthly change in projected evaporation of Lake Tana for the period (2041-2070) is presented in Figure 5-14. Projected lake evaporation for both emission scenarios (RCP4.5 & RCP8.5) showed an increasing pattern for the future period. The change in the percentage of lake evaporation is greater for the RCP8.5 emission scenario.

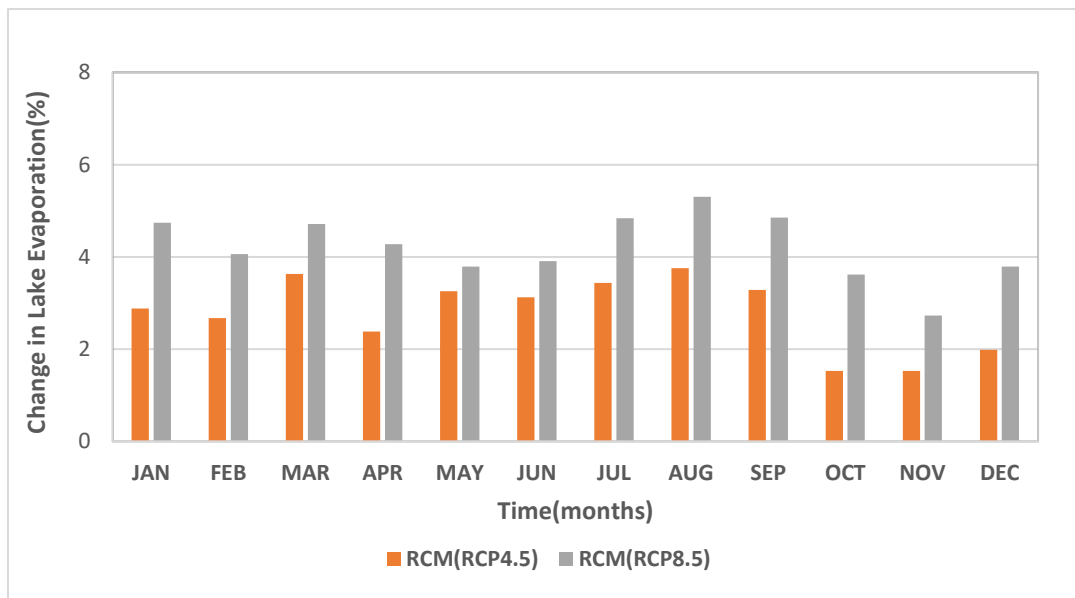


Figure 5-14: Projected change in monthly lake evaporation for the future period under RCP4.5 and RCP8.5 emission scenario

Figure 5-15 illustrates the five-year annual average lake evaporation and lake precipitation of the future period for RCP4.5 and RCP8.5 emission scenarios. As it is seen from the figures, the lake evaporation of the RCP8.5 is higher than the RCP4.5 and shows an accelerated increase over the year. Precipitation of the lake does not show a consistent change over the simulation period. However, the amount of annual rainfall is higher for the RCP4.5 scenario.

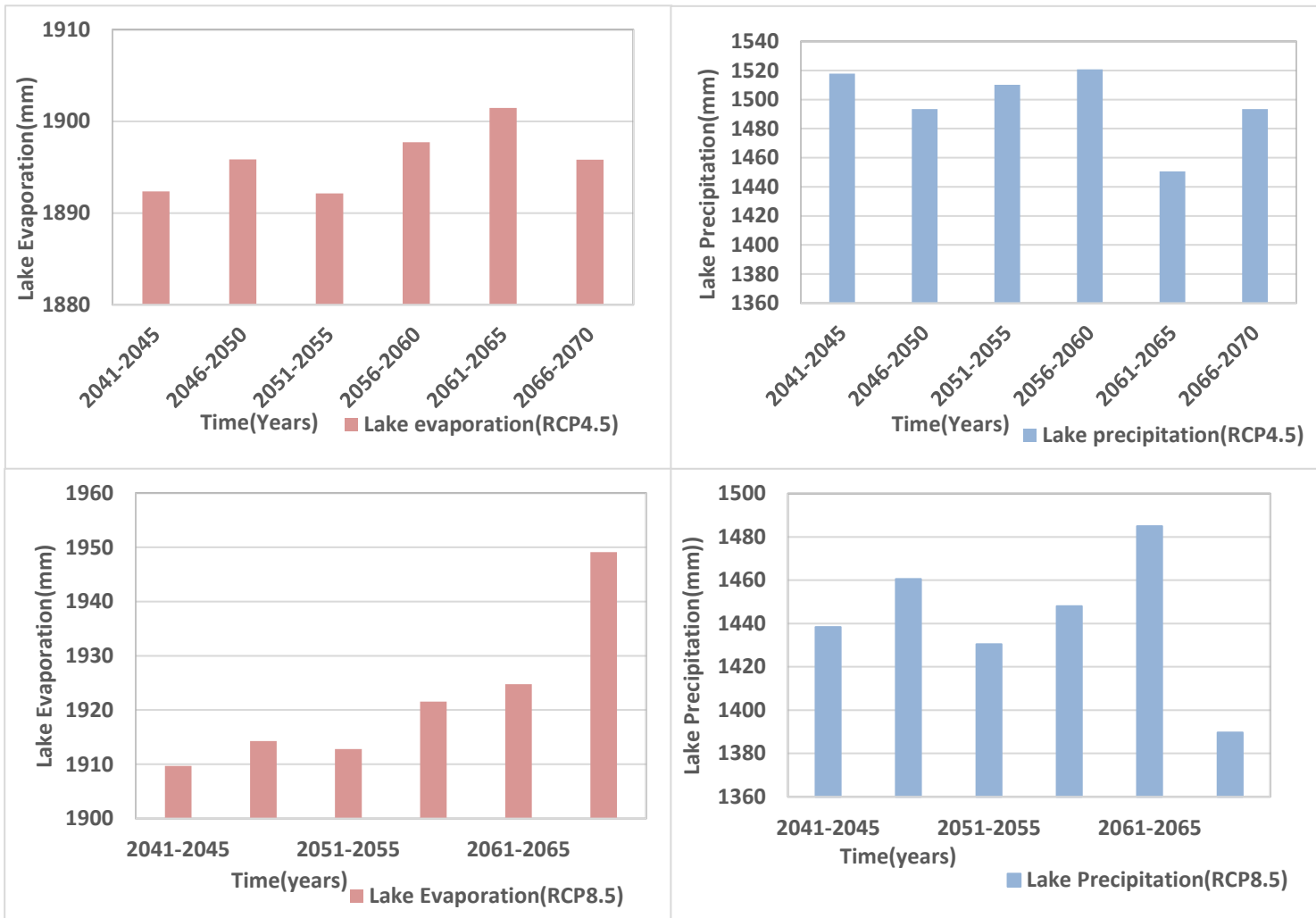


Figure 5-15: Projected five-year average lake evaporation and precipitation for RCP4.5 and RCP8.5 scenarios

#### 5.2.4. Surface Water Inflow

Bias corrected ensemble mean RCM climate data (mean temperature, potential evapotranspiration, and rainfall data) were used as input to the HBV model to simulate the baseline and future period streamflow. For this study, the HBV simulation result of the annual lake inflow under the future period showed an inconsistent pattern similar to the catchment precipitation. Although the future annual lake inflow does not show a consistent pattern, the mean annual lake inflow of the future period will likely be larger than the baseline period. Results of the HBV simulation indicated a mean yearly lake inflow of 2606 mm/year for the baseline period and 3059 mm/year, 2937 mm/year future inflow is simulated for RCP4.5 and RCP8.5 emission scenario(see Figure 5.16).

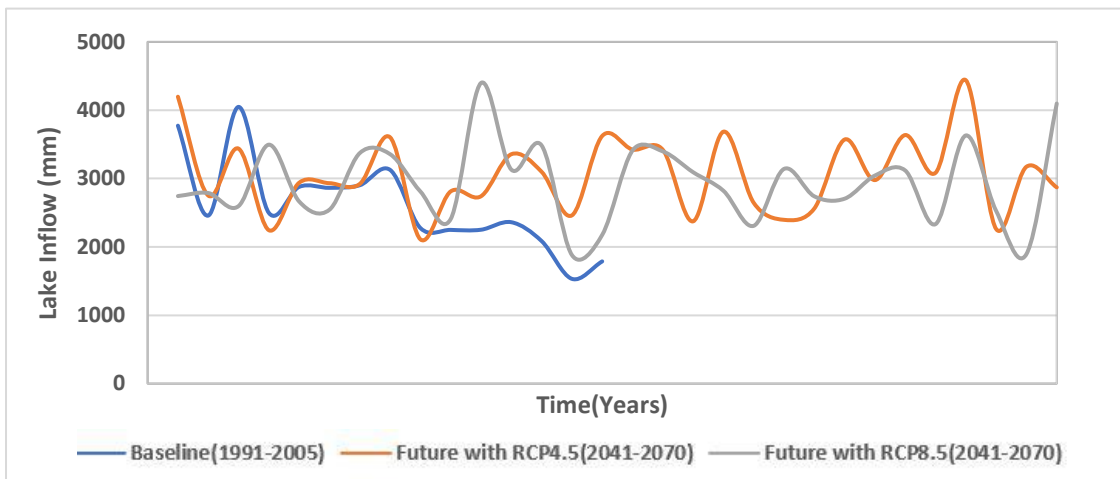


Figure 5-16: Lake Tana's annual inflow for baseline and future period under RCP4.5 and RCP8.5 emission scenario

The monthly HBV model output indicates that the future lake inflow could be affected by the change in rainfall of the future period. The future streamflow shows an increase and decrease of runoff in the wet and dry seasons, respectively( see Figure 5-17). This is mainly due to the increase in precipitation for the wet season and a decrease in the dry season.

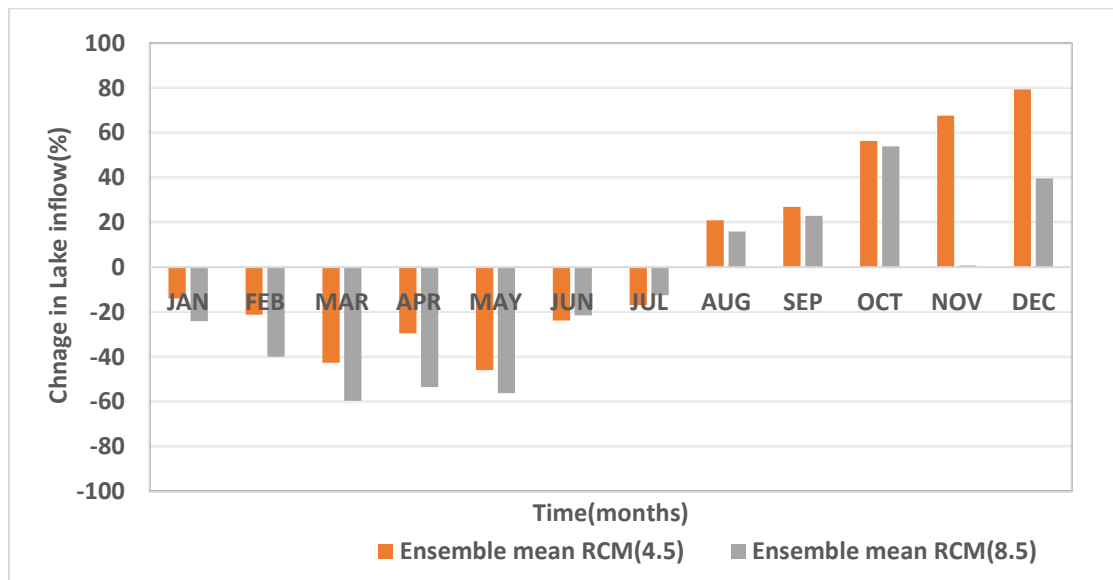


Figure 5-17: Projected change in monthly inflow for the future period under RCP4.5 and RCP8.5 emission scenario

### 5.2.5. Lake Outflow

Figure 5-18 illustrates the performance evaluation of the *Beta* coefficient to compute the lake outflow. The performance of the coefficient is evaluated for different values starting from 0.5 to 0.9. The outflow was calculated with the assumed coefficient, and the lake level was simulated by using all the water balance components. The *Beta* coefficient, which gave better NSE and R<sup>2</sup> value of was 0.865. The NSE and R<sup>2</sup> values of 0.74 and 0.78 were indicated as a result of a comparison between the simulated and observed water levels (see Figure 5-18). The observed and simulated lake level calculated with the established *Beta* is presented in Figure 5-19.

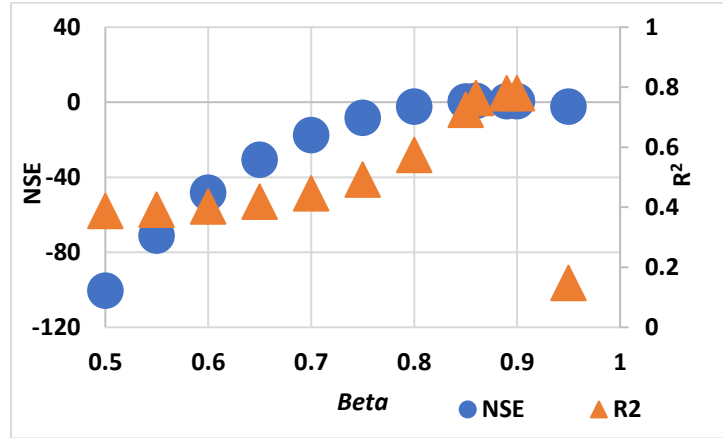


Figure 5-18: Evaluation of *Beta* coefficient for Lake Tana outflow computation (1991-2005)

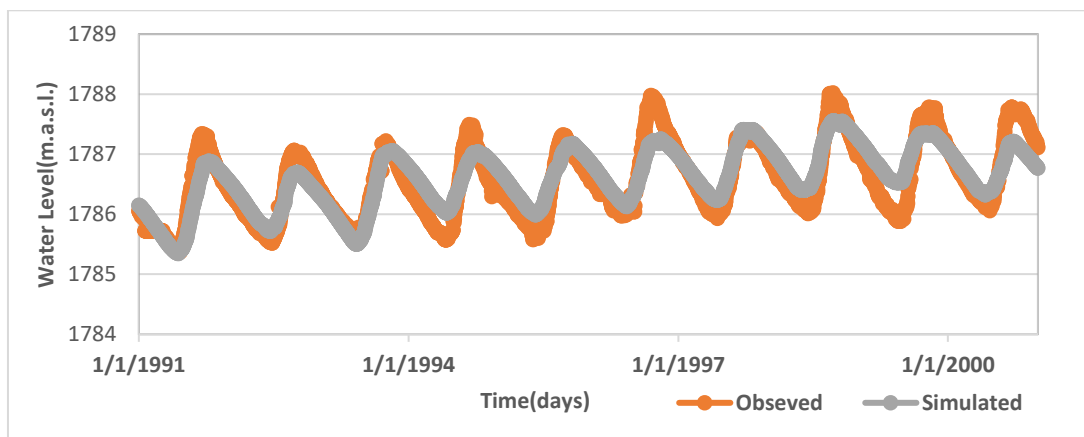


Figure 5-19: Observed and simulated lake level (1991-2005) as a result of outflow computation

Lake Tana's mean annual outflow of the baseline period is 2254 mm/year. The future outflow of the lake will likely be 2646 mm/year and 2541 mm/year, respectively.

### 5.2.6. Water Balance of Irrigation Dams

The result of the upstream flow of the irrigation dams is presented in Figure 5-20. According to the result, the flow upstream of the Gilgel Abay dam has the highest flow than the other five dams. And flow upstream of the Koga dam has the lowest flow. This is explained by the different sizes of the upstream area above the irrigation dam.

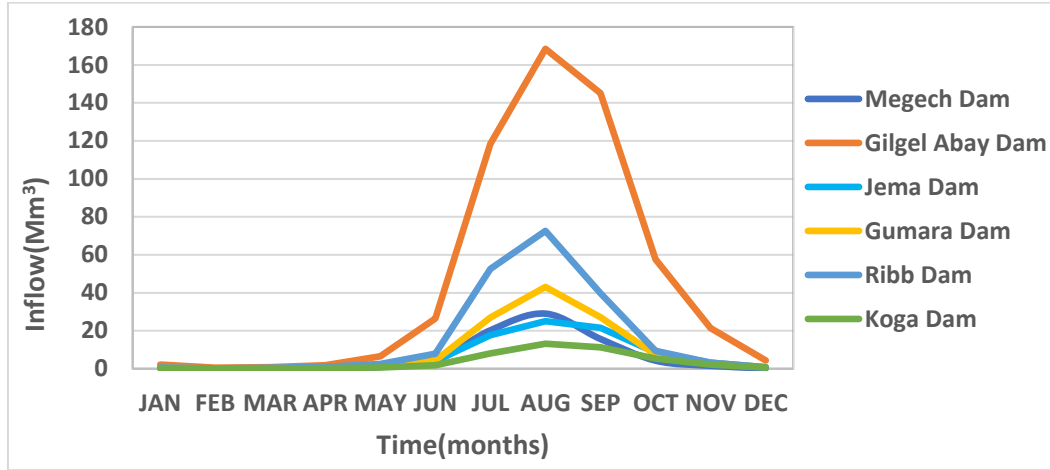


Figure 5-20: Flow upstream of the six irrigation dams

**5.2.7. Dam Precipitation and Evaporation**

Table 5-7 shows the irrigation dams' mean annual evaporation and precipitation in the Lake Tana sub-basin. The table shows that Jema dam receives the highest precipitation, and Megech receives the lowest. As explained in the data processing section of this thesis, the southern part of the sub-basin receives the highest precipitation, whereas the northern receives the lowest. The highest evaporation amount of the Megech dam can also be associated with the higher temperature Gonder station, which is a nearby station to Megech catchment.

Table 5-7: Mean annual evaporation and precipitation of irrigation dams

Dams	Mean annual evaporation(mm/year)	Mean annual precipitation(mm/year)
Ribb	1490	1372
Gumara	1510	1391
Megech	1702	1107
Gilgel Abay	1658	1581
Koga	1657	1508
Jema	1641	1943

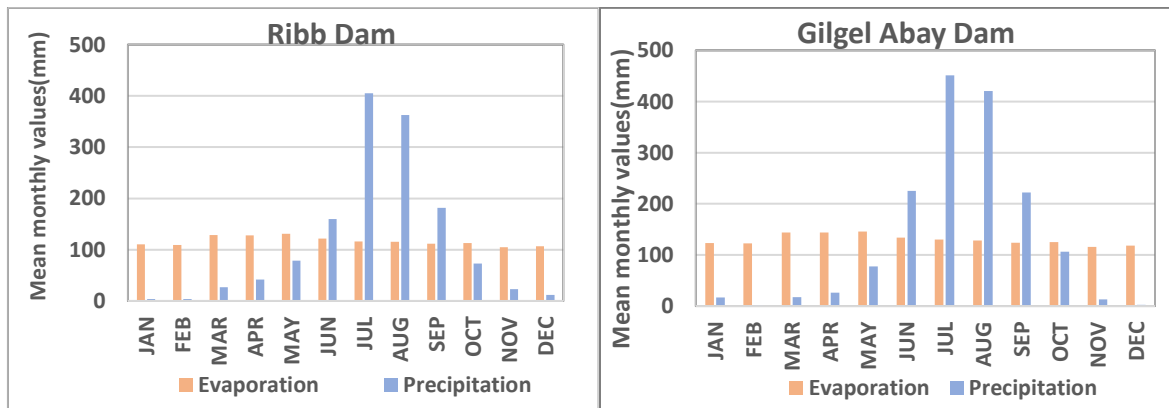


Figure 5-21: Mean monthly evaporation and precipitation for Ribb and Gilgel Abay Dams

### 5.3. Irrigation Requirement

Figure 5-22 illustrates the monthly gross irrigation requirement of 11 irrigation schemes in the Tana sub-basin for the baseline and future period under the RCP4.5 and RCP8.5 emission scenarios. According to the result, the Peak irrigation water requirement of the baseline period is in February. While the peak water requirement of the future period under RCP4.5 and RCP8.5 emission scenarios will likely be in January. This indicates that the future peak water requirement will possibly occur one month earlier than the baseline period. This shift in peak irrigation water requirement and shortening the development cycle of the future period are associated mainly with the rise in temperature and the increase in atmospheric CO<sub>2</sub> concentration of the future period under both RCP4.5 and RCP8.5 emission scenarios. In addition to the shift in the peak water requirement and the shortening of the development period, AquaCrop predicted a decrease in water requirement for both RCP4.5 and RCP8.5 emission scenarios (see Figure 5-22). The decrement is higher under the RCP8.5 scenario. Although the dry period (irrigation season) under the RCP8.5 scenario will experience higher temperature and decrease of precipitation than the RCP4.5 scenario, the irrigation requirement under the RCP8.5 emission scenario is lower.

The MaunaLoa. CO<sub>2</sub> concentration used for the baseline period irrigation requirement ranges approximately between 360 ppm to 380 ppm for the period between 1991-2005. The CO<sub>2</sub> concentration under the RCP4.5 scenario increases approximately from 460 ppm to higher than 500 ppm between the period 2041 -2070. While RCP8.5 scenario shows a high increment from 500 ppm to higher than 650 ppm between the future period.

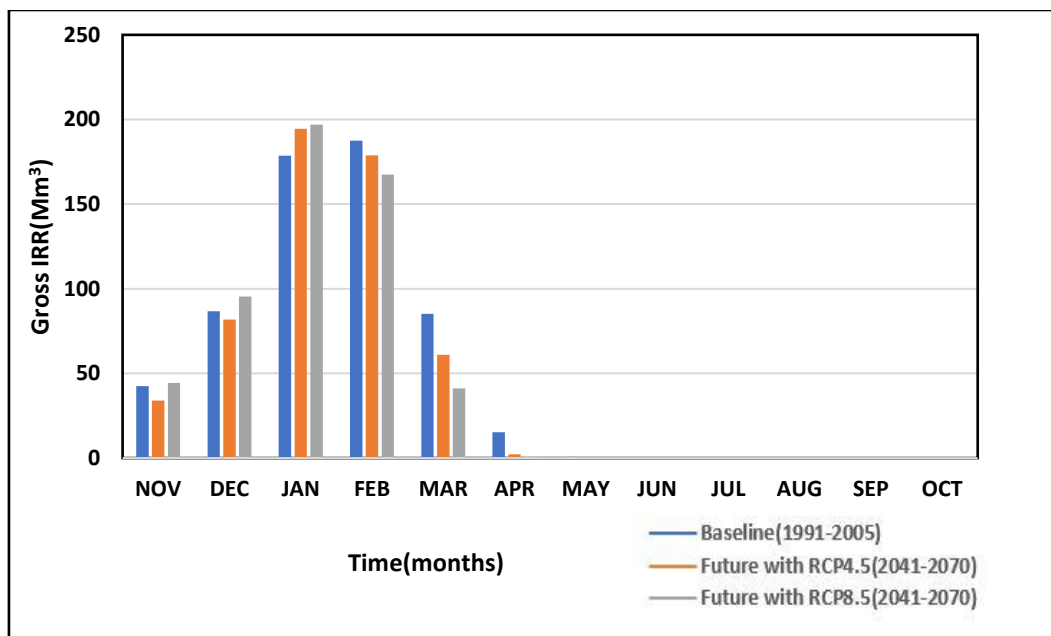


Figure 5-22: Monthly gross irrigation requirement

Table 5-8 shows the baseline and projected gross irrigation requirement of irrigation schemes in the Lake Tana sub-basin. According to the results, for overall 50% irrigation efficiency, the gross irrigation requirement in Tana sub-basin under the baseline scenario is 596.67 Mm<sup>3</sup>/year. The future period average annual gross irrigation requirement under the RCP4.5 and RCP8.5 emission scenarios is 552.50 Mm<sup>3</sup>/year and 545.72 Mm<sup>3</sup>/year, respectively. This indicates a 7.4% and 8.54% reduction of gross water requirement for the future period under the RCP4.5 and RCP8.5 emission scenarios.

Table 5-8: Annual gross irrigation requirement for baseline and future period under land use intervention scenario

Irrigation schemes	Area(ha)	Baseline	Future land use interventions (RCP4.5)	Future land use interventions (RCP8.5)
		Land use interventions	Annual gross IRR (Mm <sup>3</sup> /year)	Annual gross IRR (Mm <sup>3</sup> /year)
Gilgel Abay	11250	71.80	70.09	68.00
Gumara	14800	90.60	81.62	80.75
Jema	7559	48.02	47.09	46.88
Koga	7000	44.38	43.32	42.45
Megech	14621	96.41	84.44	86.10
Megech Ribit	6024	40.55	36.17	36.23
Megech Serbera	4040	25.45	24.97	24.50
NE Tana	3903	23.32	21.63	21.29
NW Tana	6719	41.27	35.66	34.19
Ribb	14460	78.33	73.17	71.45
SW Tana	5132	36.54	34.34	33.87
<b>Total</b>		<b>596.67</b>	<b>552.50</b>	<b>545.72</b>
		<b>(Mm<sup>3</sup>/year)</b>		

The irrigation requirement of baseline and future scenario under RCP4.5 and RCP8.5 show that irrigation requirement of Gumara, Megech, and Ribb irrigation schemes is higher with 96.41 Mm<sup>3</sup>/year, 90.6 Mm<sup>3</sup>/year, and 78.33 Mm<sup>3</sup>/year for the period 1991-2005(see Figure 5-23 & Table 5-8). Megech Serbera and NE Tana receive the lowest irrigation water of 25.45 Mm<sup>3</sup>/year and 23.32 Mm<sup>3</sup>/year for the baseline period. The size of the irrigation area mainly explains this difference in the water requirement of the irrigation schemes.

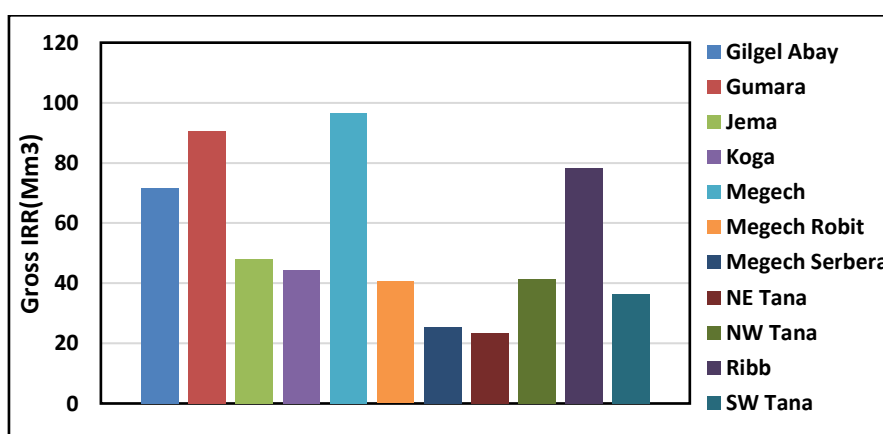


Figure 5-23: Gross irrigation requirement of the baseline period

The annual water use rate of the irrigation schemes in the Lake Tana sub-basin is presented in Table 5-9. The annual water use rate explains how much water is needed for one hectare of each irrigation scheme in the sub-basin.

Table 5-9: Annual water use rate of each irrigation scheme (Mm<sup>3</sup>/ha)

Irrigation Schemes	Area(ha)	Baseline period	Future land use	Future land use
		land use intervention	intervention (RCP4.5)	intervention (RCP8.5)
Gilgel Abay	11250	6382.28	6230.21	6044.88
Gumara	14800	6121.33	5514.97	5456.17
Jema	7559	6353.23	6229.51	6202.20
Koga	7000	6340.61	6188.75	6064.02
Megech	14621	6593.60	5775.50	5888.81
Megech Ribit	6024	6730.69	6004.81	6013.77
Megech Serbera	4040	6298.77	6179.95	6064.74
NE Tana	3903	5975.28	5541.15	5454.28
NW Tana	6719	6141.75	5306.63	5089.26
Ribb	14460	5417.21	5060.47	4941.36
SW Tana	5132	7120.64	6690.46	6598.98

## 5.4. Water Balance

### 5.4.1. Calibration of WEAP Model

The result of WEAP model calibration shows a good match between the simulated and observed lake levels for the period 1991 - 2000 (see Figure 5-24). The WEAP model well captured the pattern of the observed lake level with seasonal effects by wet and dry seasons. Model performance of the lake level simulation resulted in NSE and  $R^2$  values of 0.78 and 0.79, respectively. These values indicate adequate model simulation performance, and it appears that ensemble mean RCM data used for simulation is of sufficient quality to serve model simulations in this thesis.

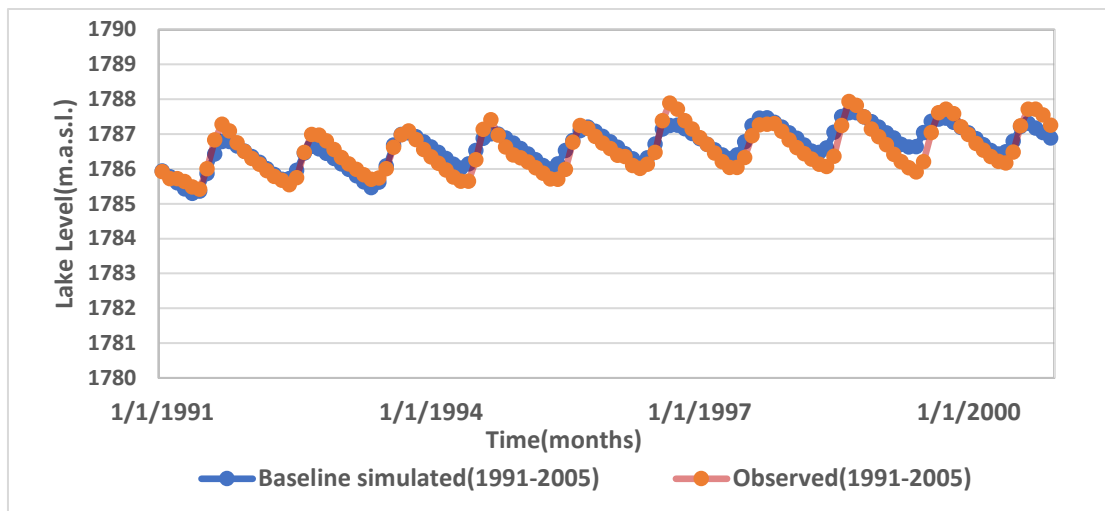


Figure 5-24: Observed and simulated lake levels for the period 1991-2005

### 5.4.2. Lake Level Simulations

#### 5.4.2.1. Baseline Scenario (1991-2005)

The baseline period, water level simulation result indicates that the mean annual lake level is 1786.45 m.a.s.l. (see Figure 5-25). According to the simulation result, the monthly maximum and minimum water level occurs in September and May, respectively. 1786.92 m.a.s.l. and 1785.93 m.a.s.l. are the maximum and minimum lake level respectively (see Figure 5-28 & Table 5-11).

#### 5.4.2.2. Baseline Period under Land Use Interventions (1991-2005)

This scenario includes irrigation consumption by planned large-scale irrigation projects and environmental flow requirements downstream of the proposed dams and Tiss Abay Falls. Figure 5-25 shows the lake level simulation for scenarios 1 & 2. Water level simulation resulted in an average annual lake level reduction of 1.2 m and volume change of 13.03% over the entire period compared to the baseline scenario. (See Figure 5-27 & Table 5-10).

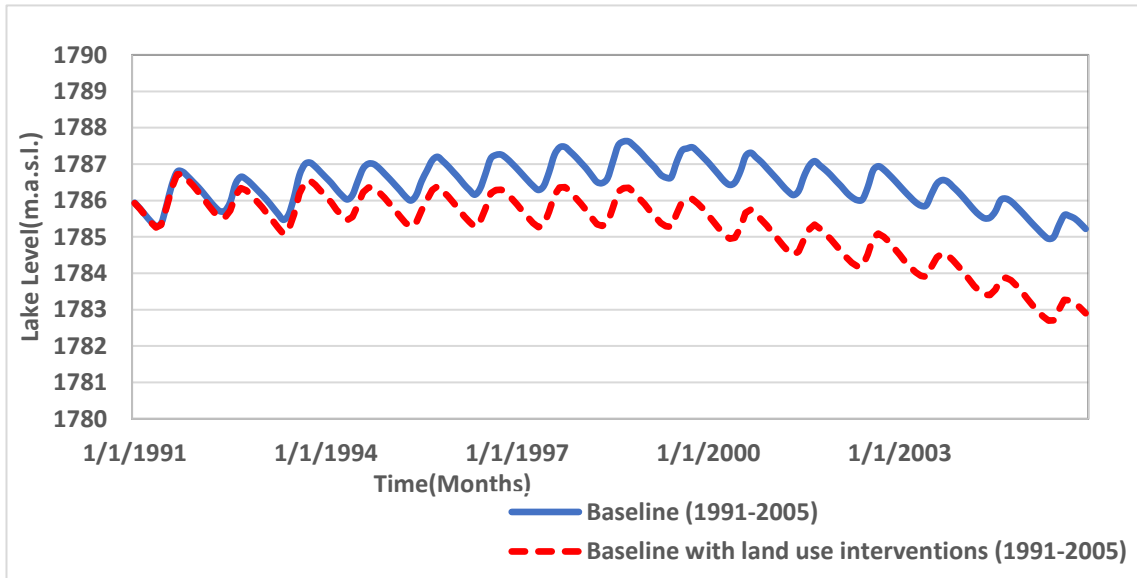


Figure 5-25: Annual Lake level for baseline under land use interventions scenario

The monthly WEAP water level simulation under this scenario indicates that the maximum and minimum water levels will likely be in September and May, respectively. According to the results, the maximum and minimum water levels will decrease by 1.25 m and 1.17 m, respectively (see Figure 5-28 & Table 5-11).

**5.4.2.3. Future Period 2041-2070**

Figure 5-25 illustrates the future period simulation result of the WEAP model. Results show that the future period average annual water level will reduce by 0.51 m and 1.74 m for RCP4.5 and RCP8.5 emission scenarios, respectively. Those levels correspond to an annual average lake volume reduction of 5.57% and 18.78% for RCP4.5 and RCP8.5 emission scenarios, respectively, compared to the baseline scenario (see Table 5-10).

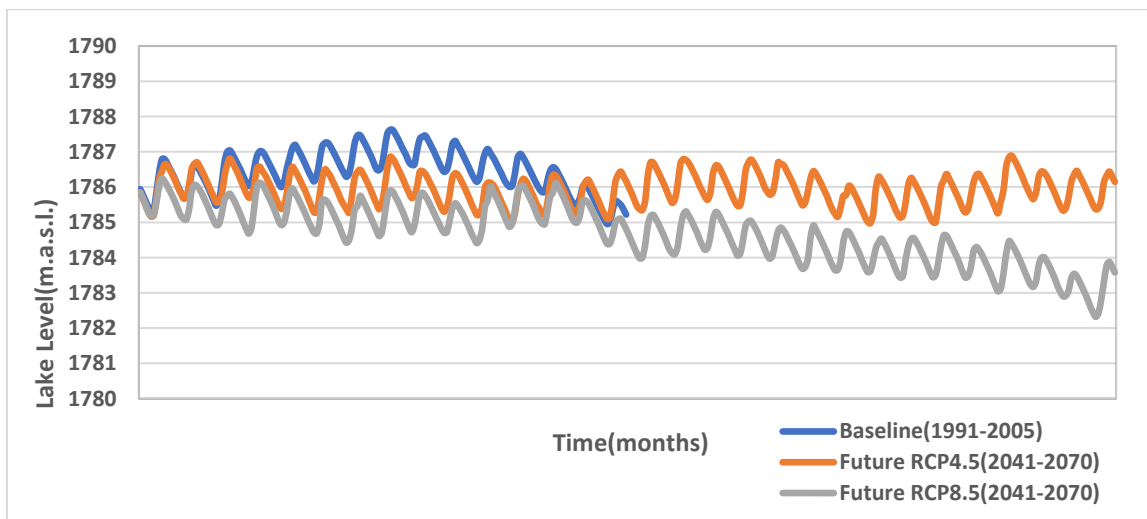


Figure 5-26: Annual Lake level for baseline and future scenario

This scenario's monthly WEAP water level simulation indicates that the maximum and minimum water levels will likely occur in October and May, respectively. The maximum water level showed a shift in the occurrence of the maximum lake level. This is mainly due to the increase of future period precipitation between August and November for both emission scenarios. According to the results, under the RCP4.5 scenario, the maximum and

minimum water levels will decrease by 0.47 m and 0.54 m from the baseline scenario. The maximum and minimum lake levels under the RCP8.5 will possibly be 1.7 m and 1.72 m, respectively (see Figure 5-28 and Table 5-11).

The annual and monthly reduction of the water level of the future period is mainly due to the increasing open water evaporation for RCP4.5 and RCP8.5 emission scenarios because of increasing temperature for both scenarios. The decrement in the lake level is higher under the RCP8.5 scenario. This is mainly related to the higher lake evaporation and lower lake precipitation of the RCP8.5 scenario than RCP4.5.

Based on the results of the simulations, it can be concluded that the effects of land use interventions will be more pronounced than the effect of climate change under the RCP4.5 emission scenario (see Table 5-10). The simulation of lake water level under land-use interventions for the baseline period resulted in a higher reduction of the water level (1.2 m) than the lake level modelling for the future period, including the climate change effect under the RCP4.5 emission scenario (0.51 m). However, water level simulation under RCP8.5 will likely have a more significant impact than the land use interventions of the baseline period, with a water level reduction of 1.74 m.

#### 5.4.2.4. Future Period under Land Use Interventions (2041-2070)

This scenario includes the combined effect of future period climate change and land use interventions on the water balance of Lake Tana. Results of lake level simulation indicate that, for implementation of all planned land use developments, the average annual water level of Lake Tana will decrease by 2.78 m and 5.16 m for RCP4.5 and RCP8.5 emission scenarios respectively. This will translate to water volume reduction of 29.53% and 52.05% for the RCP4.5 and RCP8.5 scenarios, respectively. The highest reduction is shown for the RCP8.5 scenario because of its lower lake inflow than RCP4.5 scenario. Also, the high open water evaporation due to the increasing temperature for the RCP8.5 emission scenario compared to the RCP4.5 scenario partly explains differences in reduction of the lake volume. Figure 5-26 shows annual lake level simulation results under scenarios 1,2,3,4.

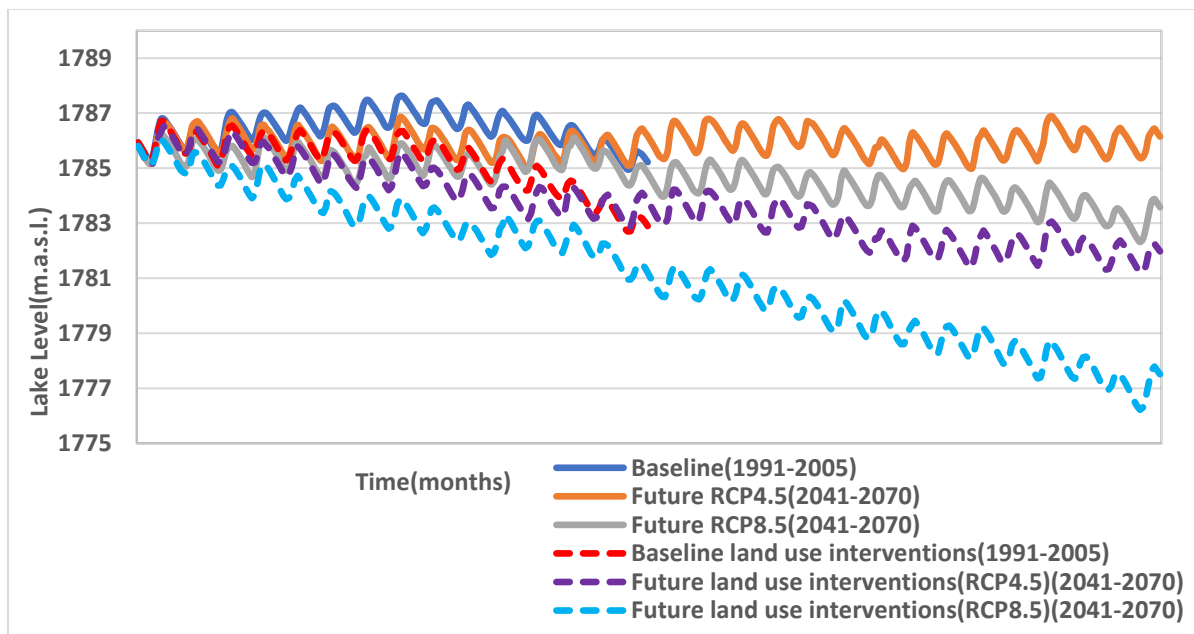


Figure 5-27: Annual Lake level under scenario 1 ,2 ,3 & 4

Similar to the future period scenario, the maximum monthly water level of this scenario showed a shift in the occurrence of the maximum lake level. Thus, the maximum and minimum water levels will likely occur in October

and May, respectively. According to the results, the maximum and minimum water levels will decrease by 2.76 m and 2.79 m under the RCP4.5 scenario. The maximum and minimum lake level reduction under the RCP8.5 will possibly be 5.22 m and 5.14 m, respectively (see Figure 5-28 & Table 5-11).

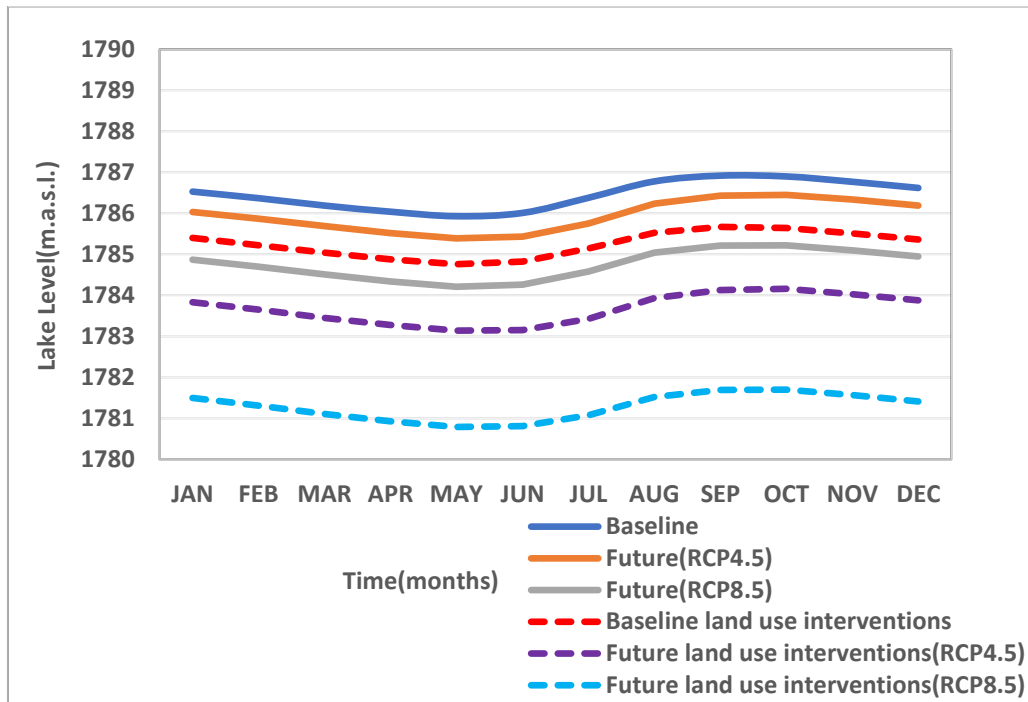


Figure 5-28: Monthly Lake level under scenario 1, 2, 3 & 4

This study reveals that climate change affects the water balance of the lake. Moreover, land use interventions in the upstream catchment are more pronounced than the climate change effect. The integrated effect of climate change and land use interventions is higher effect than the individual effects.

Table 5-10: Results of mean annual water level simulation for each scenario

Scenario	Mean lake level	Volume	Lake level change	Volume change
	m.a.s.l.	Mm <sup>3</sup>	m	%
Baseline	1786.45	27402.00		
Baseline with land use interventions	1785.25	23831.00	-1.2	-13.03
Future				
RCP4.5	1785.94	25877.00	-0.51	-5.57
RCP8.5	1784.71	22256.00	-1.74	-18.78
Future with land use interventions				
RCP4.5	1783.67	19310.00	-2.78	-29.53
RCP8.5	1781.29	13140.00	-5.16	-52.05

Table 5-11: Monthly minimum and maximum lake level for each scenario

Scenario	Maximum monthly lake level		Minimum monthly lake level		Change in maximum lake level	Change in minimum lake level
	m.a.s.l.	Month	m.a.s.l.	Month	m	m
	Baseline	1786.92	September	1785.93	May	
Baseline with land use interventions	1785.67	September	1784.76	May	-1.25	-1.17
Future						
RCP4.5	1786.45	October	1785.39	May	-0.47	-0.54
RCP8.5	1785.22	October	1784.21	May	-1.70	-1.72
Future with land use interventions						
RCP4.5	1784.16	October	1783.14	May	-2.76	-2.79
RCP8.5	1781.70	October	1780.79	May	-5.22	-5.14

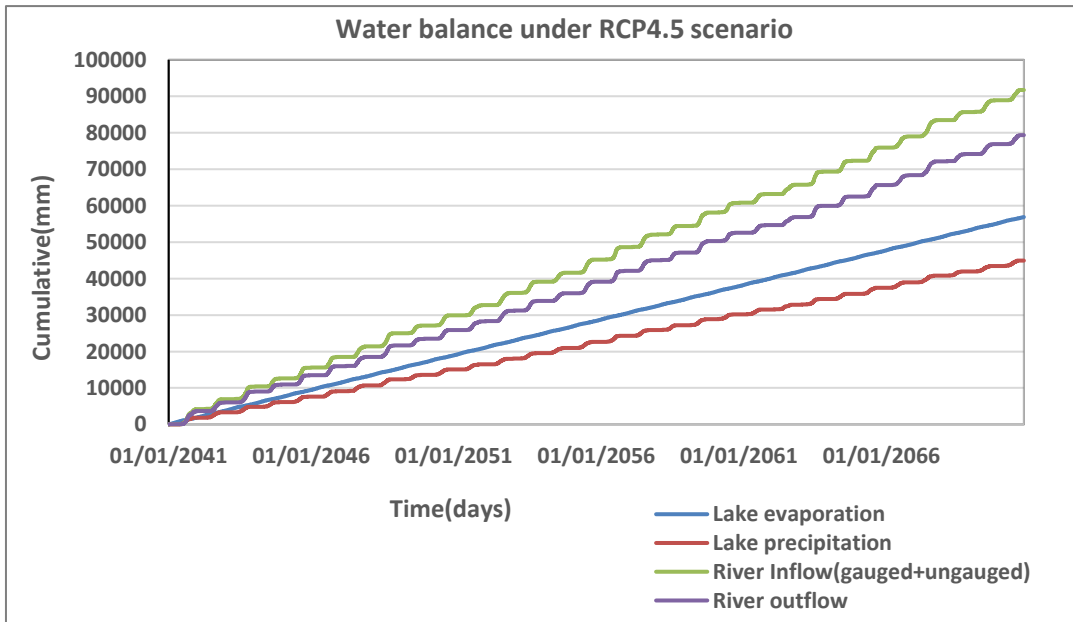
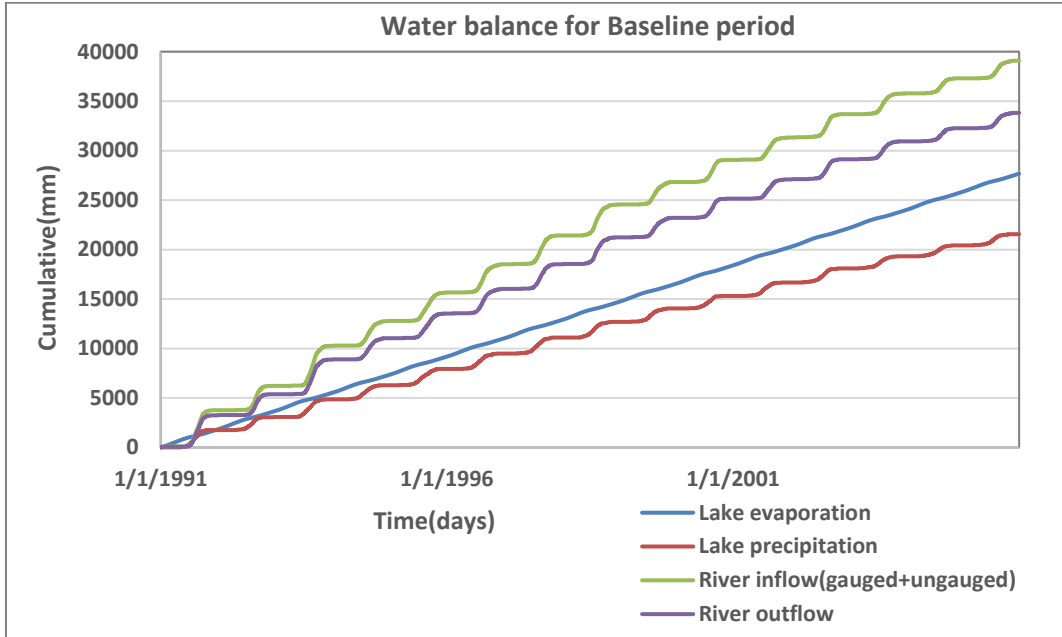
The result of the annual water balance simulation under all scenarios is presented in Figure 5-12. According to the result, the annual net evaporation under the land use intervention scenario decreases when compared to the no land use intervention scenarios. This is mainly related to the decrease in the area of the lake due to the water abstraction of the irrigation schemes. The outflow component under the land use intervention also shows an increasing pattern. This is due to the introduction of the environmental flow requirement node to Tiss Abay Falls under the land use intervention simulations.

Table 5-12: Lake Tana water balance components (Mm<sup>3</sup>/year)

Water Balance Components	No land use interventions			Land use interventions		
	Baseline	Future RCP4.5	Future RCP8.5	Baseline	Future RCP4.5	Future RCP8.5
River Inflow	7599	8918	8564	7348	8650	8087
Net evaporation	-1214	-1189	-1389	-1184	-1109	-1172
River outflow	-6574	-7714	-7408	-6639	-7790	-7493
<b>Closure term</b>	<b>-189</b>	<b>15</b>	<b>-233</b>	<b>-475</b>	<b>-249</b>	<b>-578</b>

The closure term represents an accounted loss due to uncertainty in the computation of water balance components, flow calculation, rainfall computation, evapotranspiration estimation, outflow computations. The closure term of the baseline period indicates 2.5% of the total inflow. While the future water balance simulation under RCP4.5 shows a very small balance closure term of 15 Mm<sup>3</sup>/year. The closure balance under the future period simulation of the RCP8.5 scenario shows an error of 2.7% of the total inflow. The closure term is for the water balance simulation under the land use interventions. This can be associated with additional inaccuracies in irrigation water requirement computation, computation of flows upstream of the irrigation dam, open water evaporation, and precipitation computation of the dams.

The figures below show the cumulative water balance components for the baseline and future periods under RCP4.5 and RCP8.5 emission scenarios. The result shows that river flow is higher under the RCP4.5 scenario than the RCP8.5. Also, the difference between lake evaporation and lake precipitation under the RCP8.5 scenario is higher than the difference between lake evaporation and lake precipitation under the RCP4.5 scenario.



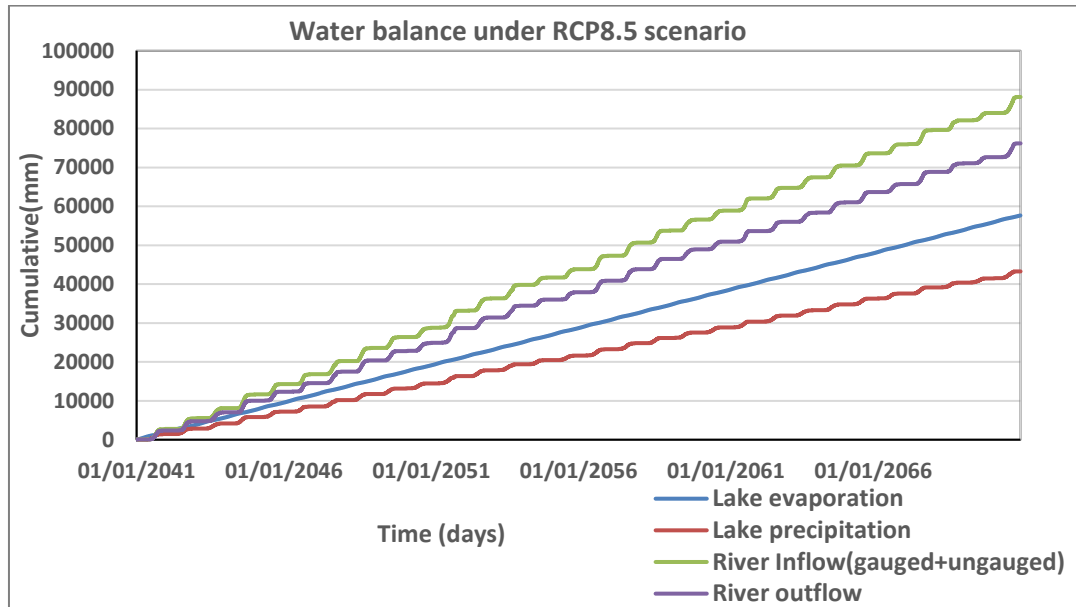


Figure 5-29: Cumulative value of water balance components for baseline and future period (RCP4.5 and RCP8.5)

#### 5.4.3. Impact of Lake Water Reduction for Navigation and Hydropower

As indicated in the earlier sections of the thesis, a minimum lake level of 1784.75 m.a.s.l. was set by Ethiopian Electric Power Corporation (EEPCO) to allow for a minimum draught needed for navigation in Lake Tana (SMEC, 2008). This level was also recommended as minimum operation level (MOL) to release an average flow of 77m<sup>3</sup>/s for Tana-Beles hydropower SMEC (2008) and Halcrow (2011). Table 5-13 shows the number of months below the recommended lake level by EEPCO.

The WEAP simulation result shows 45 months of the simulation period of scenario 2 is below the recommended minimum level. This corresponds to 25% of the simulation period. The future water level simulations under RCP4.5 show lake water levels higher than the recommended minimum water level by the EEPCO. At the same time, 48% of the months under RCP8.5 will possibly drop below the recommended level. 75% and 90% of the months under RCP4.5 and RCP8.5 scenarios, respectively, will drop below the minimum lake level recommendation by EEPCO.

Under the future land use interventions, Lake Tana's water level declines by losing its function to supply water to the hydropower plant consistently.

Table 5-13: Number of months under the minimum recommended lake level by EEPCO

Scenario	Number of months	Percentage of months
Baseline		
Baseline with land use interventions	45	25%
Future		
RCP4.5	-	-
RCP8.5	173	48%
Future with land use interventions		
RCP4.5	271	75%
RCP8.5	324	90%

#### 5.4.4. Impact of Reduced Water Supply on Irrigation and EFR Demands

Assessing the ability of water supply to satisfy the potential water demand is very important in order to evaluate the lake's sustainability for future water use management. Reduction of water supply due to climate change and land interventions can lead to not meeting the irrigation and EFR demands. The unmet demand of the irrigation schemes and environmental flow requirements due to insufficient water supply has been assessed for the baseline and future scenario. As a result, even if the release of water from the lake and the irrigation dams is unrestricted when WEAP modelling is undertaken, there is still unmet demand for the irrigation schemes and environmental flow requirement of both baseline and future periods.

Even though the future period with RCP8.5 emission scenario has lower irrigation water requirement because of the rise in temperature and increasing CO<sub>2</sub> concentration in the atmosphere, which resulted in improved water productivity, it showed higher unmet demand than the RCP4.5 (see Table 5-14). This is mainly due to the lower amount of streamflow than the RCP4.5 emission scenario.

Table 5-14: Unmet demand of irrigation schemes (Mm<sup>3</sup>/year)

Scenario	Water Demand	Supply Delivered	Unmet Demand	% Unmet Demand
Baseline with land interventions	596.67	480.8	115.88	<b>19.42</b>
Future (RCP4.5) with land interventions	552.5	489.74	62.76	<b>11.36</b>
Future (RCP8.5) with land interventions	545.72	433.64	112.08	20.54

Table 5-15 shows the unmet demand of the environmental flow requirement for the baseline and the future period (RCP4.5 and RCP8.5). The unmet demand for environmental flow requirements is small for the baseline and RCP4.5 scenario. This is mainly associated with lower streamflow under the RCP8.5 scenario. Also, the impact of reduced water supply is more significant for the irrigation requirement.

Table 5-15: Unmet demand of environmental flow requirement (Mm<sup>3</sup>/year)

Scenario	Water Demand	Supply Delivered	Unmet Demand	% Unmet Demand
Baseline with land intervention	623.33	617.47	5.86	0.94
Future (RCP4.5) with land interventions	623.33	618.37	4.96	0.80
Future (RCP8.5) with land interventions	623.33	597.56	25.77	4.13

## 6. DISCUSSION

### 6.1. Projected Change in Climate Variables

An increase in the future period (2041-2070) annual and monthly mean temperature of Lake Tana sub-basin for RCP4.5 and RCP8.5 emission scenarios was reported by this study. This change in mean temperature agrees with several studies (Nigatu et al. 2016; Liersch et al. 2018, Worqlul et al., 2018), that indicated a significant temperature rise in the sub-basin. The climate projection results are also comparable with previous studies undertaken using RCP4.5 and RCP8.5 scenarios in Ethiopia. E.g., Bekele et al. (2019) indicated an increase in minimum and maximum temperature in Keleta watershed in the Awash River basin. Findings of this thesis indicated that catchment evapotranspiration and open water evaporation tend to increase for the future period under RCP4.5 and RCP8.5 scenarios due to the increase of temperature. Accordingly, the future period catchment evapotranspiration will possibly increase by 4% and 6% for RCP4.5 and RCP8.5, respectively. While the lake evaporation increases by 2.76% and 4.17%. The increase in catchment evapotranspiration and lake evaporation of the future period is in line with the previous studies. The increase in temperature is higher under RCP8.5 scenario. This result is in line with IPCC, 2013, which indicated that the monthly and annual temperature increase of the RCP8.5 scenario is expected to be higher than the RCP4.5 due to the anticipated change in greenhouse emissions.

Annual precipitation of Lake Tana will be expected to increase in the future period for RCP4.5 and RCP8.5 emission scenarios, respectively. The monthly change in precipitation for both scenarios shows a decrease in precipitation from January to July and an increase from August to December. As seen from the result section, the increase in precipitation under the RCP4.5 is higher than in the RCP8.5 scenario. The precipitation projection results are comparable with a previous study by Ayele et al. (2016), which was conducted in the Gilgel Abay watershed for the period between 2021- 2040 and 2081-2100, in which the future precipitation amount showed an increase for the wet season and a decrease in the dry season for both RCP4.5 and RCP8.5 emission scenario. The result is also in line with previous studies performed in the Lake Tana basin (Nigatu et al. 2016, Melke and Abegaz 2017), although the magnitude of the increase in precipitation is different between the studies. The result of the precipitation projection contradicted the study by Beyene et al. (2010) in the Lake Tana Basin, which indicated a decrease of 2% in precipitation in the Blue Nile basin for the future period from 2040 -2069.

### 6.2. Rainfall-Runoff Modelling

Runoff is the most uncertain water balance component of Lake Tana since around 50% of the sub basin's area is ungauged. Therefore, findings on the computation of inflow to Lake Tana vary from study to study. Thus, it is relevant to compare the findings of this study with previous studies. The baseline period (1991-2005) long-term annual mean inflow of the lake for this study is 2606 mm/year. The result of the inflow component of Lake tana is larger than some studies previously performed. Even though the same HBV parameter sets are used for the gauged catchments, except Gilgel Abay and Gumara catchment, and a similar regionalization procedure is followed, Lake inflow modelled in this study is higher than the lake inflow calculated by Perera (2009). Perera (2009) indicated a total lake inflow of 1781 mm/year from 1994 to 2003. The inflow reported in this study is also higher than Wale (2008) reported, which indicated an annual inflow of 2160 mm/year for 1995-2000. Differences in the result between this study and the above-stated findings can be explained by factors, such as the use of RCM model output by this study. The other reason is the difference in the duration of the simulation periods between these studies. This can be supported by the result of the total inflow amount reported by Nigatu et al. (2016), who adopted HBV model parameters from (Perera 2009) but resulted in a higher inflow amount. According to the

study, the total inflow to Lake Tana for the period 2040-2069 is 2580 mm/year and 2588 mm/year under A2 and B2 emission scenarios.

The future streamflow result indicates that the effect of climate change influences the hydrology of the Lake Tana sub-basin. Although the increase in annual precipitation is inconsistent, the findings of this study showed that the annual mean precipitation of the sub-basin will increase for the future period. The increase of rainfall eventually increases the amount of surface runoff for the future period. The mean annual inflow to the Lake Tana sub-basin is projected to increase for the future period under RCP4.5 and RCP8.5 emission scenarios. The baseline period streamflow is 2606 mm/year, while the future period long-term annual mean streamflow is expected to be 3059 mm/year and 2937 mm/year for RCP4.5 and RCP8.5 emission scenarios, respectively. This increase in streamflow result is in line with (Chakilu et al., 2020), who reported an increase in streamflow in the Gumara watershed under RCP4.5 and RCP8.5 emission scenarios. Nigatu et al. (2016) also reported an increase in the lake inflow under the A2 and B2 emission scenarios between 2010 to 2099. Other studies also support a projected increase in the mean annual streamflow of the future period (e.g., Adem et al., 2016; Worqlul et al., 2018; Liersch et al., 2016).

The result of the projected monthly streamflow shows an increase and decrease of runoff in the wet and dry seasons, respectively, for both RCP4.5 and RCP8.5 scenarios. This is mainly due to the increase in precipitation for the wet season and the decrease in the dry season. The monthly climate projection results are comparable with previous studies by (Ayele et al. 2016; Haile et al., 2017).

### **6.3. Irrigation Requirement**

The gross irrigation requirement for the baseline scenario is 596.67 Mm<sup>3</sup>/year. The simulated irrigation demand under this study is lower than the gross irrigation demand reported by (McCartney, Alemayehu, Shiferaw, & Awulachew, 2010). For example, the gross irrigation demand of the Northwest irrigation scheme under this study is 41.27 Mm<sup>3</sup>/year. Whereas the irrigation demand reported by McCartney is 54 Mm<sup>3</sup>/year. This is mainly due to the crop types used, differences in simulation period, cropping pattern, the irrigation season, and the use of different crop models.

As shown in the result section of this study, the gross irrigation requirement of irrigation schemes in the Lake Tana sub-basin is highly affected by climate change. The result shows that the gross irrigation of the future period will likely decrease due to the high CO<sub>2</sub> emissions and the rise in temperature for the future period. The decrement is higher for the RCP8.5 scenario due to the higher CO<sub>2</sub> emissions and temperatures than the RCP4.5 scenario. Pugh et al. (2016) argued that elevated CO<sub>2</sub> concentration can improve water productivity of C3 plants (E.g., Wheat) and stimulates their photosynthetic activity. The study indicates that elevated atmospheric CO<sub>2</sub> concentration stimulates photosynthesis and reduces the loss of water by means of evapotranspiration. Thus, the lower water requirement for both scenarios is due to the drop in evapotranspiration and rainfall, the shortening of the crop cycle, and improved water productivity. Various studies undertaken to compute irrigation requirements of the irrigation schemes in the Lake Tana sub-basin used the CropWat model. Thus the effect of higher temperature and CO<sub>2</sub> concentration has not to been studied.

### **6.4. Water Balance of Lake Tana under Baseline Period**

The water level simulation result of the baseline period indicates that, for the implementation of the planned water resources, the lake's water level will drop by 1.2 m. This corresponds to a 13.03% storage volume reduction. The decrease of water level reported in this thesis is much larger than reported by (McCartney, Alemayehu, Shiferaw, & Awulachew, 2010) that indicated a lowering of annual lake level of 0.44 m under full implementation of the

development scenario for the period between 1959-1996. This is mainly due to the use of different elevation volume relationships, the difference in the length of the simulation period, and the use of RCM data for this study. The study by McCartney, Alemayehu, Shiferaw, & Awulachew (2010) used the volume water level relationship derived by Pietrangeli (1990). Perera (2009) evaluated the bathymetric relation developed by Wale (2008) and Pietrangeli (1990) for the period of 1994 to 2020 and resulted in higher water levels for the relationship derived by Pietrangeli (1990).

As discussed earlier, the future water balance components of the Lake will likely be affected by climate change. Consequently, the lake's mean annual and monthly future water level and volume storage will possibly decrease for both RCP4.5 and RCP8.5 scenarios. The decrement in water level and storage is larger under the RCP8.5 scenario due to the higher lake evaporation, lower lake inflow, and precipitation than the RCP4.5 scenario.

The decrement in water level by the effect of climate change and land use interventions, contradicts the result reported by Zeleke (2015). According to the study, the monthly water levels simulation results showed an increase for the near-term, medium-term, and long-term periods. The study reported a maximum lake level increase of 91 cm in August in the long-term period. These contradicting results are mainly due to the use of Lake Tana's operation rule by Zeleke (2015). Thus, the outflow component of the lake and the storage are controlled by the operational rules. However, under this study, Lake Tana is considered as a natural lake.

## 7. CONCLUSION AND RECOMMENDATION

### 7.1. Conclusion

The main objective of this research was to assess the impact of climate change and land use interventions on the water balance of Lake Tana. The Water Evaluation and Planning (WEAP) model was used to assess the baseline and future water balance and thereby to evaluate the likely impact of climate change and land use interventions. This research attempted to study the effect of Climate change and land use interventions under four scenarios using bias-corrected ensemble RCM data. The four scenarios studied under this study are baseline period 1991-2005(scenario 1), baseline period with land use interventions (scenario 2), future period 2041-2070 (scenario 3), future period with land use interventions (scenario 4). The future period water balance assessment was undertaken for RCP4.5 and RCP8.5 scenarios. By considering the simulation result of the baseline period without land use intervention scenario as a benchmark/reference scenario, the other three scenarios' water balance has been evaluated.

Water balance components of the lake served as an input to the WEAP model. Computation of water balance components such as net evaporation, lake inflow, lake outflow has been performed for the baseline and future period. Calibrated HBV rainfall-runoff model was used for the generation of streamflow from 9 gauged and 10 ungauged catchments in Lake Tana sub-basin for the baseline and future period. Gauged model parameters were adapted from a previous study by Perera (2009), except for two catchments, Gilgel Abay and Gumara, in which HBV model parameters recalibration of HBV model was undertaken. The simulated streamflow from the HBV model well captured the observed hydrographs for both catchments. A regional model was previously developed by Perera (2009) to estimate river flow from ungauged catchments. Since model recalibration was performed for Gilgel Abay and Gumara catchments, regionalization relations based on catchments should be updated, and this updating has been carried out by adapting the same regionalization procedures followed by (Perera 2009).

The water balance simulation under the land use intervention integrates water demand by the irrigation schemes. The AquaCrop model was used to compute the irrigation requirements of the 11 irrigation schemes. The result revealed that the gross irrigation requirement in Tana sub-basin under the baseline land use intervention scenario is 596.67 Mm<sup>3</sup>/year. Land use intervention scenario of the future period mean annual gross irrigation requirement is 552.50 Mm<sup>3</sup>/year and 545.72 Mm<sup>3</sup>/year for RCP4.5 and RCP8.5 emission scenario, respectively. The result showed a decrement in the gross irrigation requirement of the future period. This is associated with the increased future temperature and increased CO<sub>2</sub> concentration in the atmosphere for the future period.

The sustainability of the lake was assessed by evaluating the change in lake level simulation of scenario 2,3,4 compared to the baseline scenario (scenario 1), evaluating the number of months below a minimum lake level (1784.75 m.a.s.l.) recommendation by Ethiopian Electric power corporation and by assessing the unmet demand of irrigation schemes. Consequently, Lake level simulation under the three scenarios indicated a drop in lake level. Thus, simulated lake level indicated a reduction of mean annual lake level of 1.25 m for the baseline period land use intervention scenario. The reduction in the lake level due to climate change (scenario 3) impact will likely be 0.47 m and 1.7 m under the RCP4.5 and RCP8.5 emission scenarios. The evaluation of the percentage of months below the EEPSCO recommendation indicates, 25% of the months under scenario 2 are below the minimum lake level. The future period (scenario 3) shows 48% of the months under the RCP8.5 scenario will likely be below the minimum lake level. While the lake levels under RCP4.5 will likely be above the minimum lake level. The evaluation

under scenario 4 indicates that 75.28 % and 90% months of the simulation period under RCP4.5 and RCP8.5 scenarios will likely be below the EEPSCO recommendation

The WEAP simulation resulted in unmet irrigation demand of 115.88 Mm<sup>3</sup>/year for scenario 2. And an unmet irrigation demand of 62.76 Mm<sup>3</sup>/year and 112.08 Mm<sup>3</sup>/year for RCP4.5 and RCP8.5 of scenario 4, respectively. The unmet demand of the environmental flow requirement under scenario 2 is 5.86 Mm<sup>3</sup>/year. The unmet demand of the environmental flow requirement under scenario 4 will possibly be 4.96 Mm<sup>3</sup>/year and 25.77 Mm<sup>3</sup>/year.

Overall, the study indicates that climate change and land use interventions significantly impact the water balance of Lake Tana. The sustainability of the Lake will be affected by the integrated effect of climate change and planned dam constructions for large-scale irrigation developments. Climate and land use intervention will also affect the sustainable supply for the irrigation schemes and environmental flow requirements downstream of the proposed dams.

## **7.2. Limitations and Assumptions**

In this study, bias correction of the future RCM data was performed with an assumption that errors in the baseline RCM data would remain the same on future RCM data as well. Thus, the same bias correction coefficient is used for the baseline and future period bias corrections.

The groundwater component of the water balance is assumed negligible because of the unavailability of groundwater data. However, SMEC (2007) indicated that there could be a likely groundwater flow towards the lake since the lake is found in a wide depression of Plato.

The historical runs of the CORDEX Africa cover the period from 1950–2005, whereas the climate projections from 2006–2100 are forced by Representative Concentration Pathways (RCP). In addition to this, data assessment revealed that observed data before 1991 has a lot of missing data. Because of the mentioned the period from 1991–2005 was selected as the baseline period. Thus, uncertainty may arise when comparing 15 years mean of the baseline period with 30 years mean of future climate data.

## **7.3. Recommendations**

- A further study that incorporates currently operational and planned hydropower and water supply projects should be performed to evaluate lake sustainability under complete land use interventions in the sub-basin.
- Detail irrigation demand assessment and calibration of the AquaCrop model using field data should be performed.
- A suggestion is given on using additional climate scenarios and different climate models to improve the understanding of climate change's impact on the lake's water balance.
- Further study that accounts for the groundwater balance component should be conducted.
- A recommendation is given on sustainable water resource planning and management among responsible stakeholders and decision-makers towards achieving sustainable water allocation and abstractions.
- Since the likelihood of the community directly depends on the lake and the river basins, there is a need for a detailed environmental impact assessment study and determination of the water utilization mechanism.

## LIST OF REFERENCES

---

- Abdo, K.S., Fiseha, B.M., Rientjes, T.H.M., Gieske, A.S.M. and Haile, A.T. (2009) *Assessment of Climate Change Impacts on the Hydrology of Gilgel Abay Catchment in Lake Tana Basin, Ethiopia*. Hydrological Processes, 23, 3661- 3669. <https://doi.org/10.1002/hyp.7363>
- Acreman, M., & Dunbar, M. J. (2004). Defining environmental river flow requirements - A review. *Hydrology and Earth System Sciences*, 8(5), 861–876. <https://doi.org/10.5194/hess-8-861-2004>
- Adem, A.A., Tilahun, S.A., Ayana, E.K., Abeyou W. Worqlul, T.T., Melesse, A., Dessu, S.B., M, A., 2016. Climate Change Impact on Stream Flow in the Upper Gilgel Abay Catchment, Blue Nile basin, Ethiopia. *Landscape Dynamics, Soils and Hydrological Processes in Varied Climates* v–vi. <https://doi.org/10.1007/978-3-319-18787-7>.
- Alemayehu, T., McCartney, M., & Kebede, S. (2010). The water resource implications of planned development in the Lake Tana catchment, Ethiopia. *Ecobydrology & Hydrobiology*, 10, 211–221. <https://doi.org/10.2478/v10104-011-0023-6>
- Alemseged, T. H., & Tom, R. (2015). Evaluation of regional climate model simulations of rainfall over the Upper Blue Nile basin. *Atmospheric Research*, 161–162, 57–64. <https://doi.org/10.1016/j.atmosres.2015.03.013>
- Ali, M. (2011). *Practices of Irrigation & On-farm Water Management: Volume 2*. [https://doi.org/10.1007/978-1-4419-7637-6\\_3](https://doi.org/10.1007/978-1-4419-7637-6_3)
- Asmamaw, D. K., Janssens, P., Dessie, M., Tilahun, S. A., Adgo, E., Nyssen, J., ... Cornelis, W. M. (2021). Soil and irrigation water management: Farmer’s practice, insight, and major constraints in upper blue Nile basin, Ethiopia. *Agriculture (Switzerland)*, 11(5). <https://doi.org/10.3390/agriculture11050383>
- Asres, S. B. (2016). Evaluating and enhancing irrigation water management in the upper Blue Nile basin, Ethiopia: The case of Koga large scale irrigation scheme. *Agricultural Water Management*, 170, 26–35. <https://doi.org/https://doi.org/10.1016/j.agwat.2015.10.025>
- A.W. Worqlul, Y.D. Taddele, E.K. Ayana, J. Jeong. Impact of climate change on streamflow hydrology in Headwater Catchments of the upper Blue Nile. *Water*, 10 (120) (2018), 10.3390/w10020120.
- Ayele, H. S., Li, M.-H., Tung, C.-P., & Liu, T.-M. (2016). Assessing Climate Change Impact on Gilgel Abay and Gumara Watershed Hydrology, the Upper Blue Nile Basin, Ethiopia. *Terrestrial, Atmospheric and Oceanic Sciences*, 27(6), 1005–1018. <https://doi.org/10.3319/tao.2016.07.30.01>
- Bashar, K., Nations, U., & Hailelassie, A. (2010). *CPWF Project Report Improved water and land management in the Ethiopian*. February 2015. <https://doi.org/10.13140/2.1.4386.6406>
- BCEOM (Egis Bceom International). 1998. Abbay River Basin Integrated Development Master Plan Project; Phase 2, Section II, Vol. V- Water Resources Development: Part 1 - Irrigation and Drainage. Ministry of Water Resources, Addis Ababa, Ethiopia.
- Bekele, D., Alamirew, T., Kebede, A., Zeleke, G., & M. Melesse, A. (2019). Modeling Climate Change Impact on the Hydrology of Keleta Watershed in the Awash River Basin, Ethiopia. *Environmental Modeling and Assessment*, 24(1), 95–107. <https://doi.org/10.1007/s10666-018-9619-1>
- Beyene, T., Lettenmaier, D. P., & Kabat, P. (2010). Hydrologic impacts of climate change on the Nile River Basin: implications of the 2007 IPCC scenarios. *Climatic Change*, 100, 433–461.
- Booij, M. J. (2005). "Impact of climate change on river flooding assessed with different spatial model resolutions." *Journal of Hydrology* 303(1-4): 176-198.
- Booij, M. J., T. H. M. Rientjes, D. L. E. H. Deckers and M. S. Krol (2007). Regionalisation for uncertainty reduction in flows in ungauged basins. In: Quantification and reduction of predictive uncertainty for sustainable water resources management : proceedings of symposium HS2004 at IUGG2007, Perugia, 7-13 July 2007. / ed. by E. Boegh ...[et.al] Wallingford : IAHS, 2007. ISBN 978- 1- 90150278-09-1(IAHS Publication ; 313) pp. 329-337., IAHS Publication 313.
- Bloschl, G., & Sivapalan, M. (1995). *SCALE ISSUES I N HYDROLOGICAL MODELLING : A REVIEW*. 9(September 1994), 251–290.

- Chukalla, A. D., Krol, M. S., & Hoekstra, A. Y. (2015). Green and blue water footprint reduction in irrigated agriculture: Effect of irrigation techniques, irrigation strategies and mulching. *Hydrology and Earth System Sciences*, 19(12), 4877–4891. <https://doi.org/10.5194/hess-19-4877-2015>
- Deckers, D.L.E.H., 2006. Predicting discharge at ungauged catchments, University of Twente, Enschede, 143 pp.
- Dessie, M., Verhoest, N. E. C., Adgo, E., Poesen, J., & Nyssen, J. (2017). Scenario-based decision support for an integrated management of water resources. *International Journal of River Basin Management*, 15(4), 485–502. <https://doi.org/10.1080/15715124.2017.1345917>
- Droogers, P. (2005). Adaptation Strategies to Climate Change and Climate Variability: A Comparative Study Between Seven Contrasting River Basins. *Physics and Chemistry of the Earth, Parts A/B/C*, 30, 339–346. <https://doi.org/10.1016/j.pce.2005.06.015>
- Duan, Z., Gao, H., & Ke, C. (2018). Estimation of lake outflow from the poorly gauged Lake Tana (Ethiopia) using satellite remote sensing data. *Remote Sensing*, 10(7), 1–21. <https://doi.org/10.3390/rs10071060>
- Endris, H. S., Lennard, C., Hewitson, B., Dosio, A., Nikulin, G., & Artan, G. A. (2019). Future changes in rainfall associated with ENSO, IOD and changes in the mean state over Eastern Africa. *Climate Dynamics*, 52(3–4), 2029–2053. <https://doi.org/10.1007/s00382-018-4239-7>
- Allen, R. G.; Pereira, L. S.; Raes, D.; Smith, M. 1998. Crop evapotranspiration: Guidelines for computing crop water requirements. FAO Irrigation and Drainage Paper No 56. Rome, Italy: Food and Agriculture Organization of the United Nations.
- Gebrechorkos, S. H., Hülsmann, S., & Bernhofer, C. (2019). Regional climate projections for impact assessment studies in East Africa. *Environmental Research Letters*, 14(4). <https://doi.org/10.1088/1748-9326/ab055a>
- Gebremichael, M., Vivoni, E. R., Watts, C. J., & Rodríguez, J. C. (2007). Submesoscale spatiotemporal variability of North American Monsoon rainfall over complex terrain. *Journal of Climate*, 20(9), 1751–1773. <https://doi.org/10.1175/JCLI4093.1>
- Gedefaw, M., Wang, H., Yan, D., Qin, T., Wang, K., Girma, A., Batsuren, D., & Abiyu, A. (2019). *Water Resources Allocation Systems under Irrigation Expansion and Climate Change Scenario in Awash River Basin of Ethiopia*. <https://doi.org/10.3390/w11101966>
- Haile, A. T., Akawka, A. L., Berhanu, B., & Rientjes, T. (2017). Changes in water availability in the Upper Blue Nile basin under the representative concentration pathways scenario. *Hydrological Sciences Journal*, 62(13), 2139–2149. <https://doi.org/10.1080/02626667.2017.1365149>
- Hagan, I. (2007). Modelling the Impact of Small Reservoirs in the Upper East Region of Ghana. *Examensarete TVVR*, 7.
- Halcrow GRID, 2011. Halcrow in association with Generation Integrated Rural Development Consultants, 2011, “Water Balance Modelling and Operational Rules and Irrigation Development in the Upper Beles Catchment”, Ministry of Water Resources, Federal Democratic Republic of Ethiopia.
- IPCC. 2000. Special Report on Emissions Scenarios: A Special Report of Working Group III of the Intergovernmental Panel on Climate Change. Cambridge, UK: Cambridge University Press. 570 pp.19.
- IPCC. (2001). The Intergovernmental Panel on Climate Change. Contribution of Working Group I to the Third Assessment Report of the Intergovernmental Panel on Climate Change. *Cambridge University Press*, 94.
- IPCC, (2013). *Summary for Policymakers. In: Climate Change 2013: The Physical Science Basis. Contribution of Working Group I to the Fifth Assessment Report of the Intergovernmental Panel on Climate Change* [Stocker, T.F., D. Qin, G.-K. Plattner, M. Tignor, S.K. Allen, J. Boschung, A. Nauels, Y. Xia, V. Bex and P.M. Midgley (eds.)]. Cambridge University Press, Cambridge, United Kingdom and New York, NY, USA. [http://www.climatechange2013.org/images/report/WG1AR5\\_SPM\\_FINAL.pdf](http://www.climatechange2013.org/images/report/WG1AR5_SPM_FINAL.pdf)

- IPPC, (2014). *IPCC's Fifth Assessment Report executive summary: What's in it for Africa?*  
[https://cdkn.org/wpcontent/uploads/2014/04/J1731\\_CDKN\\_FifthAssesmentReport\\_WEB\\_.pdf](https://cdkn.org/wpcontent/uploads/2014/04/J1731_CDKN_FifthAssesmentReport_WEB_.pdf)
- IPCC, 2021: Climate Change 2021: The Physical Science Basis. Contribution of Working Group I to the Sixth Assessment Report of the Intergovernmental Panel on Climate Change [Masson-Delmotte, V., P. Zhai, A. Pirani, S.L. Connors, C. Péan, S. Berger, N. Caud, Y. Chen, L. Goldfarb, M.I. Gomis, M. Huang, K. Leitzell, E. Lonnoy, J.B.R. Matthews, T.K. Maycock, T. Waterfield, O. Yelekçi, R. Yu, and B. Zhou (eds.)]. Cambridge University Press. In Press.
- Jin, X., He, C., Zhang, L., & Zhang, B. (2018). A Modified Groundwater Module in SWAT for Improved Streamflow Simulation in a Large, Arid Endorheic River Watershed in Northwest China. *Chinese Geographical Science*, 28(1), 47–60. <https://doi.org/10.1007/s11769-018-0931-0>
- Kebede, S., Travi, Y., Alemayehu, T., & Marc, V. (2006). Water Balance of Lake Tana and Its Sensitivity to Fluctuations in Rainfall, Blue Nile Basin, Ethiopia. *Journal of Hydrology*, 316, 233–247. <https://doi.org/10.1016/j.jhydrol.2005.05.011>
- Kifle Arsiso, B., Mengistu Tsidu, G., Stoffberg, G. H., & Tadesse, T. (2017). Climate change and population growth impacts on surface water supply and demand of Addis Ababa, Ethiopia. *Climate Risk Management*, 18(August), 21–33. <https://doi.org/10.1016/j.crm.2017.08.004>
- Kim, U., & Kaluarachchi, J. J. (2009). Climate change impacts on water resources in the upper Blue Nile River Basin, Ethiopia. In *Journal of the American Water Resources Association* (Vol. 45). <https://doi.org/10.1111/j.1752-1688.2009.00369.x>
- Krysanova, V., Hattermann, F., Huang, S., Hesse, C., Vetter, T., Liersch, S., ... Kundzewicz, Z. (2014). Modelling climate and land use change impacts with SWIM: lessons learnt from multiple applications. *Hydrological Sciences Journal*, 60, 141217125340005. <https://doi.org/10.1080/02626667.2014.925560>
- Lambin, E. F. (1997). Modelling and monitoring land-cover change processes in tropical regions. *Progress in Physical Geography: Earth and Environment*, 21(3), 375–393. <https://doi.org/10.1177/030913339702100303>
- Liersch, S., Tecklenburg, J., Rust, H., Dobler, A., Fischer, M., & Kruschke, T. (2018). Are we using the right fuel to drive hydrological models ? A climate impact study in the Upper Blue Nile Are we using the right fuel to drive hydrological models ? A climate impact study in the Upper Blue Nile. 2(April). <https://doi.org/10.5194/hess-22-2163-2018>
- Loucks, D. P. (2000). Sustainable water resources management. *Water International*, 25(1), 3–10. <https://doi.org/10.1080/02508060008686793>
- Maidment, D. R. (1993). Handbook of hydrology. New York: McGraw-Hill.
- McCartney, M., Alemayehu, T., Shiferaw, A., & Awulachew, S. B. (2010). Evaluation of current and future water resources development in the Lake Tana Basin, Ethiopia. In *IWMI Research Report* (Vol. 2010). <https://doi.org/10.3910/2010.204>
- McCartney, M. P., & Menker Girma, M. (2012). Evaluating the downstream implications of planned water resource development in the Ethiopian portion of the Blue Nile River. *Water International*, 37(4), 362–379. <https://doi.org/10.1080/02508060.2012.706384>
- Mccartney, M., Alemayehu, T., Shiferaw, A., & Awlachev, S. (2010). Evaluation of current and future water resources development in the Lake Tana Basin, Ethiopia. *IWMI Research Report*, 2010.
- Melke, A., & Fantahun, A. (2017). Impact of climate change on hydrological responses of Gumara catchment , in the Lake Tana Basin - Upper Blue Nile Basin of Ethiopia. (January). <https://doi.org/10.5897/IJW>
- Mohebzadeha, H., and Fallah, M.(2019).Quantitative analysis of water balance components in Lake Urmia, Iran using remote sensing technology. *Remote Sensing Applications: Society and Environment*,13, 389-400. <https://doi.org/10.1016/j.rsase.2018.12.009>
- MoWR (Ministry of Water Resources). 1998. Abbay River Basin Integrated Development Mater Plan Project: Phase 2, vol. VI, Water Resources Development, part 2, Large Irrigation and

- Hydropower Dams. Report, Addis Ababa, Ethiopia. pp. 22-24.
- Muerth, M. J., Gauvin St-Denis, B., Ricard, S., Velázquez, J. A., Schmid, J., Minville, M., ... Turcotte, R. (2013). On the need for bias correction in regional climate scenarios to assess climate change impacts on river runoff. *Hydrology and Earth System Sciences*, 17(3), 1189–1204. <https://doi.org/10.5194/hess-17-1189-2013>
- Mukheibir, P. (2007). The Impact of Climate Change on Small Municipal Water Resource Management: The Case of Bredasdorp, South Africa. Retrieved from <https://www.africaportal.org/publications/the-impact-of-climate-change-on-small-municipal-water-resource-management-the-case-of-bredasdorp-south-africa/>
- Nigatu, Z. M., Rientjes, T., & Haile, A. T. (2016). Hydrological Impact Assessment of Climate Change on Lake Tana's Water Balance, Ethiopia. *American Journal of Climate Change*, 05(01), 27–37. <https://doi.org/10.4236/ajcc.2016.51005>
- Oweis, T., Hachum, A., & Kijne, J. (1999). *Water Harvesting and Supplemental Irrigation for Improved Water Use Efficiency in Dry Areas*.
- Perera, B. U. J. (2009). *Ungauged Catchment Hydrology: The case of Lake Tana Basin*. 111.
- Pietrangeli (1990) Studio pietrangeli, hydrological report. Government of Ethiopia, Addis Abeba.
- Raes, D., Steduto, P., Hsiao, T. C., & Fereres, E. (2018). 2018\_Aquacrop\_Chapter 2: Users guide AquaCrop Reference manual. *Reference Manual: AquaCrop, Version 6.0*, (May). Retrieved from [www.fao.org/publications](http://www.fao.org/publications).
- Rahman, M. I. (2013). Climate Change: a Theoretical Review. *Interdisciplinary Description of Complex Systems*, 11(1), 1–13. <https://doi.org/10.7906/indecs.11.1.1>
- Rawat, J. S., & Kumar, M. (2015). Monitoring land use/cover change using remote sensing and GIS techniques: A case study of Hawalbagh block, district Almora, Uttarakhand, India. *Egyptian Journal of Remote Sensing and Space Science*, 18(1), 77–84. <https://doi.org/10.1016/j.ejrs.2015.02.002>
- Rientjes, T. (2015). 'Hydrologic modelling for Intergated Water Resource', Lecture notes for Module 9-10 surface water stream.
- Rientjes, T. H. M., Haile, A. T., Kebede, E., Mannaerts, C. M. M., Habib, E., & Steenhuis, T. S. (2011). Changes in land cover, rainfall and stream flow in Upper Gilgel Abbay catchment, Blue Nile basin - Ethiopia. *Hydrology and Earth System Sciences*, 15(6), 1979–1989. <https://doi.org/10.5194/hess-15-1979-2011>
- Rientjes, T. H. M., Perera, J. B. U., Haile, A. T., Gieske, A. S. M., Booij, M. J., & Reggiani, P. (2011). Hydrological Balance of Lake Tana, Upper Blue Nile Basin, Ethiopia. In *Nile River Basin* (pp. 69–89). [https://doi.org/10.1007/978-94-007-0689-7\\_3](https://doi.org/10.1007/978-94-007-0689-7_3)
- Salini and Mid-day 2006. Environmental Impact Assessment for Beles multipurpose project. Addis Ababa, Ethiopia: Ethiopia Electric and Power Corporation.
- Sajikumar, N., & Remya, R. S. (2015). Impact of land cover and land use change on runoff characteristics. *Journal of Environmental Management*, 161, 460–468. <https://doi.org/10.1016/j.jenvman.2014.12.041>
- SEI (Stockholm Environment Institute). 2007. WEAP: Water Evaluation and Planning System – user guide. Boston, USA: Stockholm Environment Institute
- Series, P. E. (2020). *Mid-term evaluation of the project " Monitoring water productivity by remote sensing as a tool to assess possibilities to reduce water productivity gaps "*.
- Setegn, S. G., David Rayner, Assefa M. Melesse, Dargahi B., Srinivasan R., Anders Wörman, 2011. Climate Change Impact on Agricultural Water Resources Variability in the Northern Highlands of Ethiopia. In *Nile River Basin*: Springer, 241-265 pp.
- Setegn, S. G., Srinivasan, R., Melesse, A. M., & Dargahi, B. (2009, September). *SWAT model application and prediction uncertainty analysis in the Lake Tana Basin, Ethiopia [Master's Thesis]*. <https://onlinelibrary.wiley.com/doi/abs/10.1002/Hyp.7457>.
- Shewit, G., Getahun, A., Anteneh, W., Gedif, B., Gashu, B., Tefera, B., ... Alemaw, D. (2017). Effect of

- large weirs on abundance and diversity of migratory Labeobarbus species in tributaries of Lake Tana, Ethiopia. *African Journal of Aquatic Science*, 42(4), 367–373.  
<https://doi.org/10.2989/16085914.2017.1411774>
- Sieber, J. et al. (2005). Ser uide. *Environment*, (August), 343. Retrieved from  
<http://www.weap21.org/WebHelp/index.html>
- SMEC (Snowy Mountains Engineering Corporation). 2008: Hydrological Study of The Tana – Beles Sub-basins, main report. Addis Ababa, Ethiopia: Ministry of Water Resources
- Smitha, P. S., Narasimhan, B., Sudheer, K. P., & Annamalai, H. (2018). An improved bias correction method of daily rainfall data using a sliding window technique for climate change impact assessment. *Journal of Hydrology*, 556, 100–118. <https://doi.org/https://doi.org/10.1016/j.jhydrol.2017.11.010>
- Stave, K., Goraw, G. (2017). Social and Ecological System Dynamics. In *Social and Ecological System Dynamics Characteristics, Trends, and Integration in the Lake Tana Basin, Ethiopia* (Issue December).
- Steduto, P. (2008). *AquaCrop A new model for crop prediction under water deficit conditions - Calibration for potato* -. 33(80), 285–292.
- Tadesse, A., Matthew, M., & Kebede, S. (2009). Modelling to evaluate the water resource implications of planned infrastructure development in the Lake Tana sub-basin, Ethiopia. Conference Paper h042207, International Water Management Institute.  
<https://ideas.repec.org/p/iwt/conppr/h042207.html>
- Tamiru, A., & Rientjes, T. (2015). Evaluation of regional climate model simulations of rainfall over the Upper Blue Nile basin. *Atmospheric Research*, 161–162, 57–64.  
<https://doi.org/10.1016/j.atmosres.2015.03.013>
- Taye, M. T., Ntegeka, V., Ogiramo, N. P., & Willems, P. (2011). Assessment of climate change impact on hydrological extremes in two source regions of the Nile River Basin. *Hydrology and Earth System Sciences*, 15(1), 209–222. <https://doi.org/10.5194/hess-15-209-2011>
- Teutschbein, C., & Seibert, J. (2012). Bias correction of regional climate model simulations for hydrological climate-change impact studies: Review and evaluation of different methods. *Journal of Hydrology*, 456–457, 12–29. <https://doi.org/https://doi.org/10.1016/j.jhydrol.2012.05.052>
- van Vuuren, D. P., Edmonds, J., Kainuma, M., Riahi, K., Thomson, A., Hibbard, K., ... Rose, S. K. (2011). The representative concentration pathways: An overview. *Climatic Change*, 109(1), 5–31.  
<https://doi.org/10.1007/s10584-011-0148-z>
- Vanuytrecht, E., Raes, D., Steduto, P., Hsiao, T. C., Fereres, E., Heng, L. K., ... Mejias Moreno, P. (2014). AquaCrop: FAO's crop water productivity and yield response model. *Environmental Modelling and Software*, 62, 351–360. <https://doi.org/10.1016/j.envsoft.2014.08.005>
- Wale, A., Rientjes, T. H. M., Gieske, A. S. M., & Getachew, H. A. (2009). Ungauged catchment contributions to Lake Tana's water balance. *Hydrological Processes*, 23(26), 3682–3693.  
<https://doi.org/10.1002/hyp.7284>
- Welde, K., & Gebremariam, B. (2017). Effect of land use land cover dynamics on hydrological response of watershed: Case study of Tekeze Dam watershed, northern Ethiopia. *International Soil and Water Conservation Research*, 5(1), 1–16. <https://doi.org/10.1016/j.iswcr.2017.03.002>
- Woldesenbet, T. A., Elagib, N. A., Ribbe, L., & Heinrich, J. (2018). Catchment response to climate and land use changes in the Upper Blue Nile sub-basins, Ethiopia. *Science of the Total Environment*, 644, 193–206. <https://doi.org/10.1016/j.scitotenv.2018.06.198>
- Worku, G., Teferi, E., Bantider, A., Dile, Y. T., & Taye, M. T. (2018). Evaluation of regional climate models performance in simulating rainfall climatology of Jemma sub-basin, Upper Blue Nile Basin, Ethiopia. *Dynamics of Atmospheres and Oceans*, 83(October 2017), 53–63.  
<https://doi.org/10.1016/j.dynatmoce.2018.06.002>
- WWDSE (Water Works Design and Supervision Enterprise) and ICT (Intercontinental Consultants and Technocrats India (Pvt) Ltd.). 2010 and 2008. Gumara, Jema, Gilgel Abbay, Irrigation

- Project, Design, and final feasibility study report, Vol. III: Water Resources (a), annexure-7: meteorological and hydrological studies. Addis Ababa, Ethiopia.
- WWDSE (Water Works Design and Supervision Enterprise) and TAHAL Consulting Engineers Ltd. 2008. Lake Tana sub-basin four dams project, design report for Ribb Irrigation, Project, Vol. III: hydrological report. Addis Ababa, Ethiopia.
- WWDSE (Water Works Design and Supervision Enterprise) and TAHAL Consulting Engineers Ltd. 2009. Lake Tana sub-basin four dams project, final feasibility report for Megech Irrigation Project, Vol. III: hydrological report. Addis Ababa, Ethiopia.
- Zelege, B. (2015). *Evaluation of Climate Variability and Change on Water Resources Availability for Major Water Resources Development Projects in the Tana- Beles Sub-Basin* (Masters' thesis). Retrieved from <http://196.189.45.74/NADRE/2/50/TanaThesisZelege1.pdf>
- Zhang, L., Nan, Z., Xu, Y., & Li, S. (2016). Hydrological Impacts of Land Use Change and Climate Variability in the Headwater Region of the Heihe River Basin. *PLoS one Northwest*. 1–25. <https://doi.org/10.1371/journal.pone.0158394>

## ACRONYMS

---

Alfa	Parameter defining the non-linearity of the quick runoff reservoir in the HBV
Beta	Parameter in soil moisture routine in the HBV
CORDEX	Coordinated Regional Climate Downscaling Experiment
E	Irrigation Efficiency
EFR	Environmental Flow Requirement
EMA	Ethiopian Meteorological Agency
EMWR	Ethiopian Ministry of Water
EEPCO	Ethiopian Electric Power Corporation
FAO	Food Agricultural Organization
FC	Parameter defining the maximum soil moisture storage in the HBV
HBV	Hydrologiska Byråns Vattenbalansavdelning (Hydrological Bureau Water balance section)
GCM	General Circulation Model
GDD	Growing Degree Day
GIR	Gross Irrigation Requirement
Hq	Parameter representing high flow rate in the HBV
KHQ	Parameter representing a recession coefficient in the HBV
KNMI	Koninklijk Nederlands Meteorologisch Instituut, Netherlands
IPCC	Intergovernmental Panel on Climate Change
IDW	Inverse Distance Weighted
K4	Recession coefficient for lower response box in HBV
LP	Limit for potential evaporation in the HBV
LULC	Land Use Land Cover
LS	Linear Scaling
MAE	Mean Absolute Error
MP	Model Parameter
NS	Nash-Sutcliffe coefficient
PCC	Physical Catchment Characteristic
PERC	Percolation from upper to the lower response box
PET	Potential evapotranspiration
RAW	Readily Available Water
RCP	Representative concentration pathway
RMSE	Root Mean Squared Error
R <sup>2</sup>	Regression Coefficient
RVE	Relative volume error
SEI	Stockholm Environment Institute
SHMI	Swedish Meteorological and Hydrologic Institute

SREs	Special Report on Emissions Scenarios
STDM	Statistical Downscaling Method
SWAT	Soil and Water Assessment Tool
UBN	Upper Blue Nile Basin
WEAP	Water Evaluation and Planning Model

## APPENDIX A

---

### 1. Station weight for precipitation computation of the gauged catchments

Gauged catchments	Addis Zemen	Adet	Bahir Dar	D_Tabor	Dangila	Enfiraz	Gondar	Sekela	Zege	Enjebara	Total
Gelda			0.54	0.18					0.28		1.00
Koga		0.30	0.19		0.24			0.27			1.00
Gumero						0.41	0.59				1.00
Garno	0.11					0.89					1.00
Kelti					0.98					0.02	1.00
Megech						0.09	0.91				1.00
G.Abay					0.15			0.44		0.41	1.00
Gumara	0.16			0.84							1.00
Ribb	0.22			0.78							1.00

### 2. Station weight for precipitation computation of the ungauged catchments

Ungauged catchments	Addis Zemen	Aykel	Bahir Dar	Deke Istifanos	Debre Tabor	Dangila	Delgi	Enfranz	Gondar	Zege	Total
Ribb	0.69				0.15			0.16			1.00
Gilgel Abay			0.24	0.26						0.49	1.00
Garno								1.00			1.00
Gelda			0.67							0.33	1.00
Gumara			0.39	0.26						0.35	1.00
Gumero								0.68	0.32		1.00
Megech									1.00		1.00
Dema		0.41					0.59				1.00
Tanawest						1.00					1.00
Gabikura		0.24					0.16		0.60		1.00

3. Stations weight for catchment PET computation of the gauged catchments

Gauged catchments	Adet	BahirDar	Debre Tabor	Dangila	Aykel	Gondar	Total
Gelda		0.75	0.25				1.0
Koga	0.41	0.26		0.33			1.0
Gumero					0.09	0.91	1.0
Garno						1.0	1.0
Kelti				1.0			1.0
Megech						1.0	1.0
G.Abay	0.42			0.58			1.0
Gumara		0.1	0.9				1.0
Ribb			1.0				1.0

4. Stations weight for PET computation of the ungauged catchments

Ungauged catchments	Adet	Bahir Dar	Debre Tabor	Dangila	Aykel	Gondar	Total
Ungauged Ribb		0.28	0.72				1.00
Ungauged Gilgel Abay	0.16	0.45		0.39			1.00
Ungauged Garno			0.41			0.59	1.00
Ungauged Gelda	0.12	0.88					1.00
Ungauged Gumara		0.65	0.35				1.00
Ungauged Gumero						1.00	1.00
Ungauged Megech						1.00	1.00
Ungauged Dema					1.00		1.00
Ungauged Tanawest					0.63	0.37	1.00
Ungauged Gabikura					0.29	0.71	1.00

5. Stations weight for lake precipitation computation

	Bahir Dar	Zege	Deke Istifanos	Delgi	Enfranz	Addis Zemen	Total
Lake Tana	0.07	0.13	0.53	0.13	0.08	0.06	1.00

6. Stations weight for lake evaporation computation

	Bahir Dar	Adet	Debre Tabor	Gondar	Aykel	Dangila	Total
Lake Tana	0.32	0.10	0.11	0.20	0.16	0.10	1.00

## APPENDIX B: PHYSICAL CATCHMENT CHARACTERISTICS (PERERA, 2009)

Gauged Catchments	Catchment area [km <sup>2</sup> ]	Longest flow path [km]	DEM mean [m]	Hypsometric integral [-]	Average slope of catchment [%]	Catchment shape [-]	Circularity index [-]	Elongation ratio [-]	Forest [%]	Grass land [%]	Crop [%]	Bare land [%]	Woody savannah [%]	Build up area [%]	Leptosol area [%]	Nitosol area [%]	Vertisol area [%]	Luvisol area [%]	Standard annual average rainfall [mm]	Mean precipitation wet season (Jun. to Sep.) [mm]	Mean precipitation dry season (Oct. to May) [mm]	Mean annual evapotranspiration [mm]
Ribb	1408	97.67	2915	0.48	44.59	61.73	38.49	1.55	444.38	51.53	30.66	12.79	0.06	4.96	38.58	0.30	0.00	36.84	1395	9.16	1.10	1300
G.Abay	1657	81.58	2676	0.48	36.76	40.33	30.07	1.08	428.28	74.26	25.66	0.00	0.08	0.00	0.00	0.51	1.95	55.86	1750	10.61	1.84	1332
Gumara	1281	84.28	2717	0.48	33.68	53.36	34.00	1.50	420.27	64.27	31.34	3.86	0.08	0.45	9.23	0.00	3.27	87.21	1415	9.21	1.16	1307
Megech	531	43.92	2415	0.50	37.28	48.16	23.78	1.24	422.69	89.54	10.23	0.07	0.16	0.00	81.59	9.25	3.34	5.03	1117	7.09	1.00	1442
Koga	298	47.64	2429	0.43	23.48	70.16	46.68	1.75	397.48	69.61	24.25	0.03	0.00	6.11	4.11	7.69	14.67	47.61	1542	9.55	1.51	1349
Kelti	608	62.48	2229	0.46	20.00	31.24	33.48	1.39	431.05	99.99	0.00	0.00	0.01	0.00	0.20	0.00	8.25	91.55	1585	9.74	1.60	1305
Ungauged Catchments																						
Ribb	736	24.97	2264	0.46	24.91	31.15	40.55	1.36	461.27	73.71	16.06	8.74	0.02	1.47	9.86	0.00	13.37	23.94	1210	8.15	0.84	1311
G.Abay	2072	79.96	2166	0.41	18.98	19.93	38.69	1.21	389.33	76.60	19.20	0.04	0.12	4.03	22.15	3.13	13.26	53.53	1486	9.86	1.12	1352
Gumara	287	17.87	1920	0.48	16.67	16.60	39.22	1.25	380.00	80.46	19.49	0.03	0.02	0.00	0.00	0.00	23.00	54.73	1368	9.13	0.98	1386
Megech	437	36.09	2234	0.46	18.04	46.75	37.20	1.75	457.42	97.91	2.06	0.00	0.03	0.00	18.88	0.00	47.66	13.69	1162	7.16	0.96	1359
Gumero	588	44.74	2230	0.47	27.87	46.55	30.49	1.03	395.47	71.85	28.14	0.00	0.01	0.00	48.65	3.65	35.17	10.58	1120	7.39	0.89	1340
Garno	463	37.64	2338	0.46	36.06	63.42	24.58	0.85	348.10	72.90	7.91	18.62	0.04	0.54	64.86	9.51	19.20	1.40	999	6.96	0.64	1498
Gelda	391	42.81	2093	0.47	17.95	34.42	35.42	1.27	355.90	60.73	38.93	0.00	0.33	0.00	0.46	0.00	1.44	97.52	1414	9.57	1.02	1498
Dema	325	45.87	2142	0.49	15.96	40.94	42.55	2.26	397.78	97.84	2.14	0.00	0.02	0.00	22.64	0.00	68.57	6.01	1131	7.04	0.87	1498
Tana West	546	12.81	2038	0.49	21.39	22.03	52.46	4.69	365.77	66.57	33.16	0.00	0.02	0.25	0.00	0.00	19.24	34.20	819	5.33	0.67	1444
Gabi Kura	427	26.21	2003	0.48	16.09	21.88	35.39	4.80	354.63	95.85	4.13	0.00	0.02	0.00	1.22	0.00	64.38	6.99	992	6.52	0.79	1498